SRTM DEM Suitability in Runoff Studies

Mesay Daniel Tulu
February, 2005

SRTM DEM Suitability in Runoff Studies

by

Mesay Daniel Tulu

Thesis submitted to the International Institute for Geo-information Science and Earth Observation in partial fulfilment of the requirements for the degree of Master of Science in Geo-information Science and Earth Observation, Specialisation: Watershed Management, Conservation & River Basin Planning

Thesis Assessment Board

Chairman	Prof. dr. ir. Z. Su
External Examiner	Dr. P. Reggiani
Primary Supervisor	Dr. B.H.P. Maathuis
Second Supervisor	Ing. R.J.J. Dost

**INTERNATIONAL INSTITUTE FOR GEO-INFORMATION SCIENCE AND EARTH OBSERVATION
ENSCHEDE, THE NETHERLANDS**

Disclaimer

To my wife Mesi and my daughter Milki

Abstract

In GIS based hydrological modelling Digital Elevation Models are used in determining topographic parameters, drainage networks, and other relevant indices. Since the release of the 3 arc second resolution SRTM DEM (provided to the public for free) the GIS world has access to globally uniform elevation information. The elevation information from this DEM is the height of the top reflective surface that can be vegetation or any other radar opaque material, which do not represent the actual ground surface elevation. It may also exhibit typical radar artefacts including scattered voids due to shadowing effects and poor signal returns over some terrain, as well as occasional phase unwrapping errors. In this study the SRTM DEM is assessed for these limitations, uncertainties and its performance in a semi distributed hydrologic model, the Soil and Water Assessment Tool (SWAT) in runoff modelling and in the TOPMODEL base parameter, Topographic Index in comparison to a DEM generated from ASTER optical imagery. The study is conducted on the Malewa river basin (1700sq.km) located in Naivasha, Kenya. Issues related to accuracy assessment using elevation information from high order accuracy geodetic triangulation ground control points and GPS data are also presented. The raw SRTM DEM vegetation cover is removed applying vegetation height information from the field and using Ilwis map calculation and SCOP++ filtering techniques. In general quality of the SRTM DEM will be improved using two different approaches. A vegetation height attribute map is created from a detailed landcover map and this vegetation height is removed from the DEM creating a DTM. This DTM is used to qualify the other quality improvement approach; using a DEM filtering package SCOP++ to remove vegetation cover and leftover artefacts.

It is found that the ASTER DEM gives more detailed terrain features than raw SRTM DEM. The daily runoff output of the SWAT model when the ASTER DEM is used is higher than when the SRTM DEM is used. This study has shown that in this particular landcover condition and terrain complexity that the terrain details are more influential than the accuracy difference between the two DEMs in the model runoff output.

Since no significant difference is encountered in monthly runoff output of the model when the ASTER DEM is replaced by the SRTM DEM, the study has focused on the daily runoff output changes relative to the DTMs quality and resolution. The daily runoff output of the SWAT model is higher when the ASTER DEM is used.

The Topographic index has shown small change in the catchment average value to the DTMs quality and resolution, however, the distribution and range of values are affected considerably by both quality and resolution.

Acknowledgements

Table of contents

List of figures

List of tables

1. General Introduction

Runoff is the principal component of hydrological systems of a catchment. Part of precipitation that reaches on the ground moves to streams as a form of surface or subsurface flow and generates runoff. Stream responses are the main data sources to quantify the runoff volume and execute water management and planning systems and hydraulic infrastructure implementation. This is possible when a gauging station is installed at some appropriate point along the course of the stream. where streams are not equipped with sufficient gauging station distribution or no gauging history at all and in extreme hydrologic phenomena like gauging stations are overtopped by floods; hydrologists apply rainfall-runoff modelling to forecast and predict runoff volumes and floods peaks. Various types of hydrologic models are developed and in use in a GIS environment for pre and post simulation of runoff. In most such kinds of hydrologic models the spatially varying characteristics of rainfall and runoff are analyzed by using a Digital Elevation Model (Abbott, 1996). The DEM represents the topographic features providing elevation information to extract morphometric parameters and stream networks in the modelling process. In distributed models the routing of water over a surface of each grid cell is extremely related to those morphometric parameters extracted from the DEM. In addition to that topography based simplified modelling approaches as TOPMODEL (Beven, 1997) that uses a topographic index, are gaining more popularity in the modern hydrology developments. The bottleneck to increase the reliability of these modelling approaches is a source of accurate DEM. The capability to obtain quality DTM data of large areas has been an important factor for hydrological modelling. DEMs were mostly generated from optical stereo data, acquired by airborne or spaceborne sensors. DEMs derived from such optical data are generally inhomogeneous as their quality depends strongly on image feature contrast. "Cloud cover and lack of sunlight also compromised the acquisitions of suitable optical stereo data. New DEM generating technologies are prevailing and challenging these conventional counterparts, primarily due to the advances in sensor technologies coupled with the ongoing improvement of digital technologies" (Rabus, 2003). The Shuttle Radar Topography Mission (SRTM) data collected during eleven day mission of the space shuttle Endeavour in February 2000 and processed using Synthetic Aperture Radar

Interferometry (SAR Interferometry or InSAR) technique is one of the recent developments (http://www2.jpl.nasa.gov/srtm/)

1.1. Importance of the Research

SRTM DEM is widely in use in the GIS based hydrologic modelling since the 3 arc second resolution DEM is provided to the public for free. Although this globally homogeneous, high resolution DEM allows rapid analysis of topographic attributes over large drainage basins, only few researches are done to examine systematically its uncertainties and their degree to affect the representation of the land surface in hydrological modelling. (Sun, 2003) made cross validation of the elevation information from SRTM DEM made using Shuttle Laser Altimeter after verifying SLA by field observation. In this study the DEM will be assessed for its uncertainties and its performance in a semi distributed hydrologic model Soil and Water Assessment Tool (SWAT) and the TOPMODEL base parameter, Topographic Index in comparison to a DEM generated from optical imagery ASTER.

1.2. Research Objectives

The main objective of this study is to analyze the performance of SRTM DEM in runoff modelling and the accuracy of the output using different comparison techniques at watershed scale. To achieve above objective following multiple objectives were addressed

- Assess SRTM DEM height limitations and uncertainties compared to ASTER DEM
- Assess how SRTM DEM limitations and uncertainty affect runoff modelling
- Increase the resolution of the DTM and analyze the runoff model output
- Compare the SRTM DEM-runoff model output with the optical imagery DEM-runoff model output
- Check the sensitivity of the runoff model output with relation to the extent of DTM quality improvement
- Assess topographic index sensitivity to the DEM quality and resolution

1.3. Research Questions

In this research the following questions will be addressed:

- What are the limitations of SRTM DEM?
- What is the accuracy of SRTM DEM when compared to ASTER DEM?
- How SRTM DEM limitations can be removed to improve the accuracy of the hydrologic model output?
- What is the sensitivity of the runoff model output to the degree of improvements made and the resolution changes on the DEM?
- What is the response of the SWAT (runoff) model to the improved SRTM DEMs?

1.4.   Methodology

The following approaches are applied after required data are collected during the field work to meet the objectives set in the previous section. Conceptualization of the methodology is presented in figure1 and figure 2
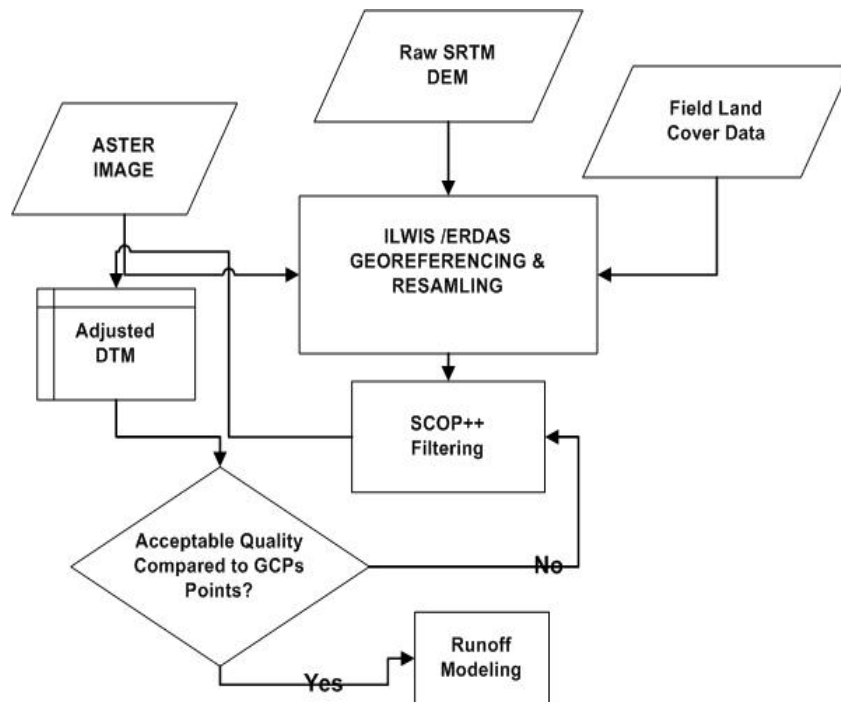
Figure 1 Flowchart of Raw SRTM DEM quality improvement

1.4.1.   RAW SRTM and ASTER DEM accuracy and quality comparison

In order to check the vertical accuracy of the raw SRTM DEM specification given by the mission, ASTER DEM is generated using ENVI DEM extraction software and comparisons are

made using geodetic triangulation ground control points and ground truth data collected by GPS during field work. Both SRTM and ASTER DEMs are compared for vertical accuracy with the Triangulation Ground Control Points (Tri.GPSs) and the GPS points separately and the RMSE and correlation coefficient of each DEM are evaluated.

The quality of these DEMs is compared by extracting drainage lines and making a comparison with a manually digitized drainage line. The drainage maps extracted from the DEMs are overlayed one the digitized drainage map one by one and assessment is made by visualizing which fits the digitized drainage network better.

1.4.2.   SRTM DEM horizontal accuracy check

 A simple procedure is applied to assess the horizontal accuracy of the DEM

1. Georeference a mosaic of ASTER image using GPS control point
2. automatic delineation of drainage network from SRTM DEM
3. overlay the drainage line on the accurately georeferenced ASTER image and measure plan distance of the drainage line from the centre of the drainage line visible on the ASTER image

1.4.3.   Quality improvement of SRTM DEM

In general quality of the SRTM DEM will be improved in two different approaches. A vegetation height attribute map is created from a detail land cover map and the vegetation height is removed from the DEM and DTM is created applying ilwis map calculation. This DTM is left untouched to be used as a control for the other quality improvement approach; that is using a DEM filtering package SCOP++ to remove vegetation cover and leftover artefacts. In SCOP++ different filtering strategies can be applied till the best output is found without losing the topographic information from the original DEM. This is done by making a difference map of the original and the applied filtering output DTM and visualizing in comparison with vegetation height attribute map. For the second time, the DTM data accuracy is derived by comparing its elevation values with corresponding point elevation values of Tri.GCPs root-mean-square error (RMSE).

1.4.4.　　　　Assessment of SRTM DEM in runoff modelling, SWAT

To assess the adjusted DTM performance in semi distributed hydrologic model the Soil- Water Assessment Tool (SWAT) will be applied. The cumulative effect of DTM extracted topographic parameters on the runoff output at the basin outlet will be assessed graphically as presented in figure 2.
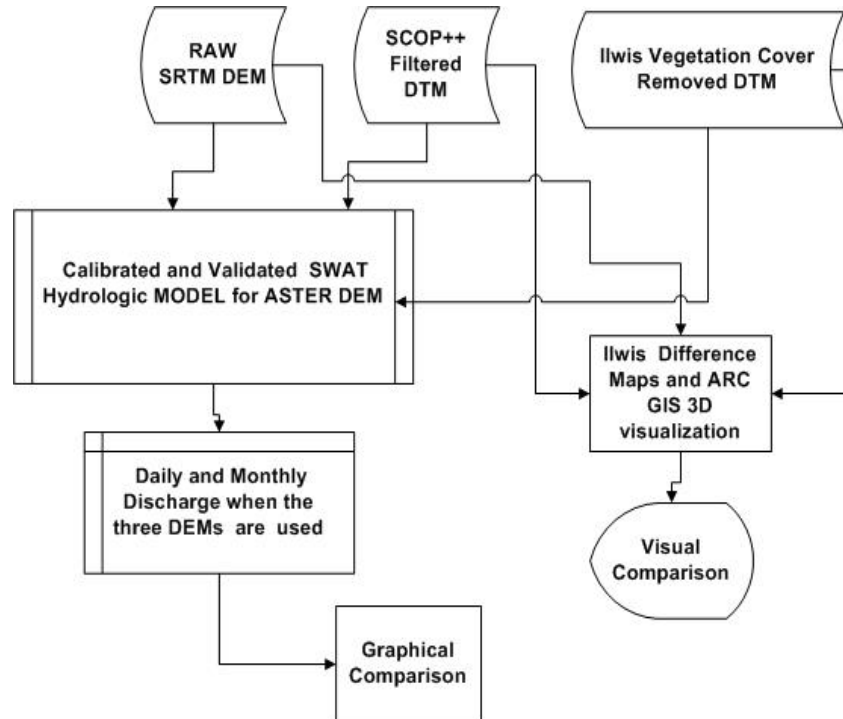
Figure 2 Flowchart of the DTMs Assessment and SWAT Runoff Outputs

Required data preparation, calibration and validation of the model was made using Advanced Spaceborne Thermal Emission and Reflection Radiometer (ASTER) DEM in previous study (Muthuwatta, 2004). The qualitatively improved SRTM DTM is applied in the model and the runoff output from the catchment is examined graphically in comparison to the output when ASTER DEM is used. Malewa catchment will be used for this assessment since it has high elevation difference, contributes the major inflow to lake Naivasha and it has long term rainfall and discharge data with little data gaps.

1.4.5.   Assessment of Topographic Index

Topographic Index will be assessed by comparing the histograms of the raw SRTM DEM and the DTMs. Visualizing saturation areas on the different maps will be applied. In addition, the maximum, mean, and minimum topographic indices of the catchment will also be evaluated.

1.4.6.   Overall Assessment

Conclusions will be drawn from the overall statistical and visualization comparison with regard to the DEM accuracy. The sensitivity of the runoff output when the ASTER DEM is replaced by the raw SRTM DEM, the vegetation cover removed DTM and the SCOP++ filtered DTM. The discharge output from these runs is plotted in the same graph and discharge differences will be evaluated.

1.5.   Thesis Structure

In chapter 2   different relevant literatures will be reviewed concerning digital elevation models sources and accuracies. A brief introduction of runoff and hydrologic models is also given in this section

Chapter 3 gives introduction about the study area topography, land cover and climate, rainfall distribution and drainage pattern of the study area.

Chapter 4 is about SRTM DEM generation and quality and accuracy assessment. Comparison of this DEM with ASTER DEM, Tri.GCPs and GPS points is also discussed in this chapter.

Chapter 5 discusses the quality improvements applied on the SRTM DEM using SCOP++ and the filtering techniques applied. Assessment of the improved DTMs is also discussed in this chapter.

In Chapter 6 the hydrologic model, SWAT discharge outputs of ASTER DEM,   raw SRTM DEM, Vegetation cover removed DEM and the SCOP++ filter DTM are analysed

In Chapter 7 conclusions and recommendations are given

2. Literature Review

2.1. Runoff Modelling

"Hydrologic phenomena are extremely complex and may never be fully understood. However, in the absence of perfect knowledge they may be represented in a simplified way by means of the system concept" (Chow, 1988)A system is a set of connected parts that form a whole. It can also be any conceptually defined region of space capable of receiving a sequence of inputs of conservative quantity, storing some amount of that quantity, and discharging outputs of that quantity (Dingman, 2002). The hydrologic cycle may be treated as a system whose components are precipitation, evapotranspiration, runoff and other phases of the hydrologic cycle. To analyse the total system the simpler subsystems can be treated separately and the results combined according to the interactions between sub systems.

A simplified representation of part of a real world system and mostly a setup to simulate a number of specific flow processes of a hydrological cycle is termed a hydrological modelling. Because of their great complications, it is not possible to describe some hydrologic process with the exact physical laws. By using the system concept, effort is focussed to the construction of a model relating inputs and outputs rather than to extremely difficult task of extracting representation of the system details (Chow, 1988). Nevertheless, knowledge of the physical system helps in developing a good model and verifying its accuracy.

Simulation models can be classified as physically based and conceptual. Physically based model accounts for observed phenomena through empiricism and use of basic fundamentals such as continuality and momentum conservation assumptions (Viessman, 1989). A conceptual model, on the other hand, relies heavily on a pre-defined and designed concept to model processes adopted in simplified manner.

Model input data and model output data are lumped or spatially distributed over the model domain. A rainfall-runoff model is termed a lumped model if the spatial variation of model input data is neglected through out the entire system and expressed by a single average value. Spatially distributed hydrologic modelling is one of the most recent developments in hydrological modelling, which gained tremendous importance starting from the late eighties. In spatially distributed rainfall-runoff model the spatial variations of model input data are simulated by uniform or non uniform grid elements through out the system. Distributed models ideally account for all spatial variability in the watershed explicitly by solving the governing equations for each pixel in the grid.

 This grid based spatial distribution demands for high computing speed and data storage space in large basin modelling applications.

Nevertheless, increase in computer resources such as processing speed, memory and data storage made a big role in advancing this type of modelling. Comparing spatially-distributed models with lumped models, which do not reflect the spatial heterogeneity, clearly reveals that grid-based modelling of hydrological processes require much more input data and process parameters. This is more challenging when the availability of data is limited and the desired project is at basin scale. Semi distributed model compromises the limitations of lumped and fully distributed models. In semi distributed model the catchment is subdivided into sub-basins or hydrologic response units and a single average spatial variable is assigned to each sub-basin or HRU giving average responses to hydrologic events. In this condition, the degree of detail information extraction from the model depends on the size of sub basin units. In order to extract more detailed information, the modeller should switch to grid-based distributed models that can solve this hydrologic response in much smaller spatial scales. Spatially distributed hydrologic models originate from the idea to use more physically based processes to define the hydrologic phenomena, rather than approximating them with empirical formulas. Thus, considering spatial heterogeneity directed the research towards using mathematically well defined conservation laws such as conservation of mass, momentum and energy to simulate the natural system (Abbott, 1996). For that reason, using advanced physically based distributed models became the current trend in hydrological modelling.

Most hydrological models, which use topographic information to predict and simulate runoff outputs from catchments are termed as topographic based models. One of the pioneering works on distributed modelling was completed by (Abbott, 1986) resulting the development of the SHE (Systéme Hydrologique Européen) model which is renowned to be one of the earliest of distributed models. Likewise, (Beven, 1985) has developed TOPMODEL to simulate runoff production from a watershed. In TOPMODEL, Topography is assumed to be of importance with respect to the hydrological behaviour of a catchment. A topographic index, which is derived from a digital elevation model, is used to determine the spatial variability of saturated areas at a given time. The concept of TOMODEL has got high consideration in the Hydro/GIS modelling environment and gave a remarkable indication that topography will be the foundation for the future advancement of runoff modelling. As (Moore, 1993) quoted "We are in the era of 'spatial modelling'. Digital elevation data and remotely sensed catchment characteristics are now viewed as essential data inputs to the new generation of hydrologic and water quality models".

2.2.   Digital Elevation Model

As reviewed in the previous section, topographically based modelling approaches are grow to be to be one of the most popular premise in catchment hydrology in view of the fact of the availability and quality of DEMs. DEMs are used in water resource projects to identify drainage related features such as watershed divides, valley bottoms, channel networks and surface

drainage patterns, and to quantify subcatchment and channel properties such as size, length and slope. The accuracy of these topographic parameters is a function of both the quality and resolution of the DEM used in the extraction (Garberecht, 1999).

Since the past decade the increasing computer speed, affordability and availability of high resolution imageries are saving money and time simplifying extraction of DEM. With a very similar method to photogrammetry using airborne and spaceborne digital remote sensing imageries automatic DEM generation is possible. As (Toutin, 1995) explained, using two images at a time and by three dimensional reconstruction of stereo model, altimetric information can be extracted. In general (Xiong, 2002) divided the procedure into three basic steps: setting up sensor mathematical model to reflect the relationship between points on the ground and pixels on the image, performing image matching to get a disparity map, and finally computing each point's altitude. Since the launch of the first of the SPOT series satellite in 1986 most stereoscopic satellite have capability of acquiring data of the same location from different positions. According to (Cuartero, 2004) today several satellites also offer the possibility for stereoscopic acquisition:

SPOT (Priebbenow, 1988) MOMS (Lanzl, 1995), IRS, KOMSAT, AVNIR (Hashimoto, 2000), TERRA (Welch, 1998) and more recently, the high resolution pushbroom scanners IKONOS (September 1999), EROS-A1 (December 2000), QUICKBIRD-2 (October 2001), SPOT 5 (May 2002), and ORBVIEW-3 (June 2003). However, these stereoscopic data acquisition techniques have some disadvantage since data are inhomogeneous as their quality depends on image feature contrast and also they are compromised by lack of sunlight and cloud cover. The latest development in DEM generation is the use of radar data such as an interferometric Synthetic Aperture Radar (InSAR) and LIght Detection and Ranging (LIDAR). InSAR has been a technique of considerable scientific interest for some years due to its three-dimensional (3D) information extraction capability, and nearly weather and sunlight independent operation (Bamler, 1999). Interferometry is the process of acquiring topographic data, or changes in the earth's surface, by calculating the interference patterns caused by the difference in phase between two radar images at two distinct times and/or distances. The result is called an interferogram, which is essentially a contour map that records the change in distance between the ground and the radar instruments.

2.3. DEM Uncertainties

DEMs generated using different techniques have some degree of uncertainties that is referred to as our lack of knowledge about the reliability of measurements representation of the true value. According to (Wechsler, 1999) survey of digital elevation model, 216 users response from 26 countries and various organizations and industries, 45% of the respondents recognized that their work is "sometimes or always" affected by uncertainty and 55% indicated that uncertainty is "very important". About 25% of users reported lack of awareness as to whether DEM errors affected their work at all. 22% of users recognized that uncertainty was very important, and the same proportion of users reported that they account for uncertainty in their work.

DEMs uncertainty impact on derived morphometric parameters has been investigated by different researchers. In each of these studies, different methods of representing DEM uncertainty were developed and implemented. (Lee, 1992) and (Lee, 1996) simulated errors in a grid DEM and determined that small errors introduced in the database significantly affected hydrologic features.

Quality and resolution should be considered in the application of DEM in hydrologic modelling. Quality refers to the accuracy of the elevation while resolution refers to the horizontal grid spacing and the precision of vertical increment.

DEM accuracy is estimated by a comparison with DEM Z values, and by contrasting many check points with elevation values from higher order accuracy. The pair wise comparisons allow the calculation of the Mean Error (ME), Root Mean Square Error (RMSE), Standard Deviation (SD) or similar statistics (Cuartero, 2004). RMSE is used widely to describe the DEM accuracy that measures the dispersion of the frequency. According to (Weng, 2002) uncertainty, instead of error, should be used to describe the quality of a DEM. To analyze the pattern of deviation between two sets of elevation data, conventional ways are to yield statistical expressions of the accuracy. In fact, all statistical measures that are effective for describing a frequency distribution, including central tendency and dispersion measures, may be used, as long as various assumptions for specific methods are satisfied. The RMSE alone is not sufficient for quantifying DEM uncertainty, because this measure rarely addresses the issue of distributional accuracy (Weng, 2002).

Quantitative assessment using ground truth data is an important component of the quality control (Maune, 2001).The number of check points is an important factor in reliability because it conditions the range of stochastic variations on the standard deviation values (Li, 1991). Another subject is the accuracy of check points that must be sufficient for the control objectives. As National Digital Elevation Program (NDEP, 2004) states, horizontal accuracy is another important characteristic of elevation data; however, it is largely controlled by the vertical accuracy requirement. If a very high vertical accuracy is required then it will be essential for the data producer to maintain a very high horizontal accuracy. This is because horizontal errors in elevation data normally (but not always) contribute significantly to the error detected in vertical accuracy tests.

3. Study Site and Data Set

This study is conducted on catchment of Malewa River which is a sub-basin of Lake Naivasha basin. Naivasha basin is situated in the Nakuru district; about 100 km northwest of Nairobi in the central part of the rift valley of Kenya with a geographic location of 0°08′13″S to 0°54′56″S and 36°04′56″E to36°42′47″E. Naivasha basin incorporates the Malewa, Gilgil and Karati rivers, which flow to lake Naivasha. The basin has area coverage of about 3287 sq.km of which Malewa river basin shares 50%. However 90% of Lake Naivasha water input is from this basin. Malewa river basin has high elevation difference that ranges from 1880m in the rift system to 3900m above mean sea level in the north eastern mountain ranges.
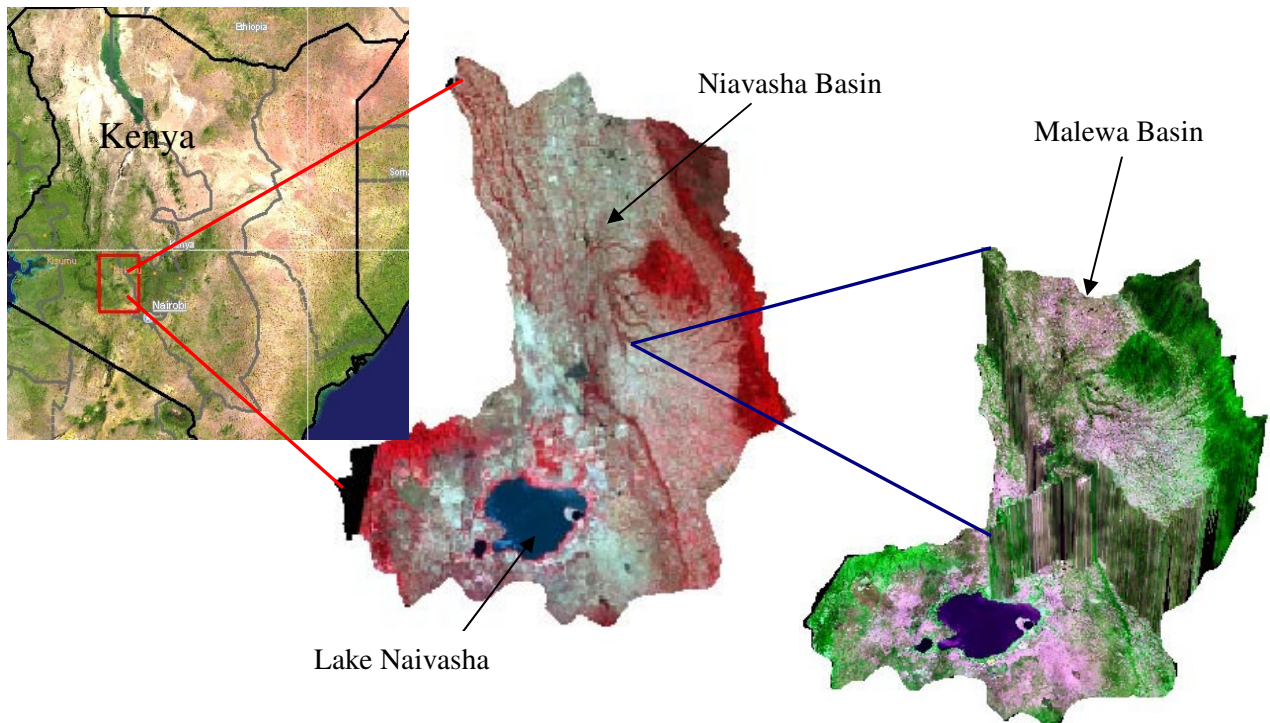
Figure 3 Study area location and 3D overview

3.1.   Topography and Landcover

The hydrological active eastern and north eastern part of Malewa basin topography can be subdivided into three terrain features. The relatively flat area in the valley system with an elevation range from 1885m to 1930 m, the Kinangop plateau in the east with gradual elevation

increment up to 2800m a.m.s.l. to the foot of the Nyandarua mountain range, and the steep mountain itself which has an elevation as high as about 4000m a.m.s.l. This relief difference provides an advantageous environment to assess the accuracy differences of SRTM DEM relative to plain areas and steep slopes.
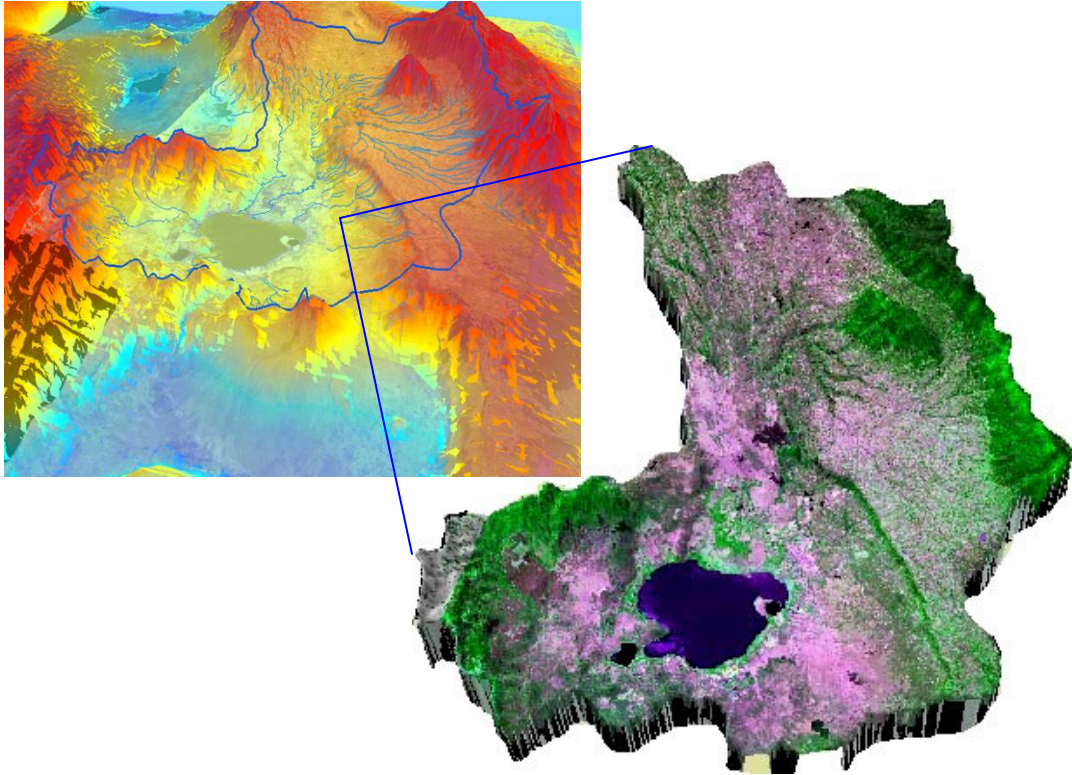
Figure 4 Naivasha catchment and the surroundings topography in 3D using SRTM DEM mosaic and ASTER image from March 2003

The landcover   varies from a semi arid grassland flats in the valley to a dense forest in the highlands. The central part of the catchment is covered by grassland and shrubs except the acacia tries along the streams and around the lake. The highlands are covered by natural dense vegetation. Hardwood vegetation like conifers, alpine trees and bamboo   are the dominant land cover types in the north eastern parts and the Nyandarua Mountain.

water
maize
Mixed Dense Forest
Dry Grass Land
Grass Land
Conifer Forest
Bushes
Natural Forest
Acacia
Bamboo
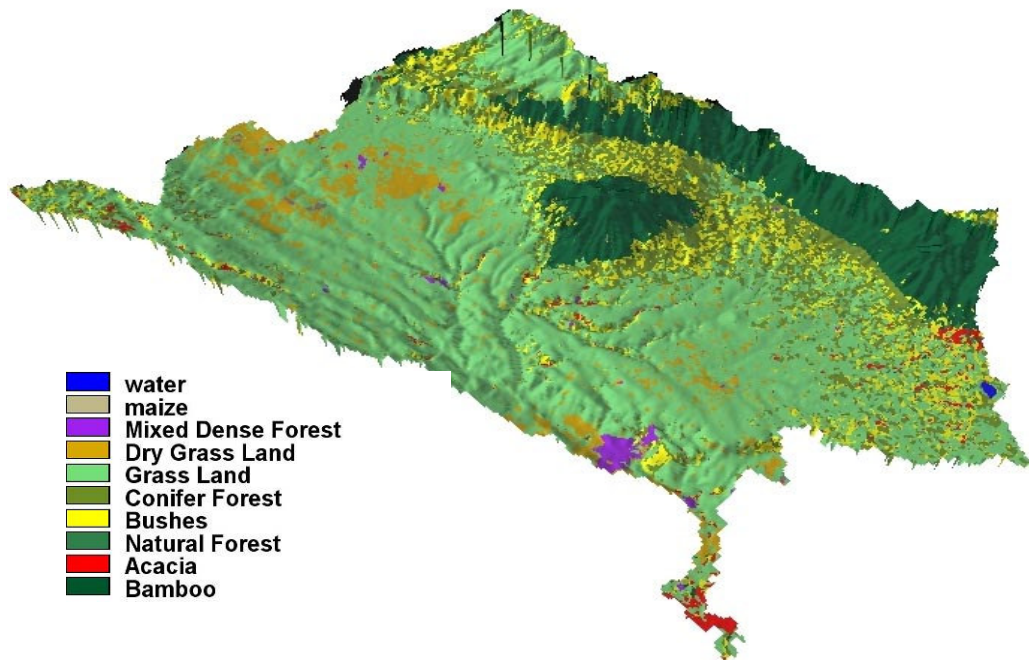
Figure 5 Landcover map produced from ASTER satellite image acquired in March 2003 draped on SRTM DEM

The main farming systems in this area are rain fed agriculture of maize, wheat, beans and vegetables on the eastern and north eastern plateau and the escarpments.

3.2.   Climate

Due to the altitudinal differences, there are diverse climatic conditions found in the basin (Muthuwatta, 2004). Naivasha basin has a typical tropical climatic condition with a   minimum temperatures of 8^oC in July, while the highest temperature occurs in March that reaches approximately up to 30^oC (Al-Sabbagh, 2001).
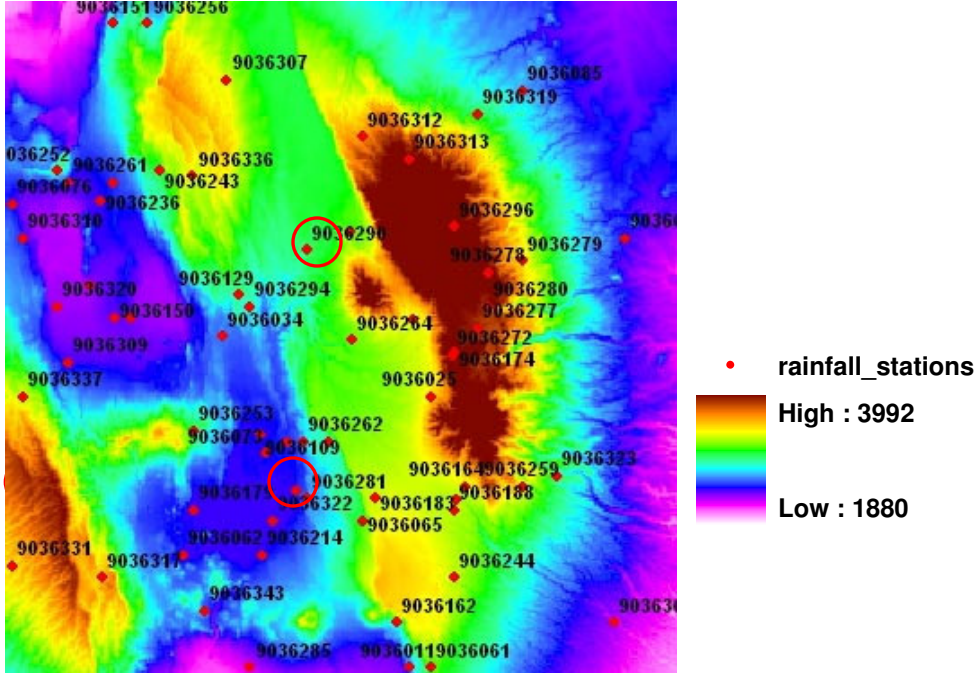
Figure 6 Rainfall stations in Naivasha area
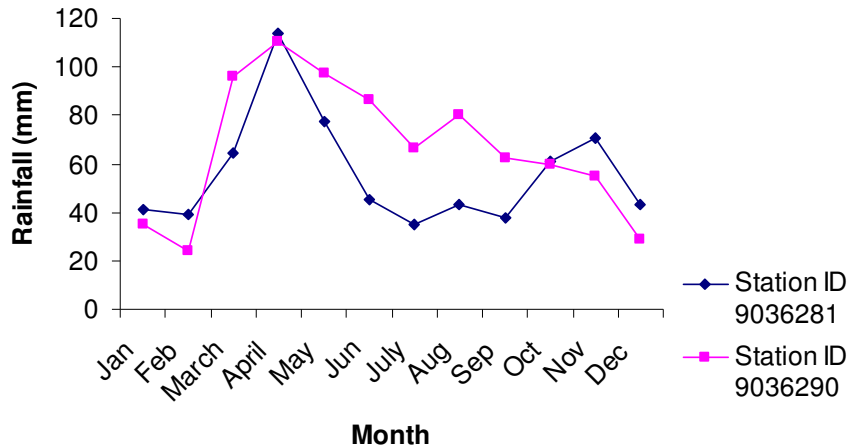
Figure 7 Average yearly rainfalls of two stations

Naivasha basin receives high rainfall peaks from April to May that reaches about 120mm per month and from mid October to December about 70mm per month. Rainfall records encircled in figure 6 and plotted in figure 7 show that, the highlands of the basin get high rainfall distribution throughout the year. The potential evapotranspiration in this catchment is about twice the annual rainfall in the semi arid area while in the upper basin humid areas, rainfall exceeds potential evapotranspiration in most parts of the year.

SRTM DEM SUITABILITY IN RUNOFF STUDIES

3.3.   Drainage Characteristics

The drainage pattern of Malewa basin is dendritic and the density varies from very low in the valley plane area to very high towards the drainage divide. Turasha, Wanjohi, Nandarasi, and Engere are the main tributaries of Malewa River.
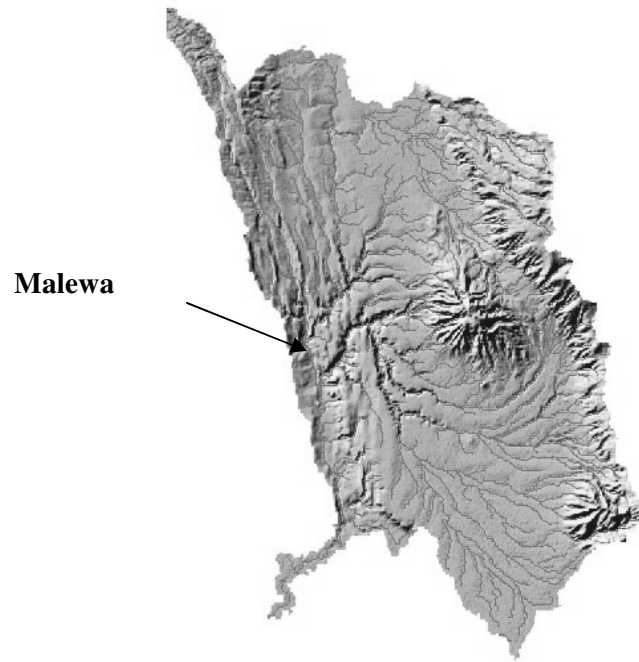
Malewa

Figure 8 Drainage Pattern of Malewa Basin

4. SRTM DEM Assessment

4.1. SRTM DEM Generation

The Shuttle Radar Topography Mission (SRTM) is a collaborative mission made by the National Aeronautics and Space Administration (NASA), the National Imagery and Mapping Agency (NIMA), the German Space Agency (DLR) and Italian Space Agency (ASI), to generate a near-global digital elevation model (DEM) of the Earth using radar interferometry technique (http://www2.jpl.nasa.gov/srtm/). SRTM DEM is the first globally uniform digital elevation model that is generated using Synthetic Aperture Radar Interferometry (SAR interferometry or InSAR) technique.

Figure 9 Single Pass InSAR DATA Acquisition by the Space Shuttle Endeavour

SAR is able to reliably map the Earth's surface and acquire information about their physical properties, such as topography, morphology, roughness, and the dielectric characteristics of the backscattering layer. As the spaceborne SAR systems operate in the microwave (cm to dm wavelength) regime of the spectrum and provide their own illumination they can acquire information globally and almost independently of meteorological conditions and sun illumination. Radar wavelength bands are described by codes such as (L-band) or (C-band) that came into use during World War II for security purpose (Mather, 2004). The commonly used wavelengths are 2.5-3.75cm (X-band), 3.75-7.5cm (C-band), and 15-30cm (L-band). SRTM used X-band and C-band radar with centre wavelengths of 3.1cm and 5.6 cm respectively (Bamler,

1999). In general, particles smaller than one forth   (1.4cm) to half (2.8cm) of the centre wavelength of C-band do not backscatter but instead allow the radiation to pass by. Cloud droplets, even falling raindrops are far smaller than the 5.6 cm wavelength of the SRTM radar signal. This gave SRTM the capability to "look through" clouds and rain (Mather 2004). The InSAR is primarily used to acquire data that can be processed and calibrated to produce digital elevation models of a target area (Mather, 2004). InSAR uses the differences in phase between the signals received by two separate SAR antennas to construct a pixel-by-pixel map of ground surface elevations. In the so called single pass interferometry the two antennae are carried by a single platform whereas in repeat pass interferometry the signals are measured from different orbits. SRTM used single-pass interferometry approach. A single-pass interferometric configuration has a number of advantages over repeat-pass system. Firstly, the target area is imaged under virtually identical condition, so that backscattering from the targets to the two antennas is effectively the same. If a repeat-pass system were used then the backscattering characteristics of the target may have changed between the dates that the two SAR images were collected, and the degree of correlation between the two images would there be reduced that leads to reduced level of accuracy in height determination (Mather 2004). SRTM consisted of a specially modified radar system called Spaceborne Radar Laboratory that flew onboard the Space Shuttle Endeavour during an 11-day mission in February of 2000. Two radars were carried during the mission. NASA re-used the C-band system from its SIR-C experiment of 1994 and the German Space Agency (DLR) contributed X-band radar (Rabus, 2003). For each instrument, one antenna was placed in the shuttles cargo and the other was located at the end of a 60m mast that was deployed after the shuttle reached its orbital altitude of 233km.

The dual antenna system of SRTM provided the best elevation data ever available at a near-global scale to generate the most complete high-resolution digital topographic database of the Earth. The SRTM swaths extended from about 30 degrees off-nadir to about 58 degrees off-nadir from an altitude of 233 km, and thus were about 225 km wide. SAR's channels measure slightly different ranges *R1* and *R2* for any ground point (De Ruyver, 2004) . Hence, the corresponding image pixels, although equally 'bright', exhibit different phase. The phase difference (or interferometric phase) of two corresponding pixels is related to the range difference (parallax) via

$$f = p\ 2\ p\ (R1 - R2)\ l \qquad \textbf{Equation 1}$$

Where *p = 2* for repeat-pass and *p = 1* for single-pass interferometry, respectively. This phase is measured pixel-wise by co-registration of the two SAR images to within a small fraction of a pixel and complex conjugate multiply of the registered images. Every pixel of the resulting interferogram carries phase, i.e. parallax, information –even in areas of low or no contrast. From this two dimensional phase field the Digital Surface Model (DSM) of the imaged area can be computed after the *2p* ambiguity of the phase measurement has been removed by a procedure called phase unwrapping (Bamler, 1999).

There are two types of data from the SRTM mission. One was processed in a systematic fashion using SRTM Ground Data Processing system (GDPS) supercomputer at Jet Propulsion Laboratory and was formatted according to the Digital Terrain Elevation Data (DTED) specification for delivery to NIMA. The GDPS data includes only the DEM and is referenced to the WGS84 Geod (Sun, 2003). The other is the PI Processor data, which was processed using the algorithm and hardware being developed for GDPS. These data are for Principal Investigators selected by NASA under the Solid Earth and Natural Hazards program and other special purposes. These data were not formatted according to DTED specification, and the terrain height data is relative to the WGS84 ellipsoid (http://edcs9.cr.usgs.gov).
SRTM Digital Terrain Elevation Data (DTED) is a uniform matrix of elevation values indexed to specific points on the ground. The horizontal datum is the World Geodetic System 1984 (WGS84) and the vertical datum is mean sea level as determined by the WGS84 Earth Gravitational Model (EGM 96) Geod (Shuttle Radar Topography Mission DTED, http://edc.usgs.gov/products/).

After NASA/JPL completes the raw data processing, NGA performs quality assurance checks on the JPL SRTM data and its contractors perform several additional finishing steps. Spikes and wells in the data are detected and voided out if they exceed 100 meters compared to surrounding elevations. Small voids are filled by interpolation of surrounding elevations. Large voids are left in the data. Water bodies are depicted in the SRTM DTED. The ocean elevation is set to 0 meters. Lakes of 600 meters or more in length are flattened and set to a constant height. Rivers that exceed 183 meters in width are delineated and monotonically stepped down in height. Islands are depicted if they have a major axis exceeding 300 m or the relief is greater than 15 m. The data are processed in one degree by one degree "cells". The edges of each cell are matched with the edges of adjacent cells to assure continuity Post processed SRTM data are organized into individual rasterized cells, or tiles, each covering one-degree by one degree in latitude and longitude. Sample spacing for individual data points is either 1 arc-second or 3 arc-seconds, referred to as SRTM-1 and SRTM-3, respectively. The resolution of the DEM during processing is 1 arc second. 1 arc second is 1/3600 of a degree. At the Equator a 1 arc second pixel in the longitude direction is approximately equal to 1 arc second in the latitude direction. An arc second equates to 1/60 of a nautical mile (1852/60 = 30.8667 meters). An arc-second of latitude remains constant while the arc-second of longitude decreases as away from the Equator to the poles. To convert the arc-second into meters the cosine of the longitude is multiplied by 30.8667, since one arc-second at the equator corresponds to roughly 30 meters in horizontal extent.

SRTM-1 data are sampled at one arc-second of latitude and longitude and each file contains 3601 lines and 3601 samples. The rows at the north and south edges as well as the columns at the east and west edges of each cell overlap and are identical to the edge rows and columns in the adjacent tiles.

SRTM-3 data are sampled at three arc-seconds and contain 1201 lines and 1201 samples with similar overlapping rows and columns. This organization also follows the DTED convention. Unlike DTED, however, 3 arc-second data are generated in each case by 3x3 averaging of the 1

arc-second data – thus 9 samples are combined in each 3 arc-second data point. Since the primary error source in the elevation data has the characteristics of random noise this reduces that error by roughly a factor of three (http://edc.usgs.gov/products).

Initial comparison between 3 arc second SRTM and older GTOPODEM (Global Topography 30 arc second DEM) of the USGS showed that the resolution of SRTM DEM is a significant improvement and will be especially useful in areas where limited topographic data are available (Reimold, 2004).

4.2.   SRTM DEM Mission Accuracy

According to the mission specification SRTM-3 DEM has an absolute horizontal and vertical accuracy of 45m and <=16m respectively. The relative accuracy attains up to 60m horizontally and <=10m vertically. These figures give only a general impression about the overall global accuracy of the DEM. The accuracy would vary depending on the steepness of the landscape and the land cover conditions of the area of interest.

4.3.   Raw SRTM DEM Quality

To understand accuracy and quality of Digital Elevation Models derived by SRTM it is necessary to illustrate possible error sources (Koch, 2000) The uncertainties influencing the data can be divided into three groups. The first one characterizes the InSAR parameters during data acquisition: baseline length and orientation, phase, slant range and position of the antenna (Zink, 1999). The second group deals with the processing steps after acquiring the raw data and the last group contains the influences of vegetation, land cover etc. InSAR DEM elevations are with respect to the reflective surface which may be vegetation, man-made features or bare earth and do not represent the actual ground surface elevation. These features cause positive bias on the elevation information from the DEM. Moreover, according to (Sun, 2003), however, InSAR can provide DEM over large area, but has inherent speckle noise. Consequently, SRTM DEM may exhibit typical radar artefacts including scattered voids due to shadowing effects and poor signal returns over some terrain, as well as occasional phase unwrapping errors (http://edc.usgs.gov/products/elevation/srtm.html)
In this study the overall uncertainties resulted form these factors will be assessed. Some of the limitations of SRTM DEM can be assessed by visual inspection. As shown in figure 6 data void due to shadows (the Longonot Caldera, in figure 10) and water bodies (Lake Naivasha in the same figure) can be clearly seen in the raw DEM.
Other limitations like blunders and land cover effects can only be evaluated using other source of elevation information. In the following subsections geodetic triangulation ground control points, GPS field data, and ASTER DEM data sources are used to evaluate the raw SRTM DEM.
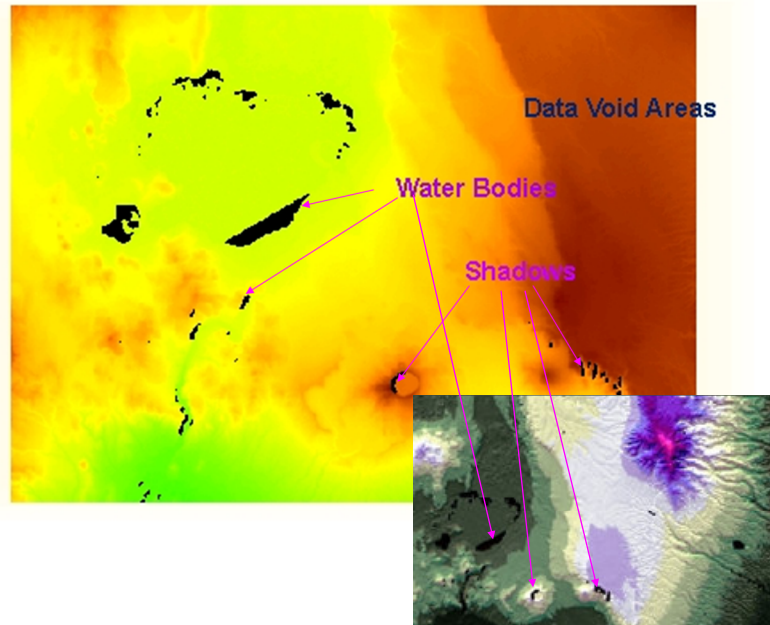
Figure 10 Data voids in raw SRTM DEM of Naivasha basin

4.4.   Vertical Accuracy Assessment of the Raw SRTM DEM

The vertical accuracy of the raw SRTM DEM is assessed by making a comparison with the automatically generated ASTER DEM. The two DEMs are compared with a selected set of geodetic Triangulation Ground Control Points (Tri.GCPs) independently. The ground control points are set by the Kenyan Survey Department with high order triangulation technique. The order of accuracy of this Tri.GCPs is in the order of centimetres. Since, some of the control points are found replaced by new GPS elevation values with no evidence about the accuracy of the GPS used, only the unaltered points are considered in this assessment. Even though this data source has an advantage in providing absolute elevation assessment, the level of confidence of the limited number of points should be taken into consideration. Therefore, an additional comparison is made using GPS points collected in the field. The GPS used was Garmin eTrex Summit occupied with a barometric altimeter accuracy of 10feet (3.048m) and horizontal accuracy of 15m. Even though, this is a reasonable accuracy, locating the Tri.GCPs in the field to calibrate the GPS was problematic since almost all of the marks were removed.

As (Li, 1991) proposed, the confidence level with respect to the check points can be evaluated by:

$$R(e) = \frac{1}{\sqrt{2(n-1)}} *100 \quad \textbf{Equation 2}$$

Where R(e) represents the confidence value in % and n is the number of check points used in the accuracy test. As an inverse example, if we wish to obtain a SD confidence value of 5%, we need

about one hundred check points. If we used 28 check points, we would reach a 20% confidence value (Cuartero, 2004).

4.4.1. 3D Transformation

The four elevation information sources have different projection, ellipsoid, and datum. To make the z value comparison between these sources the geographic information has to be transformed into the same ellipsoid and datum, i.e. a 3D transformation given that vertical datum is also transformed. The original projection information from the sources is detailed below:

 SRTM DEM
        Projection   Geographic lat/lon
        Horizontal Datum World Geodetic System 1984 (WGS84)
        Vertical Datum is the mean sea level as determined by the WGS84
ASTER DEM
        Projection UTM, zone 37 south
        Horizontal Datum World Geographic System 1984 (WGS84)
        Vertical Datum WGS84

Triangulation Ground Control Points (Tri.GCPs)
        Projection UTM, zone 37 south
        Horizontal Datum Arc 1960
        Vertical Datum Arc 1960
        Spheroid Clarke 1880

GPS Collected Points
        Projection UTM, zone 37 south
        Datum Arc 1960
All the z values are transformed to UTM coordinate system and WGS84 vertical and horizontal datum using the ERDAS 8.7 functionality, so that they have the same reference. This procedure recalculates the original z value of the Tri.GCPs and the GPS points while others remain the same.
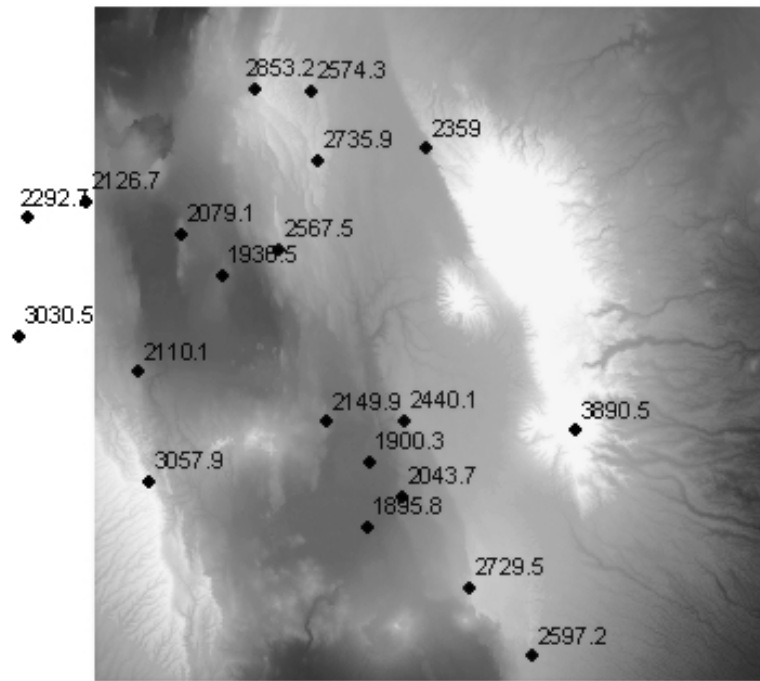
Figure 11 Geodetic Triangulation Ground Control Points

As shown in Table 1 the RMSE of the raw SRTM DEM compared to the selected Tri.GCPs is calculated 19.71m, which is 3.71m more than the absolute RMSE given by the mission. Nevertheless, this is when the highly erroneous Tri.GCP marked in table 1 is included

Table 1 Raw SRTM DEM and Triangulation Ground Control Points statistical comparison

Elevation a.m.s.l. (m)		Diff	Diff^2	Diff^2
Tri.GCPs	**SRTM DEM**			
1895.8	1896	0.04	-0.2	0.04
1900.3	1912	136.89	-11.7	136.89
2043.7	2049	28.09	-5.3	28.09
2149.9	2125	620.01	24.9	620.01
2440.1	2454	193.21	-13.9	193.21
2567.5*	2526	1722.25	41.5	
2729.5	2734	20.25	-4.5	20.25
RMSE			**19.71**	**12.90**

in the evaluation. When this check point is disregarded the accuracy of the DEM is found to be within the mission accuracy as calculated (RMSE 12.90m) in the same table.

The confidence level is calculated 71% when the Tri.GCPs are applied. The accuracy test is also made using GPS points collected during fieldwork. When corresponding points from the raw DEM are compared with 272 GPS points the RMSE is 25.31m. This value is much higher than the one calculated by using the Tr.GCPs. This shows that the error from the GPS has propagated

in the calculation of the differences. In addition, there is a probably that some points may shift horizontally and lay on vegetated area on the raw DEM. Each grid cell in the DEM reads a single elevation value throughout the 90m length. This may not represent the actual elevation information in steep areas where high elevation difference can be found within 90m horizontal distance that can result in high deference in elevation when compared to GPS point located in such kind of terrain.   The confidence level when the GPS data is used is increased to 96%, ($R(e)$=4%) low $R(e)$ value indicates high dependability in the assessment).

y = 0.9951x
R^2 = 0.9988
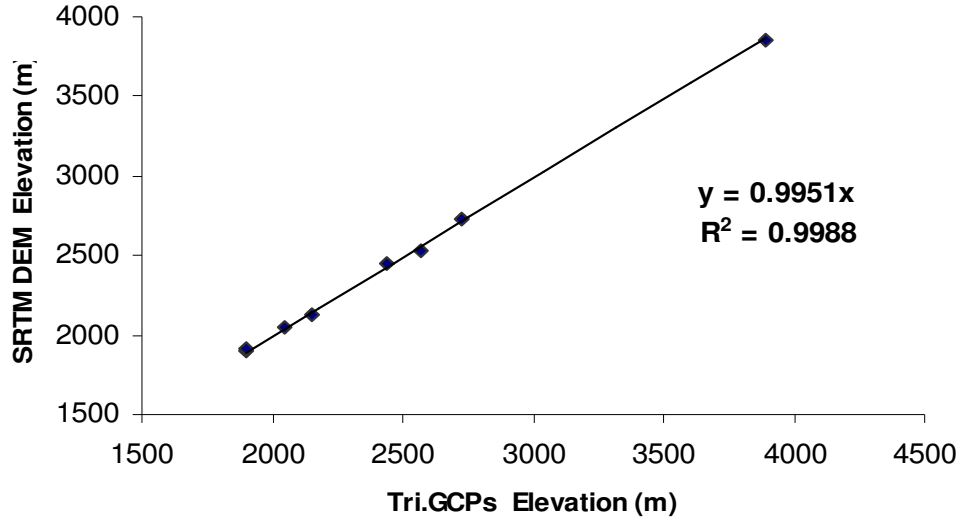
Figure 12 Correlation of points from Raw SRTM DEM and Tr.GCPs

In figure 12 the triangulation control points and corresponding values from the SRTM DEM has got 0.9979 correlations. When GPS points are plotted against the raw DEM values the correlation found is 0.9939 (figure 13). However, as illustrated in table 1 and in figure13 (encircled in the scatter plot) at higher elevations SRTM DEM gives an elevation difference that ranges from -13.9 to 24.9m.
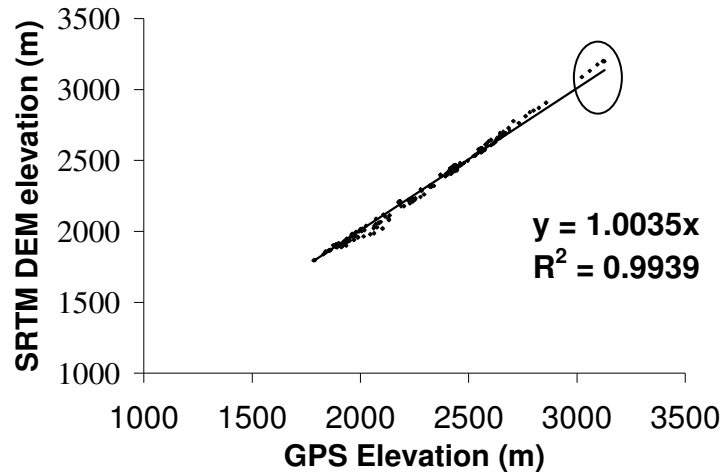
Figure 13 Correlation of points from Raw SRTM DEM and GPS points

These high differences are the effects of the unavoidable sub pixel elevation difference and shift of GPS points in the DEM. The SRTM DEM is affected by the steepness of the landscape. As it is explained by (Jacobsen, 2002) it has less accuracy on steep areas than flat areas when the terrain inclination in view direction is greater than incidence angle plus shadow and subpixel elevation difference is not considered when comparing with the control and GPS points.

4.4.2. Horizontal Accuracy

Horizontal error is more difficult than vertical error to assess in a coarse resolution DEMs. This is because of the difficulty to locate distinctive topographic features necessary for such tests. In this study the horizontal shift is assessed using a manually digitized drainage line from a 15 meter resolution ASTER image. A drainage line is delineated from the raw SRTM DEM and overlayed on the manually digitized drainage line. From this approach it can be seen that the matching of these two drainage maps is greatly influenced by the accuracy of georeferencing the satellite image from which the manual digitizing is done and the way the raw DEM is imported to the working software. In this study the raw ".hgt" SRTM DEM is imported by ENVI and saved as "tiff" format. In doing so care should be taken to correct the upper left corner of the raw DEM since the default coordinate value assigned by ENVI is wrong and creates a big mismatch with other maps form different sources. By default ENVI assigns 35°59′55.5″E, 00°00′1.5″N for the upper left corner of Naivasha area SRTM DEM, which is in fact 36°00′00″E, 00°00′00″N in geographic lat/lon coordinate. Unless a close look is made and corrected with the accurate corner values while importing and exporting the DEM form one package to another and reprojecting the DEM to a different projection and datum, the shift found at last could be beyond the acceptable limit. If care is exercised in these procedures   the inherent shift in the raw SRTM DEM is within one pixel as it is assessed in this study. This one pixel shift improvement is found to be labour

intensive and has shown no significant hydrological effect. Trying to adjust this small shift may distort the whole DEM unless it is assisted by an accurately manually digitized drainage line from a satellite image with high resolution and very high georeferencing accuracy.

4.5. Advanced Spaceborne Thermal Emission and Reflection Radiometer (ASTER) DEM Accuracy

The Advanced Spaceborne Thermal Emission and Reflection Radiometer (ASTER), on board the NASA's TERRA satellite, is one of the satellites which have a capability of back looking capability.   TERRA-ASTER was launched in December 1999 and is a quite recent sensor, which provides along-track near-IR stereoscopic images. ASTER covers a wide spectral region with 14 bands from visible to the thermal infrared with high spatial, spectral and radiometric resolution. The spatial resolution varies with wavelength; 15m in the visible and near infrared (VNIR, 0.52 to 0.86 µm), 30m in the short wave infrared (SWIR, 1.60 to 2.43µm), and 90m in the thermal infrared (TIR 8.125 to 11.65µm). From band 3N (named for "nadir") and 3B (named for "back looking") at a back ward angle of approximately 28 degrees at 15 m spatial resolution of the VNIR sensor produce a stereo pair for each ASTER image. As mentioned in the preceding sections, ENVI ASTER-DTM has a special facility of automatic DEM generation from ASTER image. The basic principle behind the DEM extraction using ENVI ASTERDTM   is the known parallax effect. An object is looked from two different angles and thus can obtain its third dimension. AsterDEM converts 3N and 3B bands into a pair of quasi-epipolar images, which have a pixel displacement in the satellite flight direction proportional to the pixel elevation. A cross-correlation method is used to determine this displacement, which in turn is transformed into elevation values (SulSoft, 2002).Table 2 shows results of some researches about accuracy in DEM derivation and derived DEM from ASTER images. Some studies show that the accuracy may also be affected by the software in use to extract the DEM as shown in table 2b.

Table 2 (a) Some works about ASTER-DEM accuracy determination and (b) Error statistics for DEMs adapted from "ACCURACY OF DEM GENARATION FROM TERRA-ASTER STEREO DATA" (by Cuartero A. ,A.M. Felicísimo, and F.J. Ariza, 2004)

Date	Reference	RMSE[a] (m)	Method[b]
2001	Tourin & Cheng	7.9	6 DGPS check points
2002	Kääb et al.	18 - 60	Photogrammetrically derived DEM
2002	Hirano et al.	7 - 15	Different methods

[a] Root Mean Square Error.
[b] Method by which RMSE has been calculated.

(a)

Source data	Software	Error (m)			
		ME [a]	RMSE [b]	SD [c]	CI [d]
TERRA-ASTER	Ortho Base	9,7	34,8	28,8	±2,3
	Ortho Engine	-1,5	12,6	12,5	±1,0
Cartographic		-1,1	7,9	7,8	±0,6

[a] Mean Error
[b] Root Mean Square Error
[c] Standard Deviation
[d] Confidence Interval for SD (95%)

(b)

When the extracted DEM is compared with the Tri.GCPs as shown in table 3 the RMSE is
21.29m and 15.55m when the extremely erroneous point is disregarded in the calculation of the
RMSE. This shows that the RMSE of ASTER DEM when the Tri.GPSs are used is greater than
the raw SRTM DEM. This comparison is also assisted by the GPS points and scatter plots. A
RMSE of 35.45m is found in comparing the ASTER DEM with GPS points.

Table 3 ASTER DEM and Triangulation Control Points statistical comparison

Elevation a.m.s.l. (m)		Diff	Diff^2	Diff^2
Tri.GCPs	**ASTER DEM**			
1895.8	1889	278.89	6.8	46.24
1900.3	1917	18.49	-16.7	278.89
2043.7	2048	894.01	-4.3	18.49
2149.9	2120	193.21	29.9	894.01
2440.1	2454	1722.25	-13.9	193.21
2567.5*	2526	20.25	41.5	
2729.5	2734	19.92	-4.5	20.25
RMSE			**21.29**	**15.55**
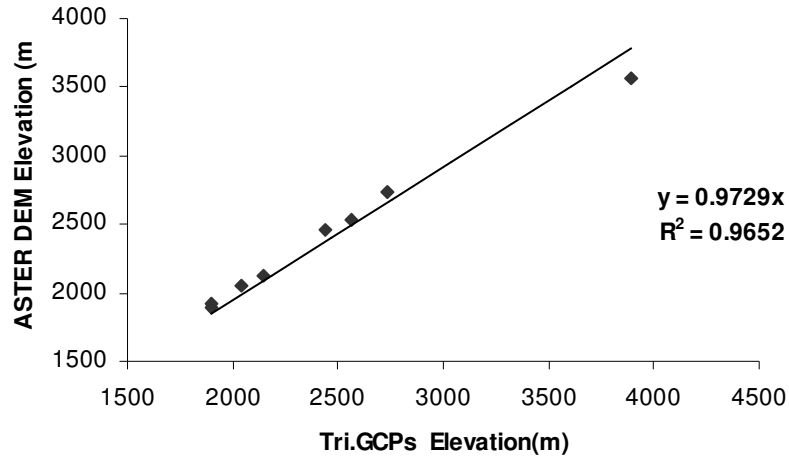
Figure 14 Correlation of points from ASTER DEM and TR. GCPs
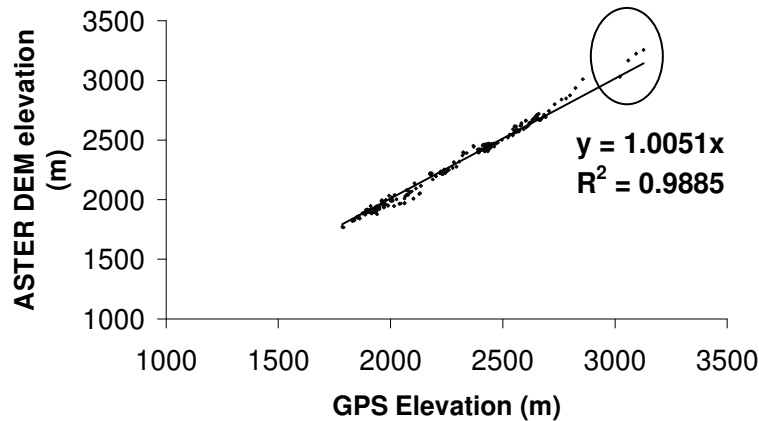
Figure 15 Correlation of points from Raw ASTER DEM and GPS points

From figure 13 and figure15 at higher elevations (points encircled) both SRTM DEM and ASTER DEM gave higher elevation values than the GPS records. These points lie on the steep area that causes high elevation difference for a small horizontal shift as the GPS used has a horizontal accuracy of ±15m in addition to the effect of subpixel elevation differences in the DEM.

4.6. Raw SRTM DEM and ASTER DEM Comparison

Comparisons made in the previous sub sections are made at discreet points spread all over the DEMs. To visualize the trend of the surface in the two DEM sources a profile is put up together from a layer stack of ASTER and SRTM DEMs. A section is made along the steepest areas to assess major differences that encountered in these areas in the RMSEs.

ASTER DEM was extracted in 30m horizontal resolution and resampled to 90m resolution so that it has the same level of detail as the raw SRTM DEM. However, as it is shown in figure 18 SRTM DEM missed a considerable detail of the terrain both in flat and steep areas. In the left side, ASTER DEM gives lower elevations than SRTM DEM and in the right side it gives higher values. This shows that ASTER DEM has some inclination as illustrated in figure 16 towards the west during its generation in ENVI-ASTER DTM software. This could be because of poor distribution of control points or the inclination of the image during acquisition.
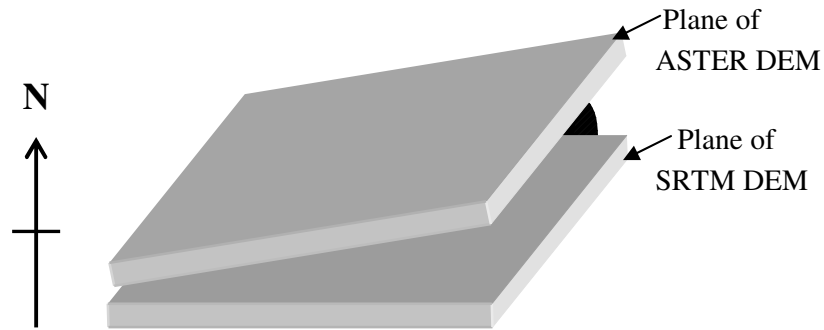
Figure 16 Exaggerated representation of ASTER DEM generated in ENVI-ASTER DTM inclination relative to SRTM DEM
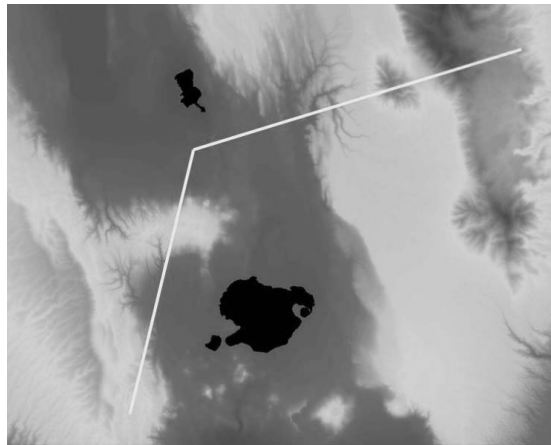
Figure 17 Section line along steep areas of ASTER and SRTM DEMs layer Stack of the profiles in figure 18
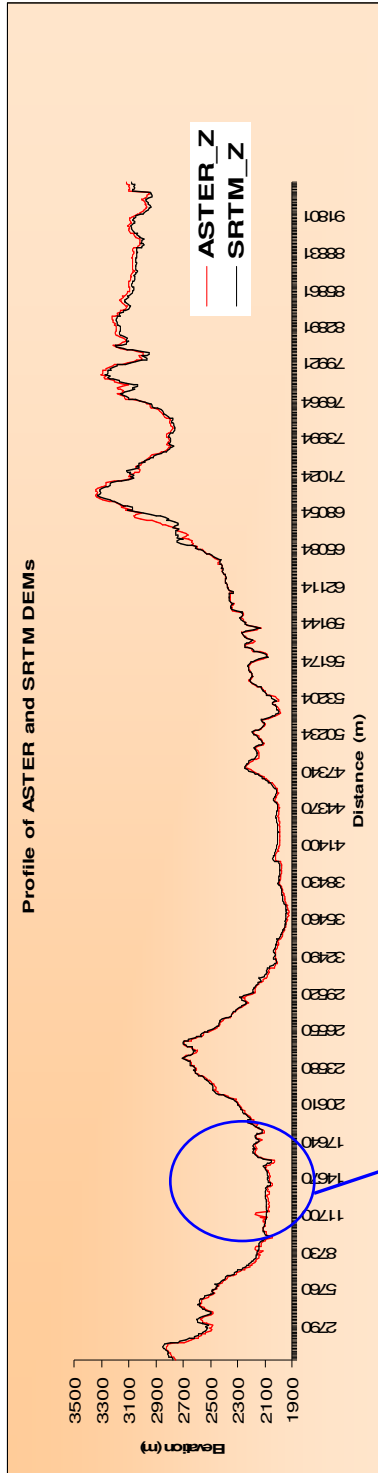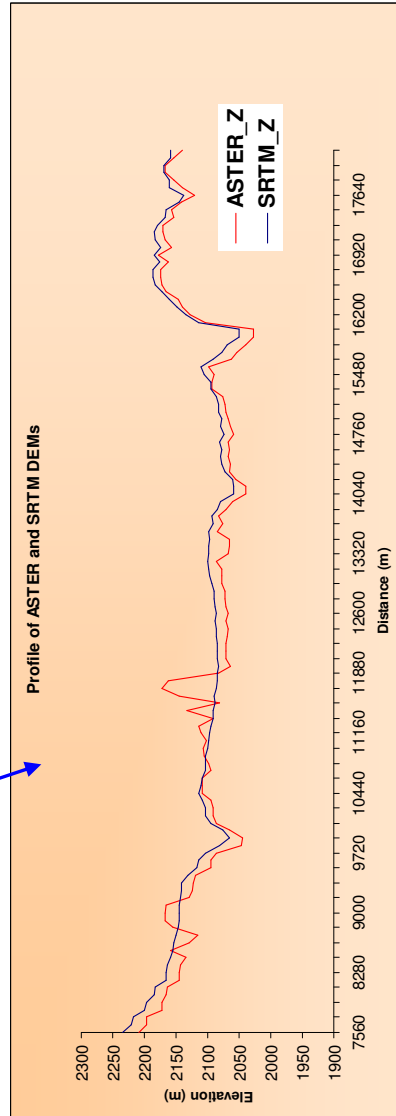
Figure 18 (a) Profile of ASTER and SRTM DEMs in steep areas. (b) Loss of detail in SRTM DEM compared to ASTER DEM
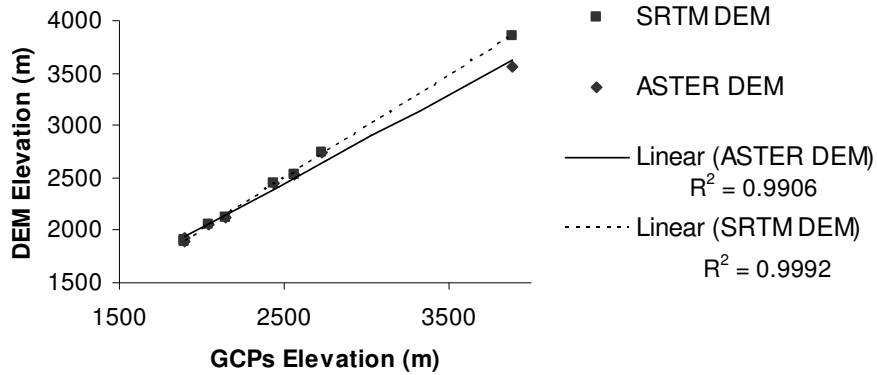
Figure 19 ASTER and SRTM DEMs compared to Tri.GCPs

Correlation and RMSE calculations depend on the number of check points considered for the comparison and the accuracy of the point values. ASTER DEM does not cover the whole area covered by SRTM DEM. Therefore, only points which intersect with both DEMs are considered in the comparison. (Table 4)

Table 4 Triangulation Ground Control Points used to compare Aster and Raw SRTM DEM

	Tri. Gaps	ASTER DEM	Raw SRTM DEM
1	1895.8	1889	1896
2	1900.3	1917	1912
3	2043.7	2048	2049
4	2149.9	2120	2125
5	2440.1	2454	2454
6	2567.5*	2526	2526
7	2729.5	2734	2734
8	3890.5	3559	3847

As shown in the preceding graphs and tables it can be concluded that SRTM DEM has high correlation to the high accuracy of the triangulation ground control points and the GPS data than ASTER DEM. However, ASTER DEM gives much more ground feature details which are smoothened in the SRTM DEM. This is the influence of the SRTM DEM averaging from 30m to 90m horizontal resolution and the vegetation cover effect. It should also be proved that if optical parallax is giving more terrain detail than interferogram parallax.

5. SRTM DEM Quality Improvement

5.1.　　　Vegetation Cover Removal

Two approaches are applied to remove the vegetation cover form the raw DEM. The first is to use field collected vegetation cover data to create vegetation height attribute map from landcover detail map applying Ilwis map calculation. The landcover map is created using a combined approach of supervised classification, Normalized Difference Vegetation Index (NDVI) and Slicing in Ilwis software from a mosaic of ASTER image acquired in March 2003.
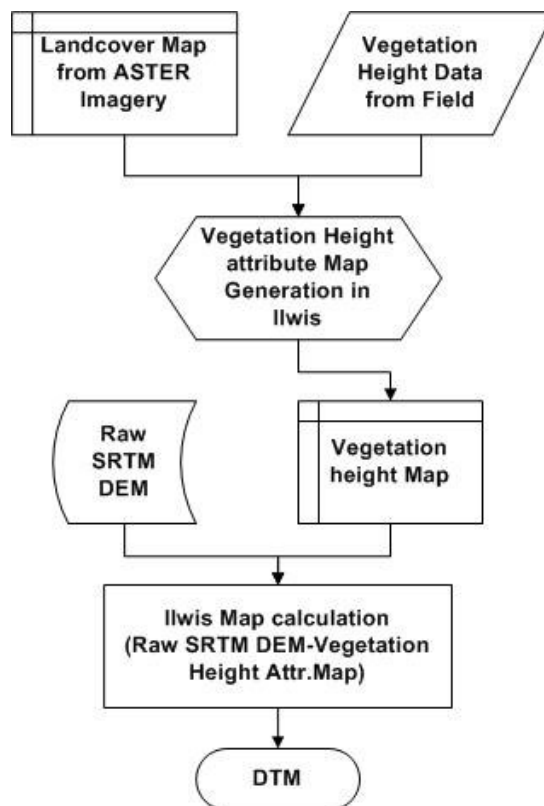
Figure 20 Flowchart of vegetation cover removal from SRTM DEM in Ilwis

With regard to landcover map preparation much effort is made to make it a good representative of the area applying full human knowledge   in the classification. Subtracting the vegetation height map from the raw DEM gave a realistic output of DTM without modifying the discontinuities and the landscape detail information. However, for big catchments with inaccessible areas this is uneconomical approach, as it needs a huge amount of field data

collection and image interpretation. Since the information in the original raw DEM is least affected by this processing, it is used as a validation to the DTM outputs from the automatic vegetation cover filtering applied that will be discussed in section 5.2.

(a)

(b)

(c)
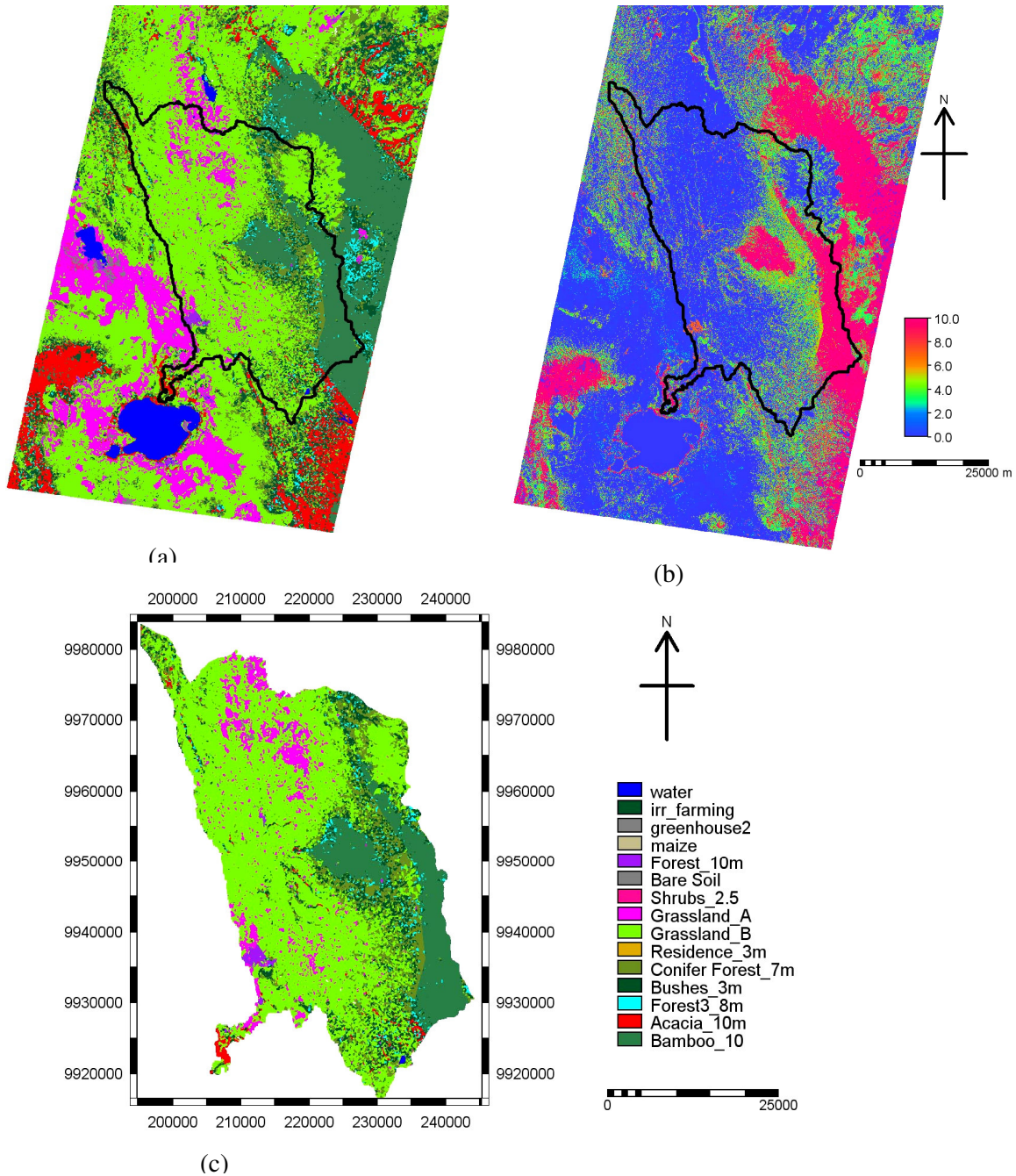
Figure 21 (a) Landcover map of Naivasha area made from ASTER Image acquired in March 2003, (b) Vegetation height attribute map generated from the landcover map, and (c) Landcover map of Malewa basin with approximate vegetation height

Table 5 Distribution of Landcover in Malewa Basin

Landcover Type	Area (%)
water	0.1
Irr. farming	0.1
Forest-10m	0.6
Bare Soil	0.1
Grassland-A	6.5
Grassland-B	57.3
Conifer Forest-7m	12.2
Bushes-3m	8.3
Forest -8m	1.7
Acacia 10m	1.1
Bamboo-10m	12.1

5.2.   Filtering the Raw SRTM DEM

Points which are located on the top of vegetation surface also can be removed using a carefully selected filtering sequence of steps (strategy). The term filter can have various meanings (Pfeifer, 2001). On one hand it can mean the filtering (smoothing) of random measurement errors, on the other hand it is stands for filtering (elimination) of gross errors, which is also a classification. Unless stated, otherwise we use the term in its second meaning. According to (Jacobsen, 2002) there are several methods or procedures for filtering. Among them are:

- Spline approximation
- Shift invariant filters
- Linear prediction
- Morphological filters

Although morphological filters are the most frequently used, linear prediction, also named as Linear Least Squares Interpolation, is a very robust methodology for digital surface model filtering. (Maire, n.d.) also found what they called a very good result using a non stationary Bayesian filter to remove noise and small artefacts which spread through the SAR DEM while preserving structures and information content, nevertheless, large artifacts cannot be filtered and some artifacts remain.

In SCOP++ linear prediction filtering method is available. Here it is applied via summation of surfaces; that is the cumulative surface consists of a sum of elementary surfaces around the reference points. The elementary surfaces are rotating bell curves which allow a statistical analysis. To apply this filtering procedure the SRTM DEM raster map is imported into SCOP++ as xyz point data since, the filtering and interpolation procedure are based on point data. The method and results are explained in the next sections.

Using only visual interpretation of the filtered DEM do not guarantee the quality improvement applied on the DEM since, each pixel value may be raised or lowered even could be doubled by

the filtering procedure applied. A comparison is made with the DTM found from landcover attribute map elimination to see the extent of height removal from the original DEM. The removal of spikes and blunders are assessed using the drainage extraction and comparison.

5.2.1.   The Programme SCOP++

SCOP++ is a commercial software package, which is designed for interpolation, management and visualization of digital terrain data, with special emphasis on accuracy (Vienna University of Technology, 2002-2003). It is   a joint development and continues improvement of the company Inpho, Germany, and remote sensing of the Vienna University of Technology, Austria. The software involves a high accuracy DTM interpolation by the method of linear prediction. For the description of the terrain surface it uses a subdivision into rectangular interpolation areas of constant size (Computing Units). The surface in each rectangular piece is described by a mathematical function.

To classify off terrain and into terrain points from different filtering strategy are given in SCOP++. Here we use a hierarchic robust filtering technique described in (Kraus, 1998). In addition to its complexity, the default filtering strategies set in SCOP++ are for LIDAR point cloud. The hierarchic robust filtering strategy employs four different processing steps referred to as thin out, interpolate, filter and sortout. As (Wagner, 2004) the flexibility in the design of the strategy, combined with possibility to select a number of parameters in each processing step, has the advantage in getting (with exception of few problem areas) satisfactory results for LIDAR data without manual editing. But, for the cases the default strategies offered in SCOP++ not produce satisfactory result, which is the case for SRTM DEM, even experienced interpreters need many working hours to experiment with different filtering strategies and parameter setting. In this study to remove the vegetation cover from the raw SRTM DEM a logical approach is applied considering the very course uniform distribution of the points. A number of trials are ran and compared to the DTM found by Ilwis map calculation, in which vegetation attribute map is used. After each trail a difference map of the run output and the raw DEM is created and the quality improvement and any information losses like discontinuities in the DEM are assessed and the next strategy is readjusted. The four steps can be applied consecutively, in a so many arrangements whereby there are few rules that restrict the order of application or the number of iterations. The decision on which filtering strategy to use best depends on the expert judgment of the human interpreter.

ThinOut refers to a raster based thinning algorithm which lays a grid over the complete data domain and selects one point (e.g. the mean) of each cell. A set of points is reduced in its details, the data is thinned out. The input for this step is a set of points and the output is a reduced set of points

Interpolate is a step by which a terrain model is derived from the current data set by interpolation without differentiating the data points using linear prediction.

In **Filter** also a terrain model is derived , but this time a weight function designed to give low computational weight to points with gross errors those are likely off-terrain points and high weight to likely terrain points is used. The aim is to remove these gross errors completely and build a ground model with the remaining points.

 In **SortOut** step points are compared to a DTM. Only data points within a certain distance from a previously calculated DTM are retained for the next step.

In SCOP++, the iterative robust interpolation, a rough approximation of the surface is computed first. Next, the residuals from the surface to the original points are computed. Each original elevation value is given a weight according to its distance value, which is the parameter of a weight function. A new surface is then recomputed under the consideration of the weights. The point with high elevation value attracts the surface, resulting in a small residual at that point. In contrast a point that has got a low weight will have a little influence on the new computed surface. During these iterations if an oriented distance is above or below certain values, the point is classified as off terrain point and eliminated completely from the interpolation of the new surface.

5.3.   Assessment of the improved DEMs

The DEM is processed using different convenient strategies by trial and error. The protocol files of the different strategies are found in Appendix A. The assessment is made quantitatively and qualitatively.

5.3.1.   Quantitative assessment

Unless a good guess and logical approach is applied the formulated strategy in SCOP++ may do a" cut and fill" on the DEM reducing elevation values of hill tops and raising elevations of narrow valleys. To improve this problem different trials are made for instance like choosing the "lowest" option in the thinout step and no decent for lower values for the weighting function and assigning lower upper tolerance. Nevertheless, since SCOP++ has 20 parameters and four procedures which can have more than 100 different combinations, it needs so many trials and running time to get a best output from it.   The DTM found by subtracting the vegetation height attribute map is used here as a control to check each SCOP++ run outputs and   to readjust the next trial.
From 20 trails made 8 trials gave comparable RMSE when compared to the GPS collected points. The comparison made between the filtered DTMs and the Tri.GCPs gave high RMSE variation as a result of few number of check points compared to the GPS points. The RMSE when the GPS points are used is comparable. These RMSE results in each case are given rank and sum of the ranks is used to judge the quantitative quality of the improved DEMs as shown in table 6.
In this approach the DTM with R*ank 1* in the 3rd column implies the accuracy of the DTM when compared to the Tri.GCPs and *Rank 2* in the 5th column implies the accuracy of the DTM when compared to the GPS points. *Rank1+Rank2* in the 6th column is the sum of *Rank 1* and *Rank 2*.

For instance the Raw DEM has *(Rank 1+Rank 2)* of 3 that shows that in the overall RMSE comparison when Tri.GCPs and GPS points are used has got the highest accuracy. Here, both comparison methods have equal weights. The Tri.GCPs are less in number but has much better accuracy than the GPS points, meanwhile the GPS points give high confidence value because of their sufficiency in number as discussed in section 4.4.

Table 6 Comparison of Improved DEMs with Tri.GCPs and GPS points

	DEM	RMSE Tri.GCPs	Rank 1	RMSE GPS	Rank2	Rank1+Rank2	Remark
1	Raw SRTM DEM	17.94	1	24.98	2	3	
2	DEM9	34.29	5	24.87	1	6	SCOP++ output
3	DEM10	26.44	2	26.16	6	8	SCOP++ output
4	DEM11	29.05	4	25.97	5	9	SCOP++ output
5	DEM14	26.50	3	26.20	7	10	SCOP++ output
6	DEM7	55.10	7	25.89	4	11	SCOP++ output
7	Vegetation Cover Removed DEM	58.99	8	25.68	3	11	No if Tri.GCPs check points used are less
8	DEM8	51.74	6	27.87	9	15	SCOP++ output
9	DEM6	148.73	9	26.91	8	17	SCOP++ output
10	DEM12	149.89	10	28.76	10	20	SCOP++ output

Fewer number of Tri.GCPs are used to assess Ilwis map calculation applied vegetation cover removed DEM, given that it intersects with fewer number of points. Hence, even though, its total rank is 11 it is considered in the qualitative assessment.

This assessment is further supported by qualitative assessment to check loss of information by the applied filtering procedures by taking a section along stream channels. As illustrated in figure 22 SCOP++ filter outputs: DEM8, DEM 6, and DEM 12 are greatly modified by the applied filtering strategy. Stream sections are widened and raised in level considerably. This may influence the hydraulic property of the stream channels in the channel routing stage in the hydrologic modelling runoff generation. These terrain modifications also lowered the accuracy level of the DEMs extremely. Consequently, these three DEMs are rejected from further assessments since they have the least overall quality in the quantitative assessment.
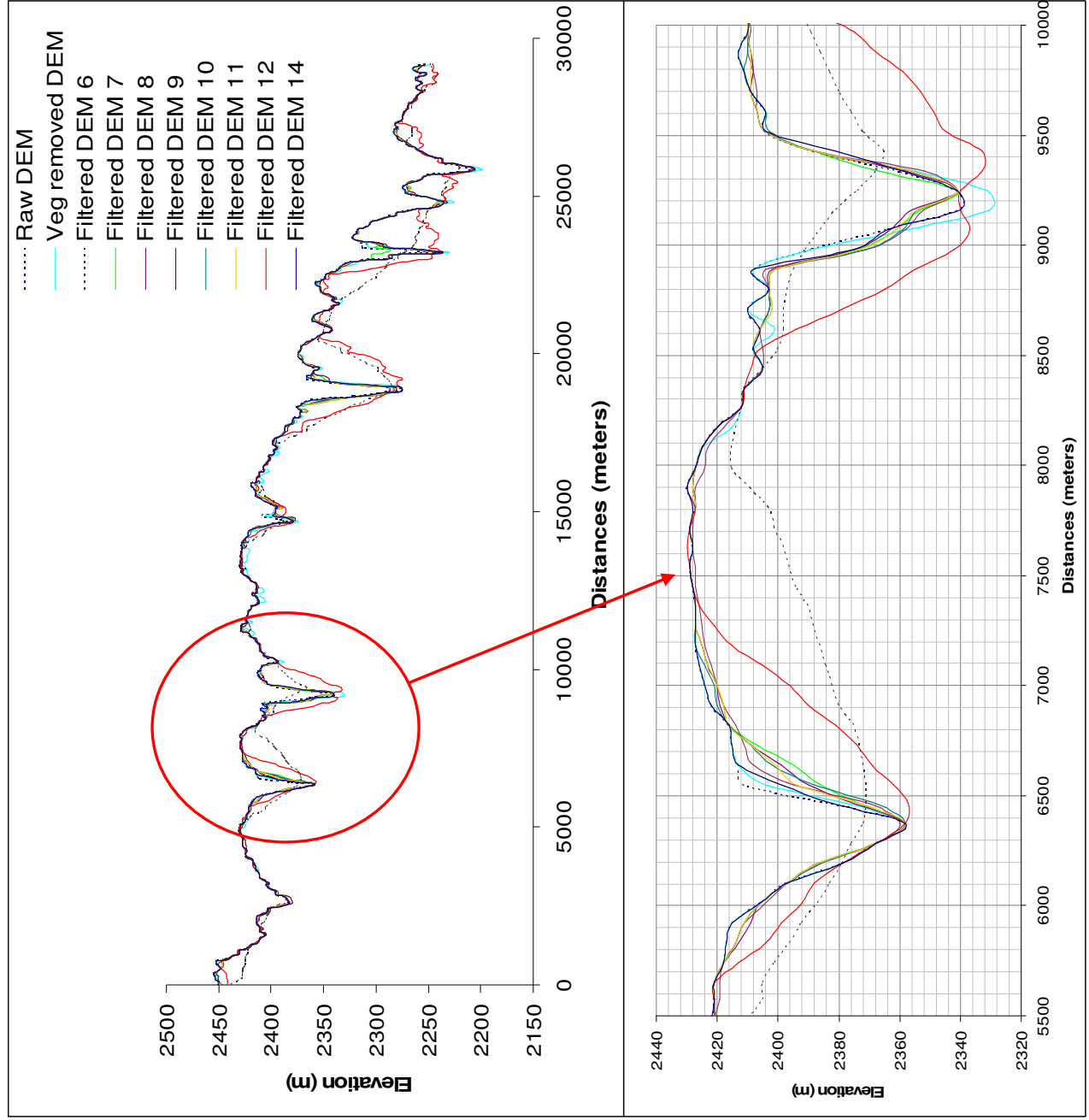
Figure 22 Profile of raw and Improved SRTM DEMs section taken at drainage lines of Malewa basin
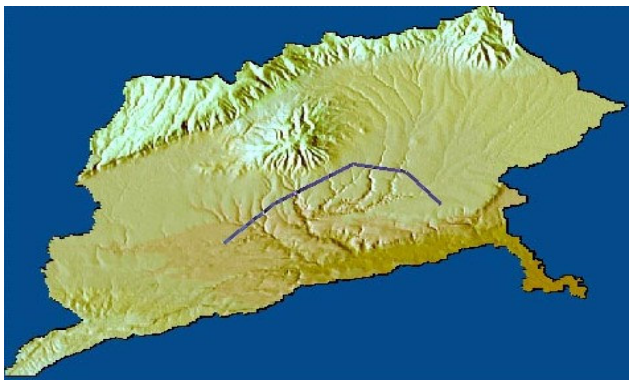
5.3.2.   Qualitative assessment of the DTMs

This assessment is made by visualizing in 3D rendering and making a profile of layer stacks drainage network comparison and visualization of difference maps between the vegetation cover removed DEM by Ilwis and the filtered DTMs by SCOP++.

In this study area the highlands and stream channels are covered by a dense vegetation cover. This makes the raw SRTM DEM non representative of the actual channel depth. When compared to the SCOP++ filtered DTMs the Ilwis map calculation applied DTM gave better result in forcing down the channels depth by removing only the vegetation cover without modifying the channel width. The SCOP++ filtered DTMs also performed well in less steep areas with negligible loss of detail as visualized in figure 23. However, all these outputs failed to force down the channels bed elevation. In the contrary, because of the linear prediction calculation the elevations are raised to some degree. This problem can be overcome by DEM optimization algorithms available in different GIS packages after the DEM is filtered. Automatic drainage line extraction from all the raw DEM and the output DTMs is done. This extraction is processed in Ilwis, which uses the D8 flow direction algorithm. DEM optimization (forcing down stream channels in the DEM) is not applied in the extraction procedure so that the drainage generated from the DEM is not forced to follow the actual drainage lines having the concept that the drainage extracted from the best DEM could follow the natural drainage path better without optimizing the DTM. In all cases the drainage network is extracted from the 90m resolution DTMs. The drainage density and the minimum length of a drainage line that should be visible in the network are specified after a number of trials so that the visualization would not be obscured by dense drainage pattern and unconnected drainage line fragments. The drainage network outputs are compared with the drainage network extracted from the raw SRTM DEM overlaying on 15m resolution false colour composite of ASTER image. All the DTMs gave satisfactory results relative to the network extracted from the raw DEM. Specially no significant difference is seen in well defined channel sections. However, some discontinuities of drainage lines are available in narrow drainage sections and flat areas. This is clearly visible along the main Malewa drainage line in figures 26 to 30.
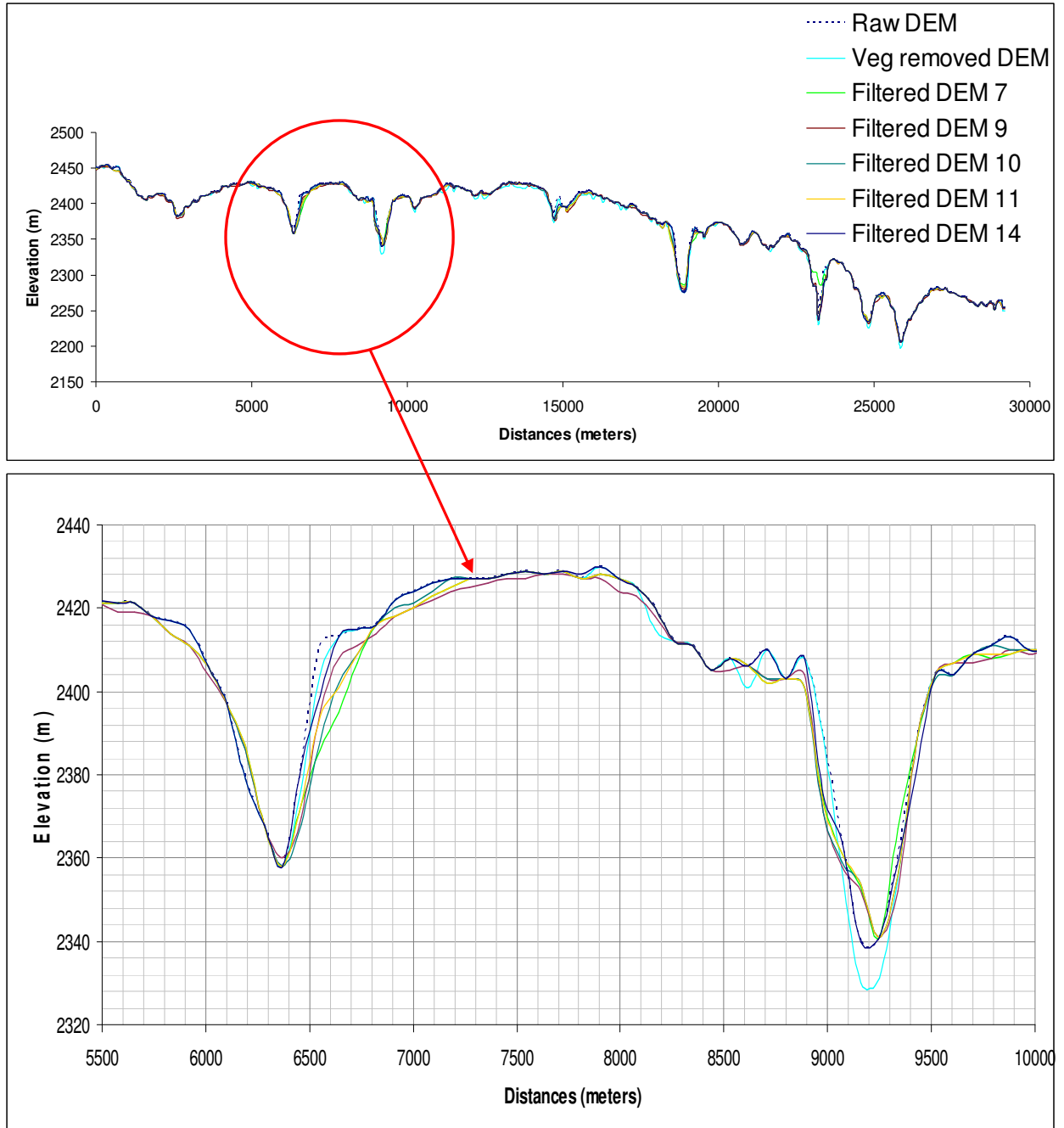
Figure 23 Profile of the raw SRTM DEM and DTMs selected for qualitative assessment
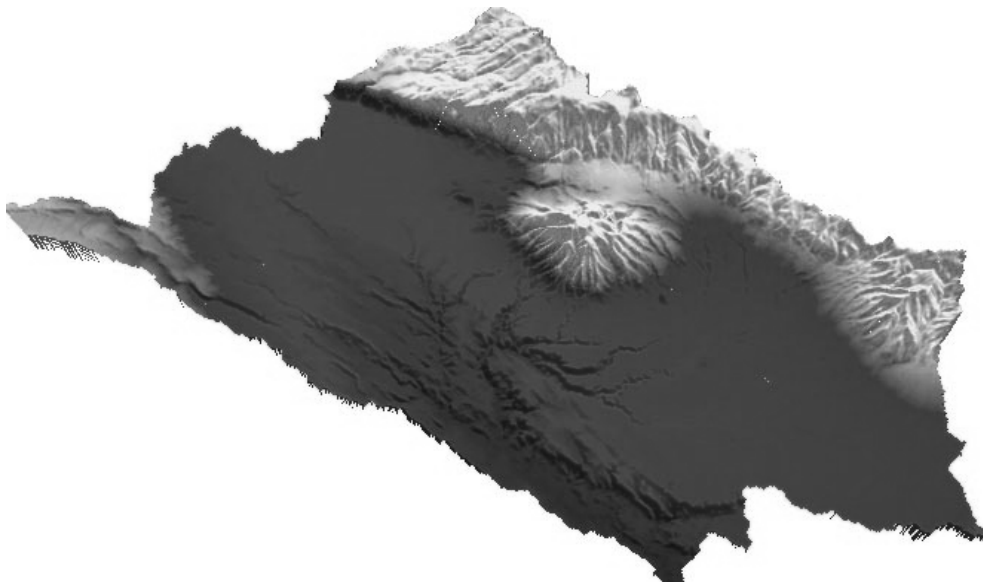
(a)
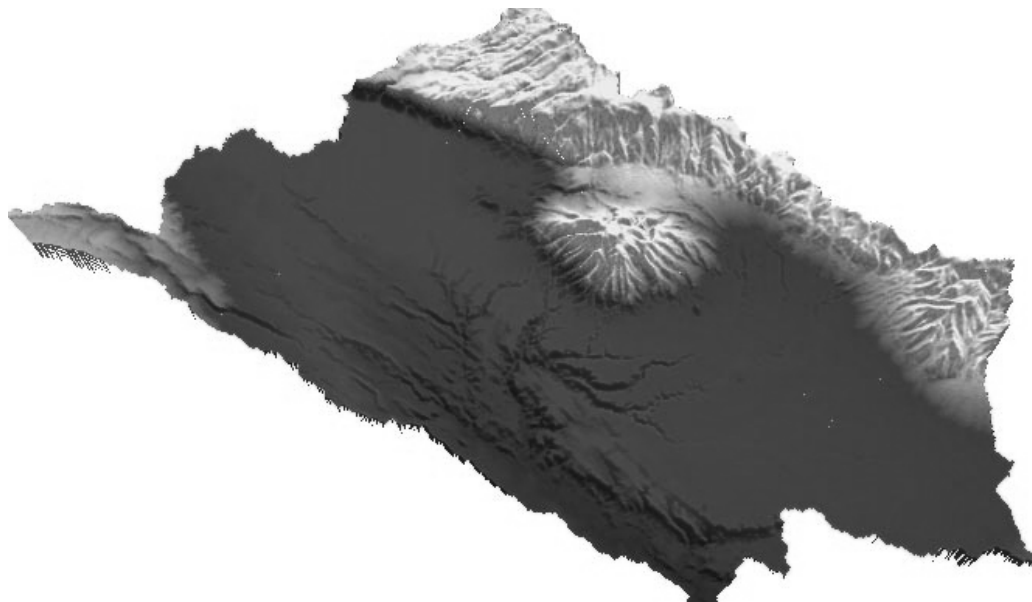
(b)

Figure 24 (a) Raw SRTM DEM and (b) Vegetation Cover Removed DEM by Map calculation in Ilwis
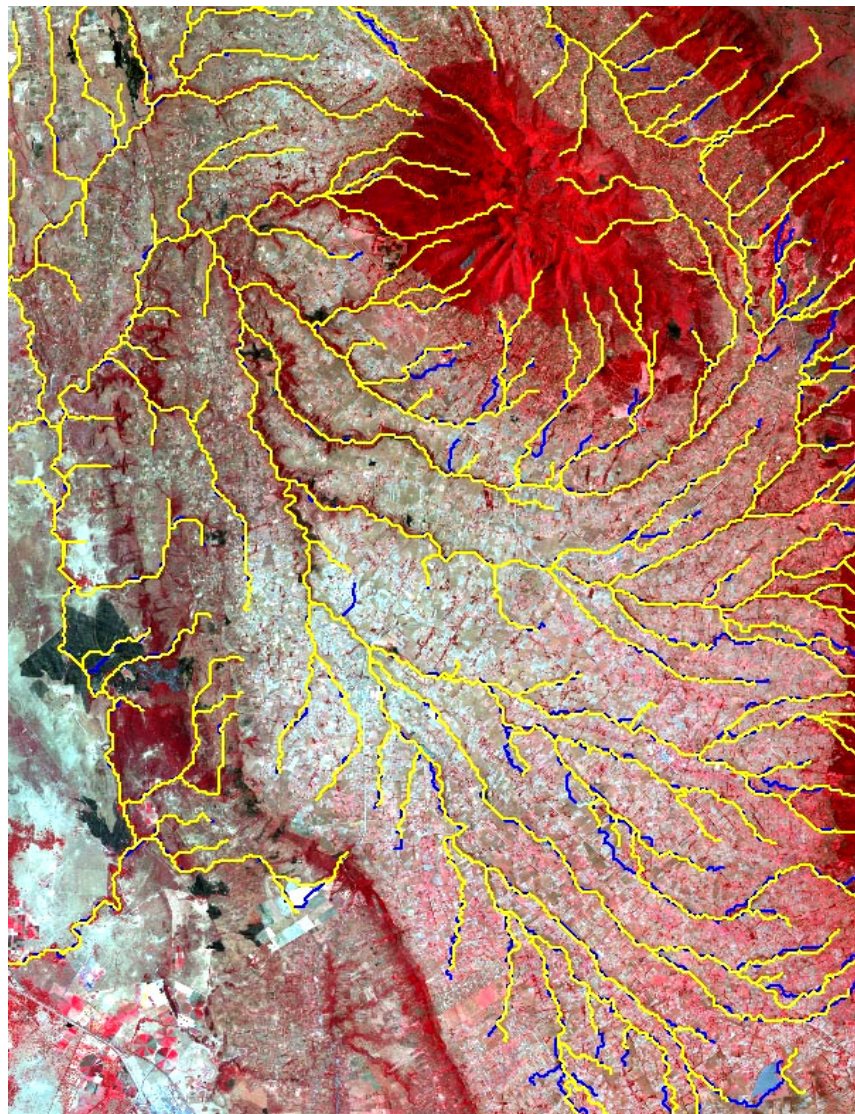
Drainage Network Extracted from
the Raw SRTM DEM

Drainage Network Extracted from
Ilwis DTM

Figure 25 Drainage Networks extracted from the raw SRTM DEM and the vegetation cover removed DEM overlayed on false colour composite of ASTER image acquired in March 2003
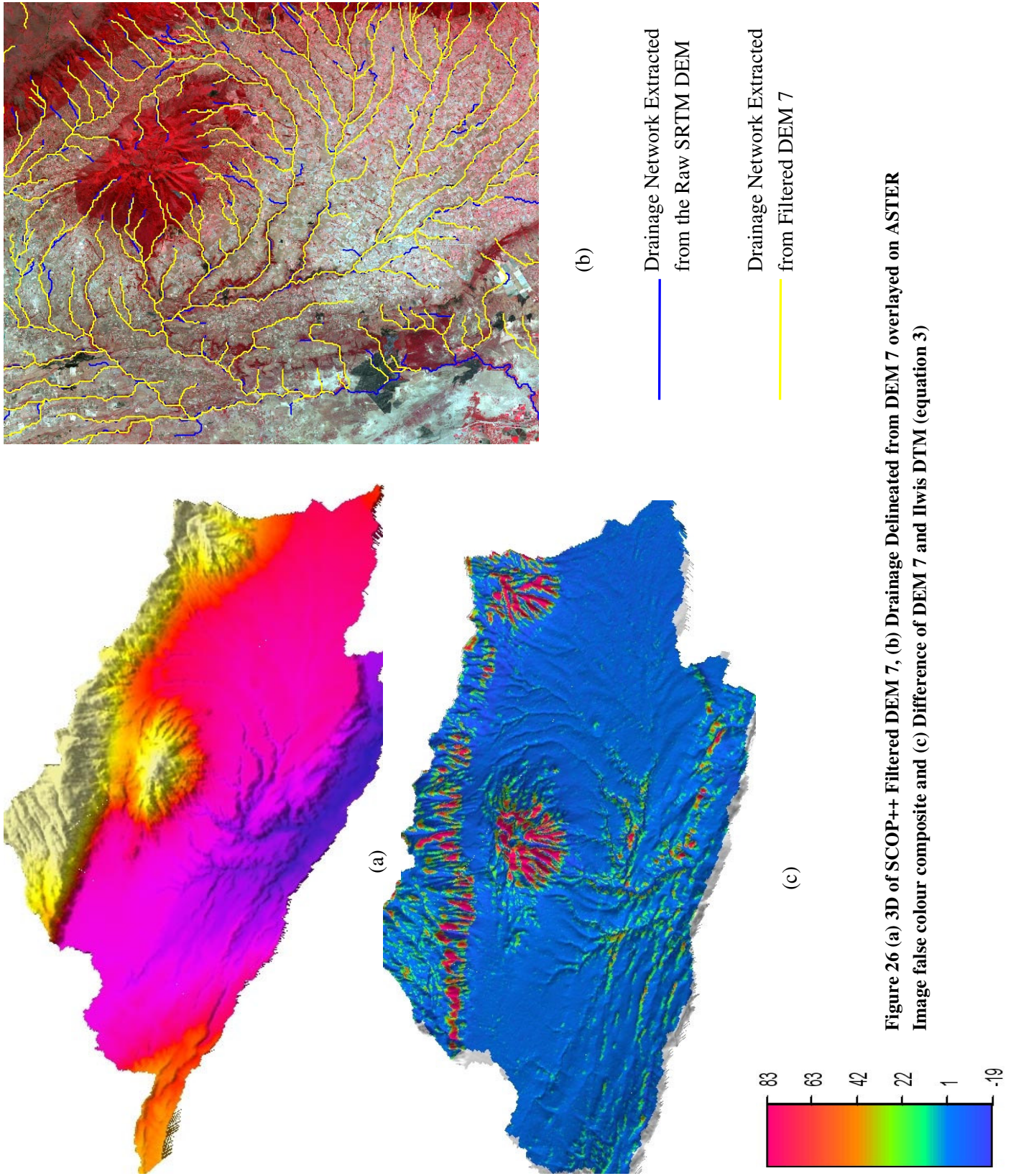
Figure 26 (a) 3D of SCOP++ Filtered DEM 7, (b) Drainage Delineated from DEM 7 overlayed on ASTER Image false colour composite and (c) Difference of DEM 7 and Ilwis DTM (equation 3)

(b)

Drainage Network Extracted
from the Raw SRTM DEM

Drainage Network Extracted
from Filtered DEM 9

(a)

(c)

21
13
6
-2
-9
-17
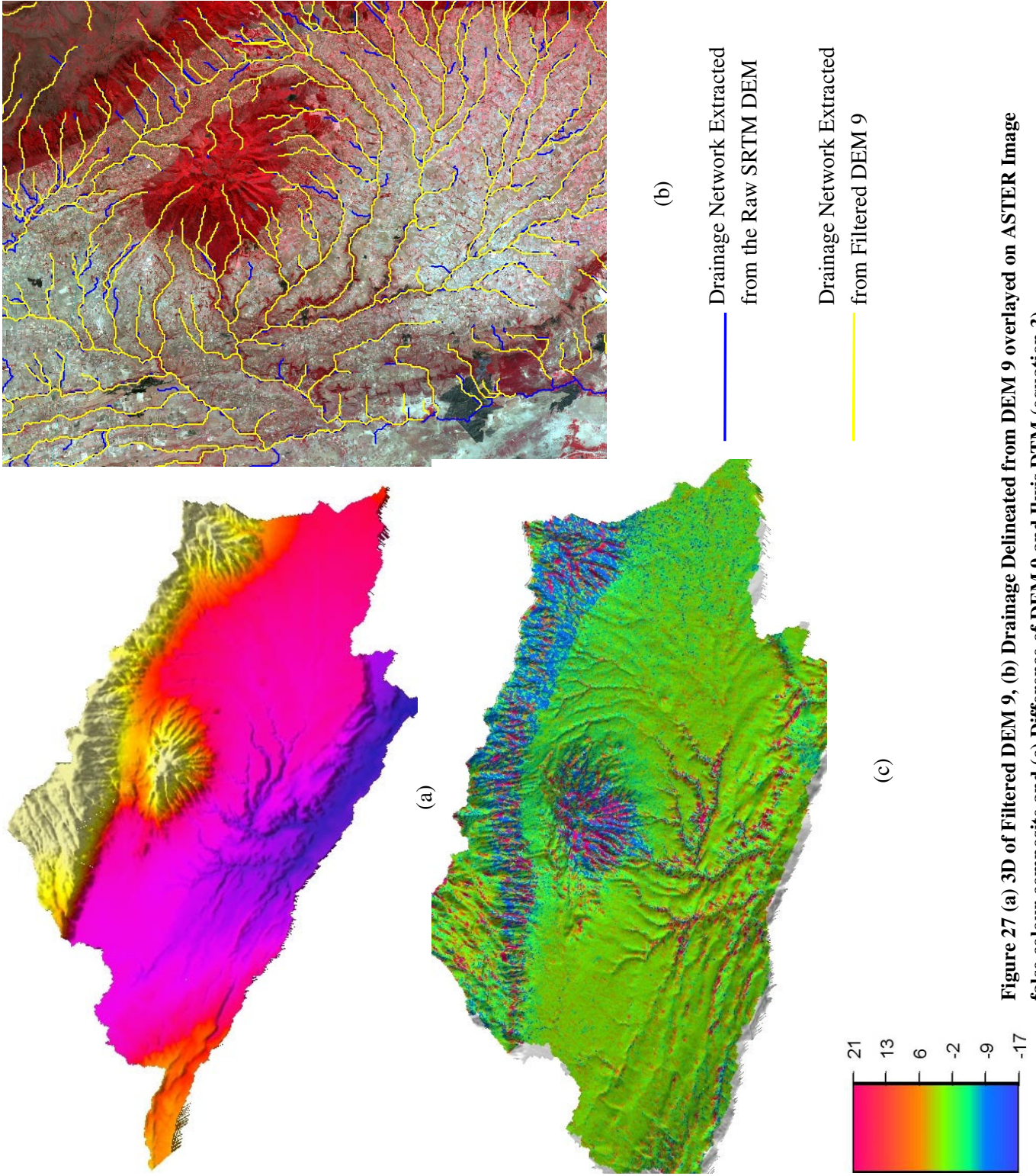
Figure 27 (a) 3D of Filtered DEM 9, (b) Drainage Delineated from DEM 9 overlayed on ASTER Image false colour composite and (c) Difference of DEM 9 and Ilwis DTM (equation 3)

(b)

———— Drainage Network Extracted
from the Raw SRTM DEM

———— Drainage Network Extracted
from Filtered DEM 10

(a)

(c)

26
17
8
0
-9
-18
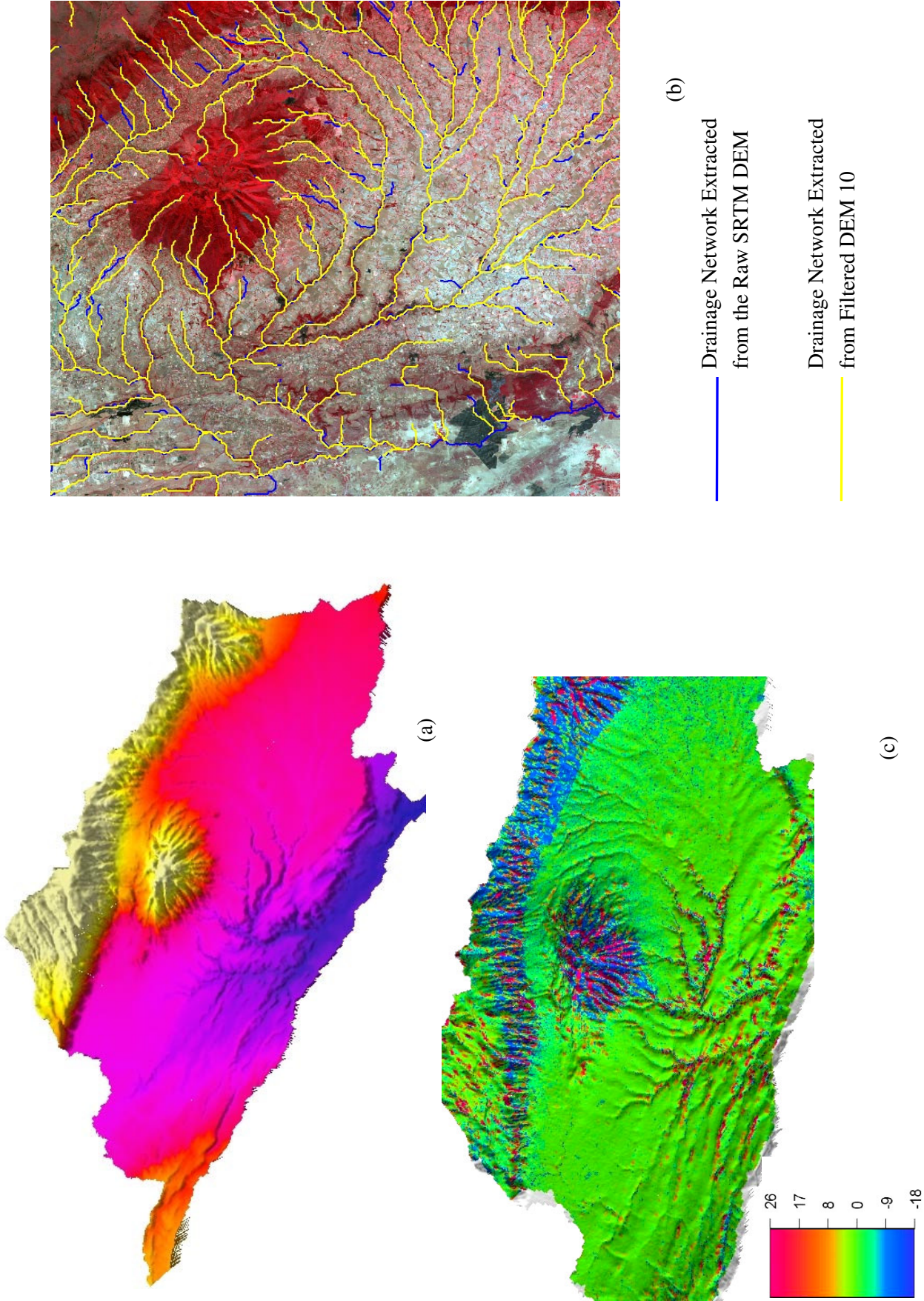
Figure 28 3D of Filtered DEM10, (b) Drainage Delineated from DEM 10 Overlayed on ASTER Image false colour composite and (c) Difference of DEM 10 and Ilwis DTM (equation 3)
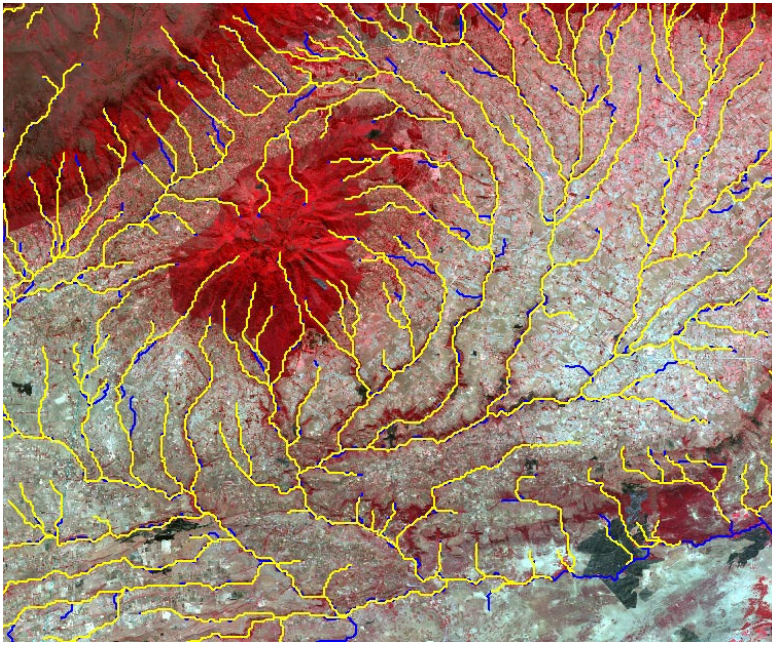
(b)

Drainage Network Extracted
from the Raw SRTM DEM

Drainage Network Extracted
from Filtered DEM 11

(a)

(c)

29

19

10

0

-9

-19
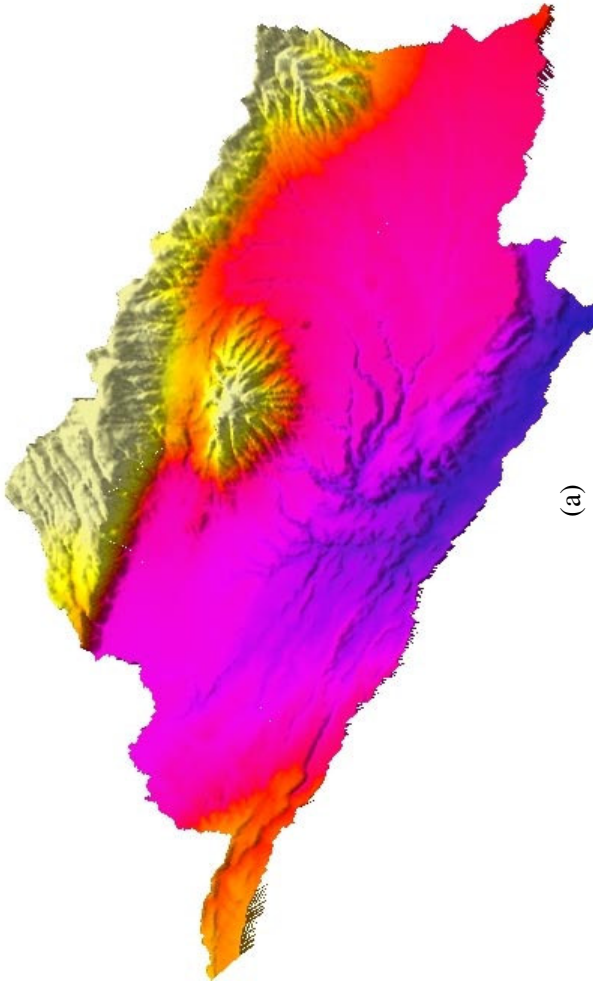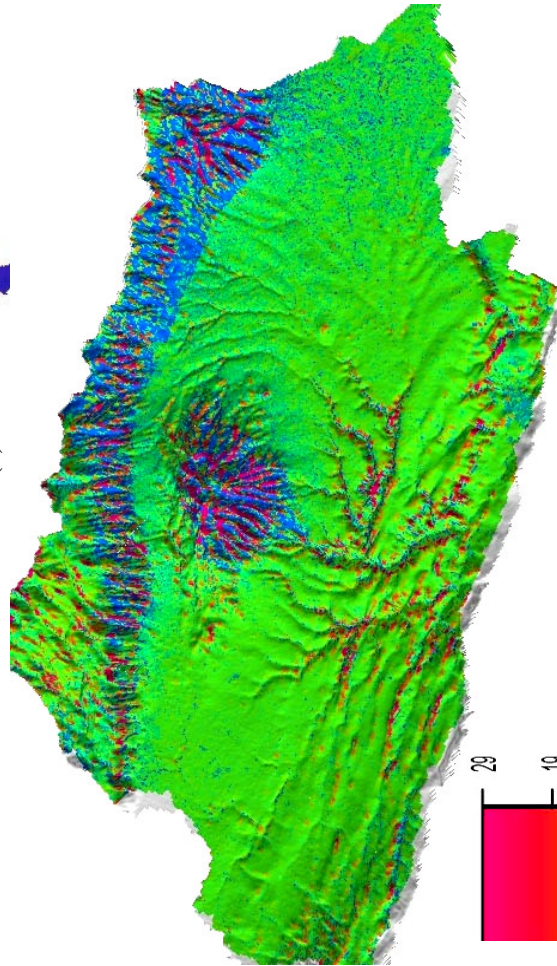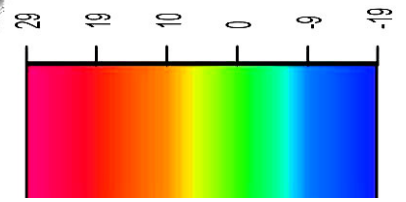
Figure 29 DEM 4 (a) 3D of Filtered DEM 12, (b) Drainage Delineated from DEM 11 overlayed on ASTER Image false colour composite and (c) Difference of DEM 11 and Ilwis DTM (equation 3)

Drainage Network Extracted
from the Raw SRTM DEM

Drainage Network Extracted
from Filtered DEM 14
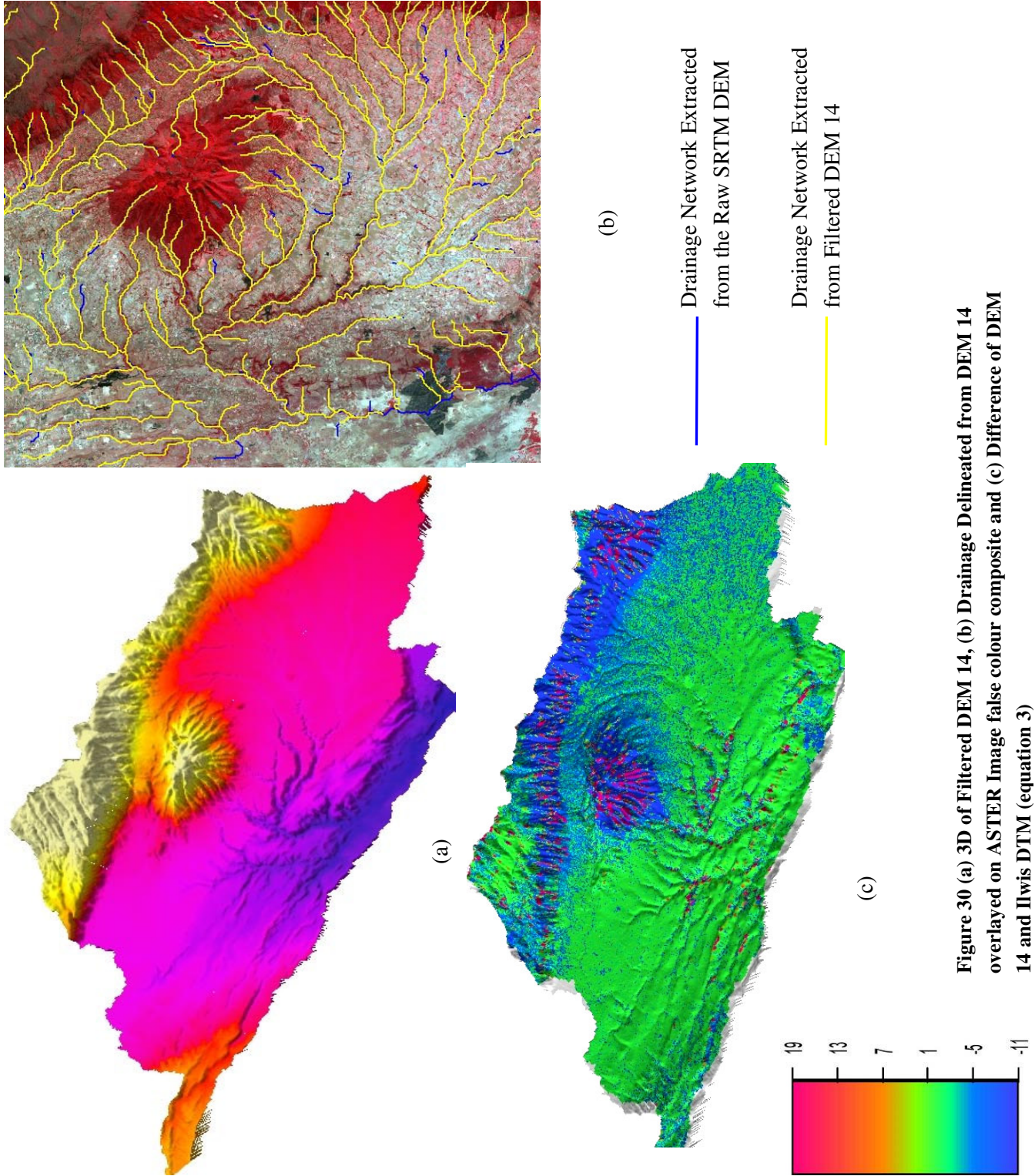
Figure 30 (a) 3D of Filtered DEM 14, (b) Drainage Delineated from DEM 14 overlayed on ASTER Image false colour composite and (c) Difference of DEM 14 and Ilwis DTM (equation 3)

Difference in elevation between the Ilwis map calculation DTM and the SCOP++ filtering outputs is made to evaluate the performance of the applied filtering strategies in SCOP++ (equation 3). The DTM from Ilwis is used as a reference for this assessment. From the successive output difference maps, it is found that SCOP++ gave reasonable results in removing the vegetation cover except in areas where the terrain features are complex and discontinuous. In such type of terrain features the linear prediction in SCOP++ performs a smoothening of the ridges and pits. In the preceding figures of the difference maps, the smoothening effect of the filtering strategies applied can be seen in the steep and vegetated areas of the basin. The reddish in the difference map shows excessively trimmed areas by the applied filter and the blue colour indicates the locations where the elevations are raised by the filtering. In the subsequent sections assessment will be made if this smoothing effect could affect the runoff output from SWAT and the Topographic Index.

Difference Map = [Vegetation Cover Removed DEM in Ilwis] – [SCOP++ filtered DTM] Equation 3

5.4.　　　　Resolution effect on Drainage Extraction

The 90m resolution DTM found by applying landcover attribute map by Ilwis map calculation is resampled to 45m and 30m resolution and drainage is extracted from the DTMs. As it is displayed in figure 31 the high resolution DTMs performed well in delineating the lower order drainage lines from the confluences to where they start to form. In figure 31 the green colour (top drainage line) is extracted from 30m resolution DTM, the yellow from 45m resolution and the blue from the 90m resolution DTMs as they are ordered in the legend. All of the three drainage networks suitably represented the higher order channels. However, the lower order drainage lines are well represented by the 30m resolution DTM followed by the 45m resolution DTM. In some areas the 45m resolution DTM gives better drainage representation than the 30m resolution DTM. This is may be the effect of the D8 flow direction algorithm used in Ilwis. Other more complex algorithms like D infinite, can give consistency in drainage network when the DTM resolution is increased.
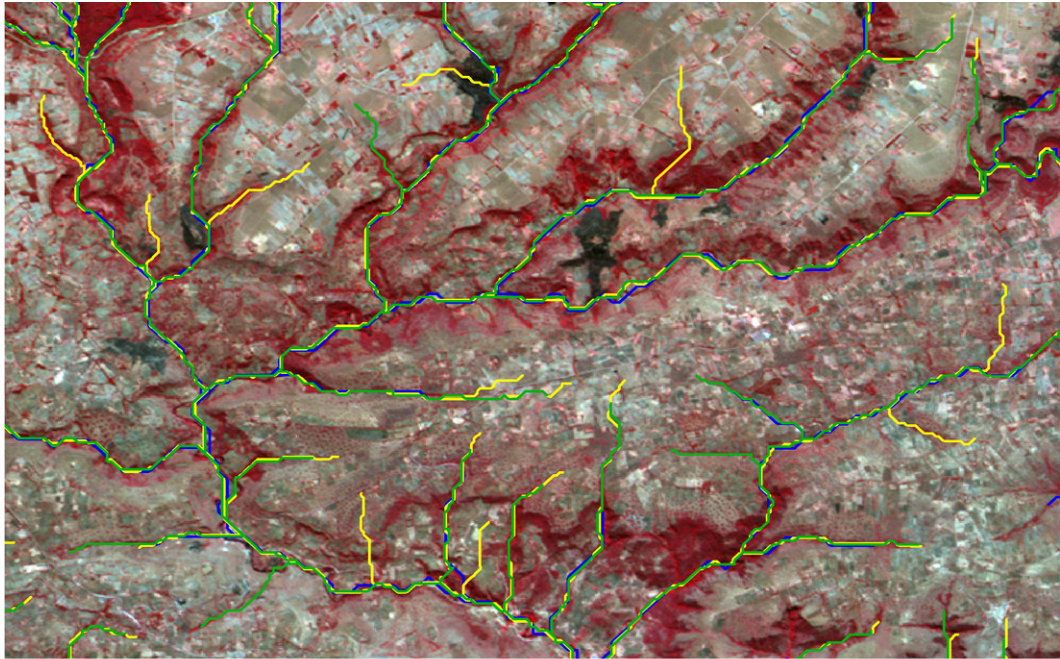
	Drainage Extracted from 30m resolution DTM
	Drainage Extracted from 45m resolution DTM
	Drainage Extracted from 90m resolution DTM

Figure 31 Drainage network extracted from 30m, 45m, and 90m vegetation cover removed DEM by Ilwis using the D8 flow direction extraction algorithm

6. Hydrologic Model Selection

The choice of a model for a particular problem is inevitably based on personal experience and preferences, as well as purely hydrological considerations and scientific rigour (Anderson, 1995).There are numerous criteria which can be used for choosing the "right" hydrologic model. These criteria are always depending on the objectives set in the project. Further, some criteria are also user depended (and therefore subjective), such as the personal preference for graphical user interface, computer operating system, input output management and structure or user add-on flexibility. (Beven, 1982) identified four major areas which offer the greatest potential for the application of distributed models. They are: forecasting the effects of land use change, the effects of spatially distributed variable inputs and outputs, the movement of pollutants and sediments, and the hydrological responses of ungauged catchments where no data are available for calibration of lumped model (Anderson, 1995). When a model is selected, the assumptions and limitations of the model structure should always be remembered and the degree of uncertainties associated with model predictions should always be known, especially for distributed models (Beven, 2000). It is not the intention of this research to make a good representative model of Malewa river basin. The model that is going to be selected is used to address the objectives set in this research with regard to SRTM DEM. Therefore, a model with simple modelling strategy and less number of parameters is highly preferred in addition to the criteria mentioned below.

The distributed model selected for this particular research has to fulfil the following according to their priority:

1.   Availability and Cost of the software
2.   The model should use a DTM as input and extracted topographic characteristics of sub-basin and stream network from it
3.   Less number of input parameters and data requirement is preferred
4.   The model have to be capable to simulate large ($>1000km^2$) river basins
5.   Processes modelled; all the hydrologic processes (continuous simulation, infiltration ,and saturation excess) should be considered in the model
6.   Low scientific expertise requirement in order to use the model adequately
7.   Technical support and documentation, such as user guides, reference manuals, webpage or support to setup and calibrate the model should be available.

This section provides a brief summary of four models considered as per the above criteria from which one distributed and one semi distributed models are selected based on the criteria listed above.

6.1.   Selection of Semi Distributed Models

HBV-Model (Hydrologiska Byråns Vattenbalansacdeling) and SWAT (Soil and Water Assessment Tool) get high priority in the selection of semi distributed model based on the criteria listed in section 6.0

6.1.1.   HBV

The HBV-Model is a general purpose hydrologic model developed at the Swedish Meteorological and Hydrologic Institute (SHMI, 2003). The HBV model is a standard forecasting tool in merely 200 basins throughout Scandinavia, and has been applied in more than 40 countries worldwide. The model is designed to run on a daily time step (shorter time steps are available as an option) and to simulate stream flow of various basin size. The basin can be disaggregated into sub basins, elevation zones, and landcover types. Input data include precipitation, monthly estimates of evapotranspiration, actual discharge (for calibration) and basin geographical information. A simple model base on bucket theory is used to represent soil moisture dynamics (Lindström, 1997). There is a provision of channel routing of runoff from tributaries, using a modified Muskingum method.

6.1.2.   SWAT

SWAT is a basin scale model developed to predict the impact of land management practices on water, sediment, and agricultural chemical yields in large, complex watersheds with varying soils, land use, and management conditions over long periods of time. The model is physically based, computationally efficient, and uses readily available inputs (Di Luzio, 2002).

SWAT is capable of performing continuous, long term simulations for watersheds composed of various sub basins with different topography, soils, land uses, crops, weather, etc. Because SWAT requires specific inputs for certain parameters, it is a physically based model that can directly model the system rather than use regression equations to describe relationships between the inputs and outputs.

SWAT offers the SCS curve number equation and Green - Ampt infiltration method to estimate the surface runoff volume. It lumps canopy interception in the term initial abstraction. Then SWAT estimates the peak runoff rate, time of concentration for overland and channel flow and surface runoff lag separately for each sub-basin (complete description is given in Neitsche, 2002). When using the curve number method to compute surface runoff, canopy storage is taken into account in the surface runoff calculations. However, if methods such as Green-Ampt are used to model infiltration and runoff, canopy storage must be modelled separately. SWAT allows the user to input the maximum amount of water that can be stored in the canopy at the maximum leaf area index for the land cover. This value and the leaf area index are used by the model to compute the maximum storage at any time in the growth cycle of the landcover.
The climatic variables required by SWAT consist of daily precipitation, maximum/minimum air temperature, solar radiation, wind speed and relative humidity.

6.2.   Selection of Fully Distributed Model

Distributed model have an advantage over lumped models in the ability to disaggregate the source of stream flow to ungauged locations upstream of the calibration location (Bandaragoda, 2004). The major drawback of lumped models is the incapability to account for spatial variability. As computers had become more powerful and less expensive, many hydrologists began using distributed parameter models. These models offer the possibility of a significant improvement over lumped models due to the ability to integrate spatial variability of hydrological processes. Therefore, effort was made to include a fully distributed hydrologic model in the assessment and the TOPMODEL and TOPOFLOW are considered as per the criteria set in the preceding section.

6.2.1.   TOPMODEL

Proposed by Beven and Kirby (1979), TOPographic MODEL (TOPMODEL) is a rainfall-runoff physically based watershed model that bases its distributed predictions on analysis of basin topography. Calculations are made based on the distribution of the Topographic Index. It is a catchment scale rain-fall-runoff model, which makes an explicit link between catchment topography and the generation of streamfow. The model predicts saturation excess and infiltration excess surface runoff and subsurface stormflow.
Since 1974 there have been many variants of TOPMODEL but never a "definitive" version (Beven, 1995). The idea has always been that the model should be simple enough to be modified by the user so that the predictions conform as far as possible to the user's perceptions of how a catchment works (http://www.es.lancs.ac.uk/hfdg/topmodel.html). This model requires a DEM data and a sequence of rainfall and potential evapotranspiration data, and it predicates the resulting stream discharges. TOPMODEL has become increasingly popular and widely used in various applications in recent years, as it provides computationally efficient prediction of distributed hydrological responses with a relatively simple framework for the use of DTM data (Beven, 1997).

The simplicity of the TOPMODEL comes from the use of the topographic index, $k = a/tan\ \beta$ where a is the upslope contributing area per unit contour draining through a point and $tan\ \beta$ is the local slope angle (Beven, 1997) . This index indicates the potential of surface and subsurface contributing areas. TOPMODEL seeks to represent the dynamics of this contributing area in both time and space providing predictions of total catchment streamflow subsurface and surfaceflow contributions and, via the distribution of the topographic index, visualization of the changing spatial distribution of soil moisture deficit and contributing area. The upslope area, a, reflects the tendency for subsurface water to drain to i, whereas $tan\ \beta$ can be considered to be an approximation of the hydraulic gradient forcing water downslope (Brasington, 1998). According to Beven (1997) high index values will tend to saturate first and will therefore have high contribution. The form of the index distribution known to be dependent on the DTM grid size from which it is derived. This strong link found between grid size and other calibrated parameter values may also reflect the loss of physical information at larger grid size. Other physical information may be lost even at fine scales.

The fundamental assumptions underlying the topographic index of hydrological similarity used in TOPOMODEL are:

1. The dynamics of the water table can be approximated by uniform subsurface runoff production per unit area
2. The hydraulic gradient of the saturated zone can be approximated by the local surface topographic slope, *tan β*
3. Exponential decline of transmissivity with depth or soil moisture deficit

The rainfall and potential evapotranspiration data are averaged for the whole catchment. Their units are depth/ time area as well as the observed discharge at the basin outlet. The time step is given in hours.

One of the aims of the TOPMODEL approach has been to keep the number of parameters required to a minimum. Those required are the mean soil surface transmissivity, a transmissivity profile decay coefficient, a root zone storage capacity, an unsaturated zone time delay, a main channel routing velocity and internal subcatchment routing velocity. To use the infiltration excess mechanism, a hydraulic conductivity (or distribution), a wetting front suction and the initial near surface water content should be added. The initialization of each run requires an initial stream discharge and the root zone deficit.

6.2.2.   TOPOFLOW

One of the recently developed distributed models is TOPFLOW (www.rivix.com). TOPOFLOW is a process based and spatially-distributed hydrological model. Its purpose is to model many different physical processes in a drainage basin with the goal of predicting how various hydrologic variables will evolve in time. Meteorological data (radiation components, relative humidity, air and ground temperature, precipitation, and wind speed) are used to drive the model. The currently supported physical processes are: (1) snowmelt, (2) precipitation, (3) evapotranspiration, (4) infiltration, (5) overland/channel flow and (6) subsurface flow.   It gives a choice to include and exclude each physical process in the model. The user specifies the input data that is required for that method and the output variables that are of interest (http://instaar.colorado.edu/topoflow).

6.3.   Selected Model

Studies in modelling the Booro-Borotou catchment in the Cot d' Ivoire (Quinn, 1991), Australia (Barling, 1994) and catchments in the Prades mountains of Catalonia, Spain (Pinol, 1997) suggests that TOPMODEL will only provide satisfactory simulations once the catchment has wetted up. TOPMODEL is suited to catchment with shallow soils and moderate topography, which do not suffer from excessively long dry periods. Catchments with deeper ground water systems or locally perched saturated zones may be much more difficult to model. Such catchments tend to go through a wetting up sequence at the end of the summer period on which the controls on recharge to any saturated zones may change with time. This makes the model

inappropriate for this particular study since Malewa basin is in a semi arid region and affected by long dry periods. Therefore, TOPOFLOW was given high priority to be applied in this assessment because of its availability, less number of input parameters and capability to model large basins. However, it is found difficult to make the model run continuously because of its huge number of bugs, and long running time. Because the software is at its development stage, much effort was put to go though the code and correct the bugs. The program is written in Interactive Data language (IDL). Because of the limited programming knowledge of the researcher and support from developer it was not merely possible to apply the model in the limited research time available. After a considerable time has been spent on input data preparation and trail runs, it is discovered that the model is not at its applicable stage at least in such kind of time constrained research work and it is disregarded from this research. Consequently, this study focused on the TOPMODEL's, base parameter, topographic index assessment with regard to DTM quality and resolution.

From the semi distributed models considered, SWAT model is selected for the assessment because of the researcher expertise with it. In addition, its wide literature cover and detail documentation makes it more preferable to be applied in this kind of study.

6.4.   Modeling in SWAT

SWAT requires particular information about weather, soil properties, topography, vegetation, and land management practices occurring in the watershed.

No matter what type of problem will be studied with SWAT, water balance is the driving force behind everything that happens in the watershed. There are two interrelated divisions in the model. The first division is the land phase of the hydrologic cycle that controls the amount of water fillings to the main channel in each subbasin. The second division is the routing phase of the hydrologic cycle which can be defined as the movement of water through the channel network of the watershed to the outlet.
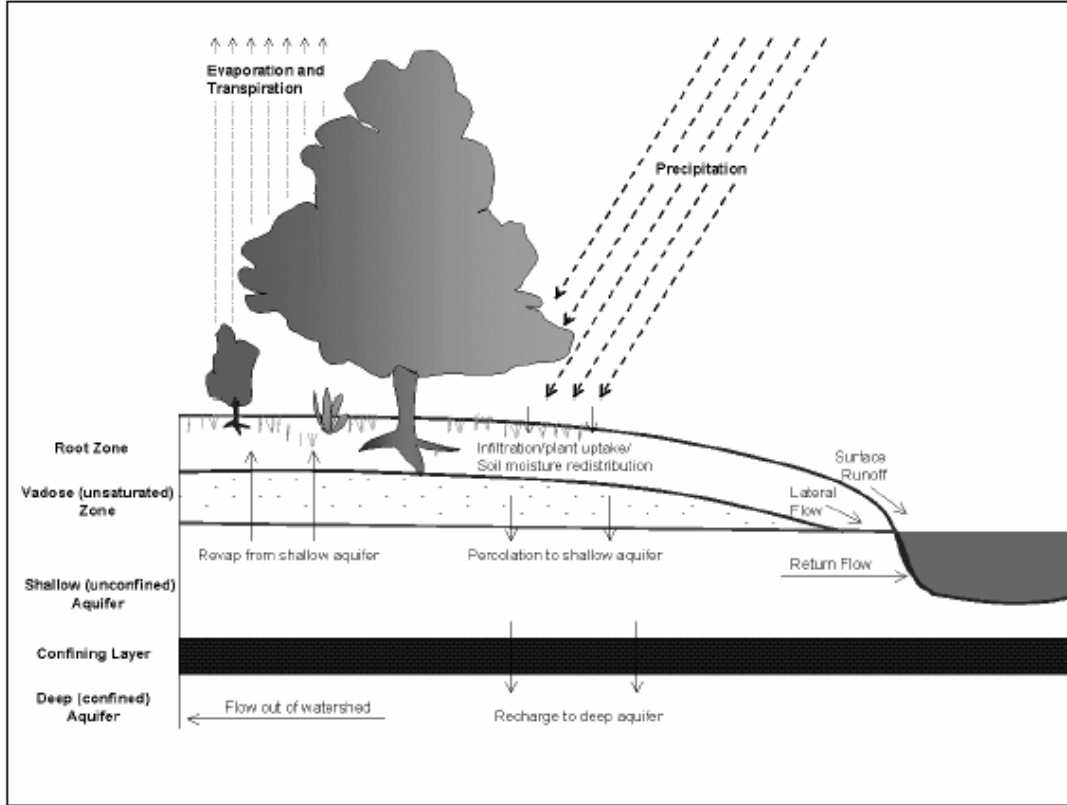
Figure 32 Schematic representation of the hydrologic cycle

The hydrologic cycle as simulated by SWAT is based on the water balance
Equation:

$$SW_t = SWo + \sum_{t=1}^{t} (R_{day} - Q_{surf} - ET_a - W_{seep} - QR_{gw})$$

where SW_t is the final soil water content, SW_0 is the initial soil water content on day i, t is the
time (days), R_{day} is the amount of precipitation on day i,, Q_{surf} is the amount of surface runoff on
day i, Ea is the amount of evapotranspiration on day i, W_{seep} is the amount of water entering the
vadose zone from the soil profile on day i, and Q_{gw} is the amount of return flow on day i all in
(*mm H_2O*).
In SWAT, a watershed is divided into multiple subwatersheds, which are then further subdivided
into HRUs that consist of homogeneous landuse, management, and soil characteristics. The
HRUs represent percentages of the subwatershed area and are not identified spatially within a
SWAT simulation. Runoff is predicted separately for each HRU and routed to obtain the total
runoff for the watershed.
Three options exist in SWAT for estimating surface runoff from HRUs – combinations of daily
or subhourly rainfall and the Natural Resources Conservation Service Curve Number (CN)
method or the Green and Ampt method. For estimating potential evapotranspiration also three

methods are provided: Priestly-Taylor, Penman-Monteith, and Hargreaves. (Neitsch, 2002) provides further details on input options. Hargraves method is used in this assessment.

The different processes involved in this phase of the hydrologic cycle and related to topography directly or indirectly are summarized in the following sections. More detailed descriptions of the model components can be found in (Neitsch, 2002) Using daily or subdaily rainfall amounts, SWAT simulates surface runoff volumes and peak runoff rates for each HRU. It can be computed using a modification of the SCS curve number method or the Green & Ampt infiltration method. In this assessment the SCS curve number method is applied.

Peak runoff rate predictions are made with a modification of the rational method. In brief, the rational method is based on the idea that if a rainfall of intensity i begins instantaneously and continues indefinitely, the rate of runoff will increase until the time of concentration, tc, when all of the subbasin is contributing to flow at the outlet. In the modified Rational Formula, the peak runoff rate is a function of the proportion of daily precipitation that falls during the subbasin tc, and the daily surface runoff volume. The proportion of rainfall occurring during the subbasin tc is estimated as a function of total daily rainfall using a stochastic technique. The subbasin time of concentration is estimated using Manning's Formula considering both overland and channel flow.

The main channel and tributary (minor or lower order) channels are defined within a subbasin. Each tributary channel within a subbasin drains only a portion of the subbasin and does not receive groundwater contribution to its flow. All flow in the tributary channels is released and routed through the main channel of the subbasin. SWAT uses the attributes of tributary channels to determine the time of concentration for the subbasin.

Transmission losses are losses of surface flow via leaching through the streambed. This type of loss occurs in ephemeral or intermittent streams where groundwater contribution occurs only at certain times of the year, or not at all. Water losses from the channel are a function of channel width and length and flow duration. Both runoff volume and peak rate are adjusted when transmission losses occur in tributary channels.

Lateral subsurface flow, or interflow, is stream flow contribution which originates below the surface but above the zone where rocks are saturated with water. Lateral subsurface flow in the soil profile (0-2m) is calculated simultaneously with redistribution. A kinematic storage model is used to predict lateral flow in each soil layer. The model accounts for variation in conductivity, slope and soil water content.

Once SWAT determines the loadings of water to the main channel, the loadings are routed through the stream network of the watershed. Flow is routed through the channel using a variable storage coefficient method or the Muskingum routing method. In this study the variable storage method is applied.

6.5.   DTM Effect in the SWAT Runoff Output

SWAT Model that was calibrated and validated for monthly discharge output of the Malewa and Gilgil Rivers in one of the previous studies (Muthuwatta, 2004) is used to test the DTMs effect in

the runoff output. The Model was calibrated for a 100m resolution ASTER DEM generated using the OrthoEngine module of the Geomatica Focus software developed by PCI Geomatics. In this assessment this DEM is resampled to 90m to make it at equal resolution level with the raw SRTM DEM. The model is rerun using the resampled 90m resolution ASTER DEM and using the raw SRTM DEM only considering Malewa basin. During stream definition equal threshold area is used to keep the consistency of no of subbasins in the different runs.

In order not to alter the calibration, all the prepared data and methods used in the previous study are used in all the runs.

After running the model for the resampled 90m resolution ASTER DEM for daily and monthly time step for the period from January 1, 1965 to December 31, 1975, it is rerun using the raw SRTM DEM and the Ilwis DTM and the DTMs processed by SCOP++ filtering technique.

The specified year is selected, since it is the period in which least rainfall data gap is encountered and the discharge rating curve used to calculate the discharges from the measured stages of the gauging station at the outlet of the basin was giving accurate results according to one of the previously made research (Podder, 1998).
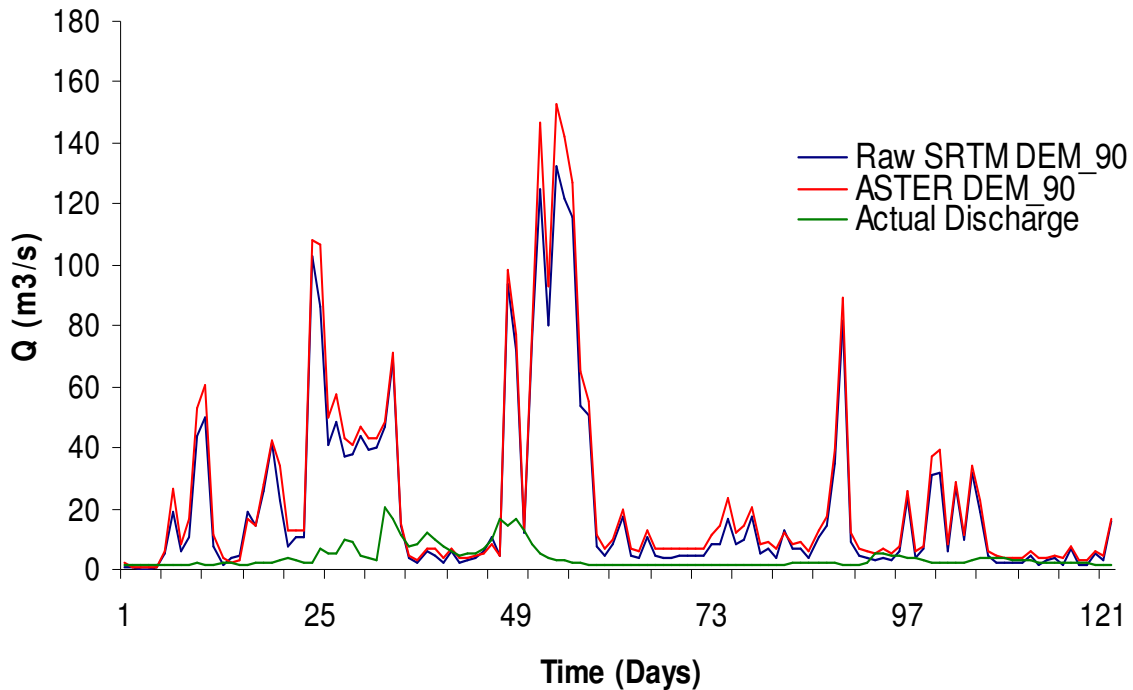
Figure 33 SWAT daily runoff output of Malewa basin for raw SRTM and ASTER DEMs.

The optimized parameters for which the model is sensitive and calibrated in the previous study are used in the modeling and the daily and monthly average outputs for the year 1995 are compared. No significant difference is encountered in the monthly runoff output of the model when the ASTER DEM is replaced by the SRTM DEM. Therefore, more focus is given to the daily runoff output

changes relative to the DTMs quality and resolution. A number of runs made to assess the sensitivity of the model output to the DTMs quality and resolution. As illustrated in figure 33, a considerable difference in the SWAT model output is found when the raw SRTM DEM replaced the resampled 90m resolution ASTER DEM in the model. The output of the model when ASTER DEM is used is higher than when SRTM DEM is used. Depending on this result, further runs were made to assess the underlying causes of this difference.

First, the SWAT runoff output is checked if the difference is resulted from the quality of the SRTM DEM. To assess these the DTMs made by Ilwis map calculation using vegetation attribute map and the best DTM (DEM 14) found by the SCOP++ filtering technique are used in the model. However, as shown in figure 34 the output from the model when these DTM are used perfectly fit with the output when the   raw SRTM DEM is used. Therefore, it is concluded that the SWAT output difference is not because of the DEM quality effect. Secondly, the cause of the difference is assessed for the resolution   effect running the model by resampling the DTM 14 to 30m and 45m resolution using the nearest neighbor resampling method in Arcview.
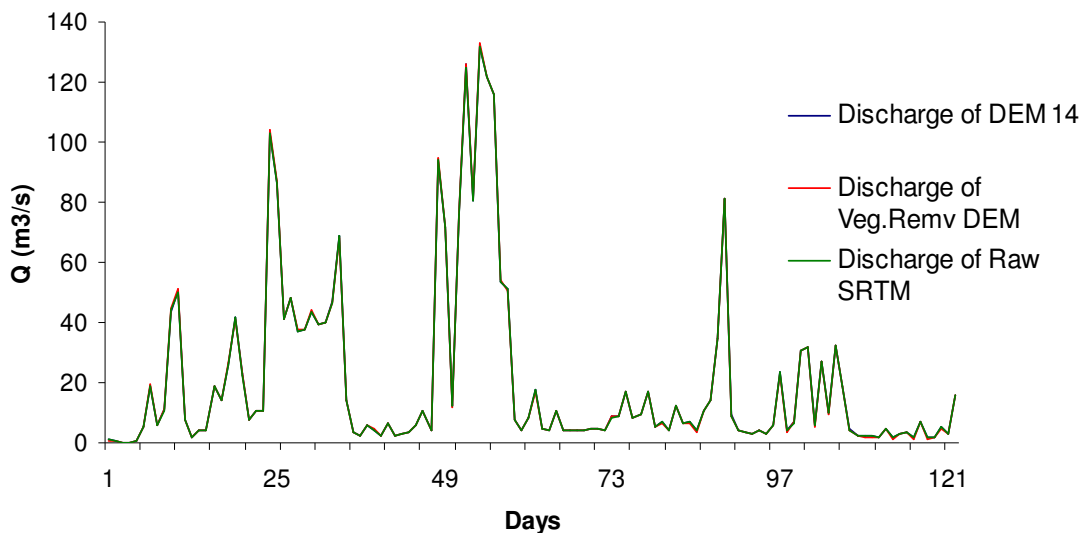
Figure 34 SWAT Model Runoff output of Malewa River for improved and Original SRTM DEMs

As shown in figure 35 the higher resolution DTMs gave a little bit higher discharge at picks than the original 90m resolution DTM. Since raw SRTM DEM supplied by NASA is an averaged to 90m resolution from 30m resolution, resampling back to higher resolutions may recover to a little extent the details lost by the averaging processes. This implies that the model output when higher resolution DTM is used is more actual than when lower resolution is used since the 30m resolution DEM represents the terrain features better than the raw 90 resolution SRTM DEM. As it is discussed in section 4.6 ASTER DEM generated in 30m resolution even after it is resampled to 90m resolution gives more detail terrain feature than the 90m resolution raw SRTM DEM.
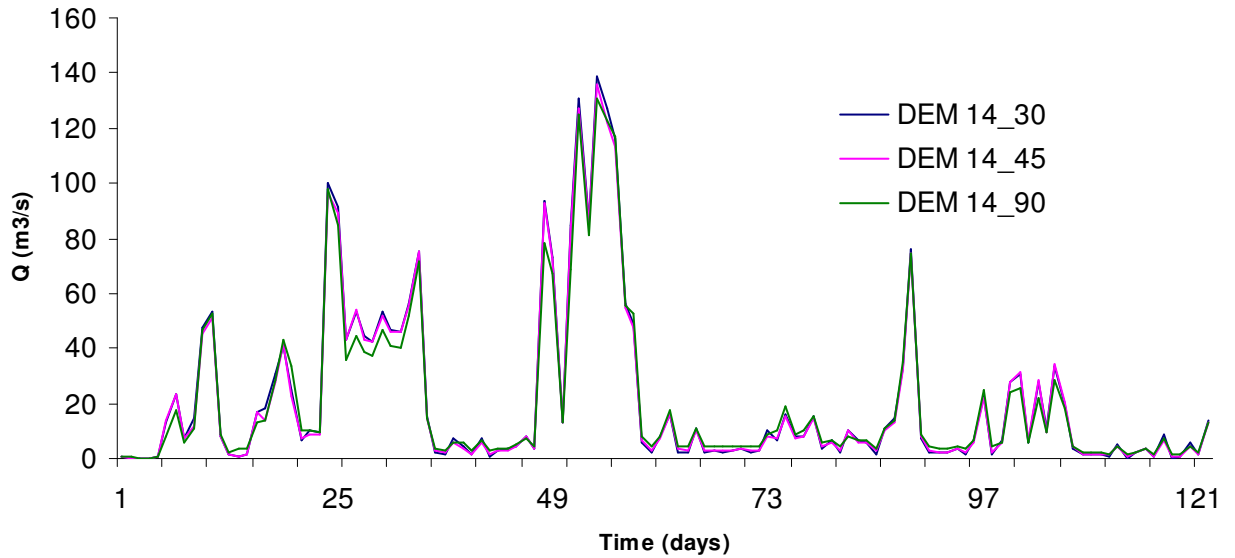
Figure 35 SWAT Model runoff output of Malewa River for filtered and resampled SRTM DTMs of 30m, 45m, and 90m resolutions
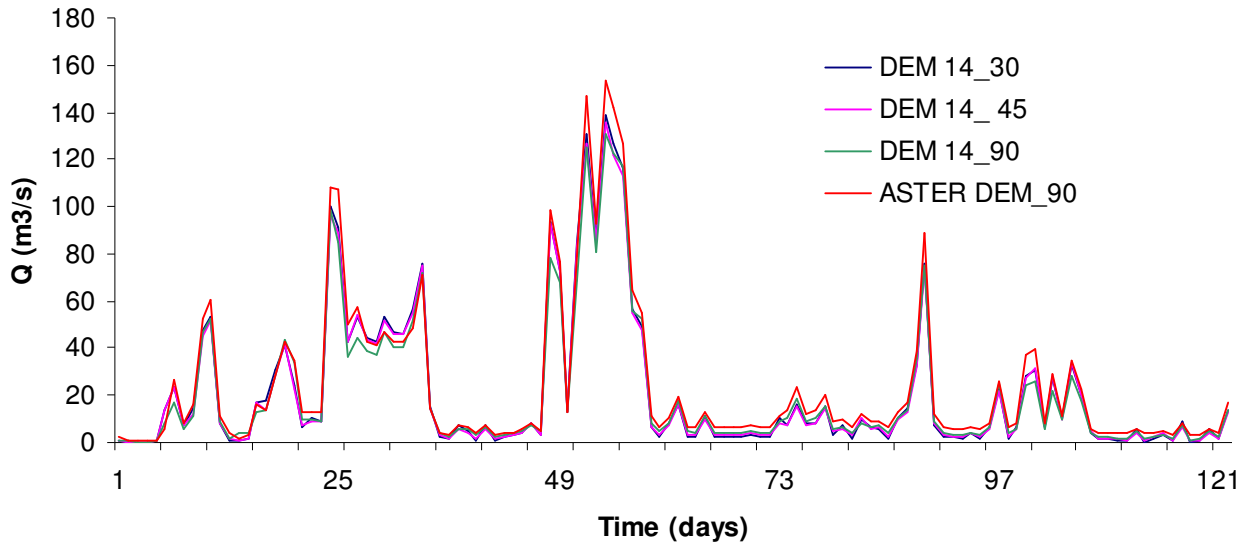
Figure 36 SWAT Model runoff output of Malewa basin for filtered and resampled SRTM DTMs and ASTER DEM

Therefore it can be concluded that the output difference is the result of lose of detail during the averaging of the SRTM DEM from 30m to 90m resolution. But this loss of accuracy in the discharge output can be recovered to a certain degree by resampling it to higher resolution as

shown in figure 36. In the preceding sections the accuracy of the raw SRTM DEM is proved to be higher than the ASTER DEM, however, it does not give much terrain detail as ASTER DEM. From the SWAT model output it is shown that the terrain detail is more influential than the accuracy difference between the two DEMs. This drawback of SRTM DEM can be improved to a certain extent by increasing the resolution as it is illustrated in figure 36.

6.6.   DTM Effect on Topographic Index

Spatial heterogeneity of the topographic index, *ln(a/tanβ)* varied in the catchment depending on the DTM quality and resolution. DTM quality effect on the topographic index output and distribution is approached by comparing the index distribution histogram, the maximum, minimum and weighted average of the map (table 7 and table 8). The topographic index is derived using the Ilwis slope, and flow accumulation algorithms, after avoiding slopes with zero values from the catchment so that the index is defined throughout the catchment. This is done by replacing the zero slope values by a very small number. The Ilwis script used in the calculation is found in Appendix B. The index calculated for the SCOP++ filtered DTMs, which have different level of terrain detail and accuracy. As illustrated in figure 38(a), the smoothened DTMs (DEM 9, DEM 7, DEM 10, and DEM 11) by the applied filtering strategy in SCOP++   shifted to higher topographic index values. This is because of the reduction of the steepness of the slopes of the terrain that resulted in the increase in the index. The topographic index has inverse relation to the local slope of the pixel. In the same figure it is shown that the index has high heterogeneity to higher values of the index. The average of the index is calculated by weighing the index values by the number of pixels. These averages of the index for the different quality DTMs from SCOP++ does not show much difference as compared in table 7 except the DTM found by Ilwis map calculation output, the "Veg. Cover Rem. DEM".

In case of the different resolution DTMs (figure 38 (b) and figure 39) the degree of the regularity in the index has increased not only for higher values but also for the medians. The range of the index distribution is also affected by the resolution. Higher resolution DTMs has got wider distribution range, but in the lower index values than the lower resolution DTMs.
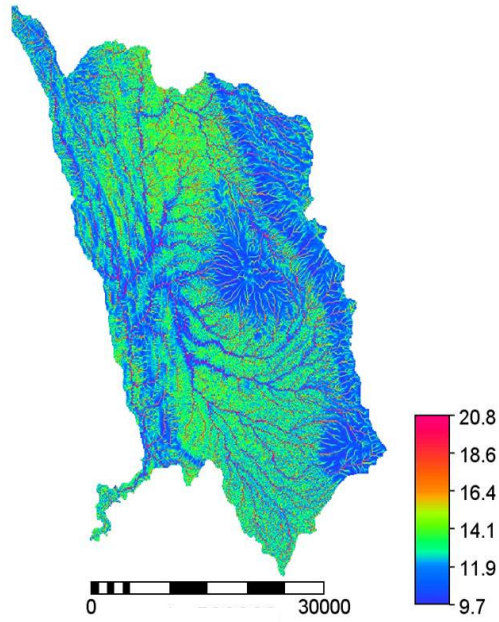
Figure 37 Topographic Index map of Malewa Basin extracted from the raw SRTM DEM

Table 7 Statistical Comparison of Topographic Index for the Qualitatively Improved DTMs

Improved DEMs	DEM 10	DEM 11	DEM 14	DEM 7	DEM 9	Ilwis DTM
Weighted average TI	26.26	26.26	25.90	26.36	26.44	24.23
Min TI	8.9	8.9	8.9	9.4	8.8	8.5
Max TI	27.1	25.5	25.9	25.4	26.2	27.2
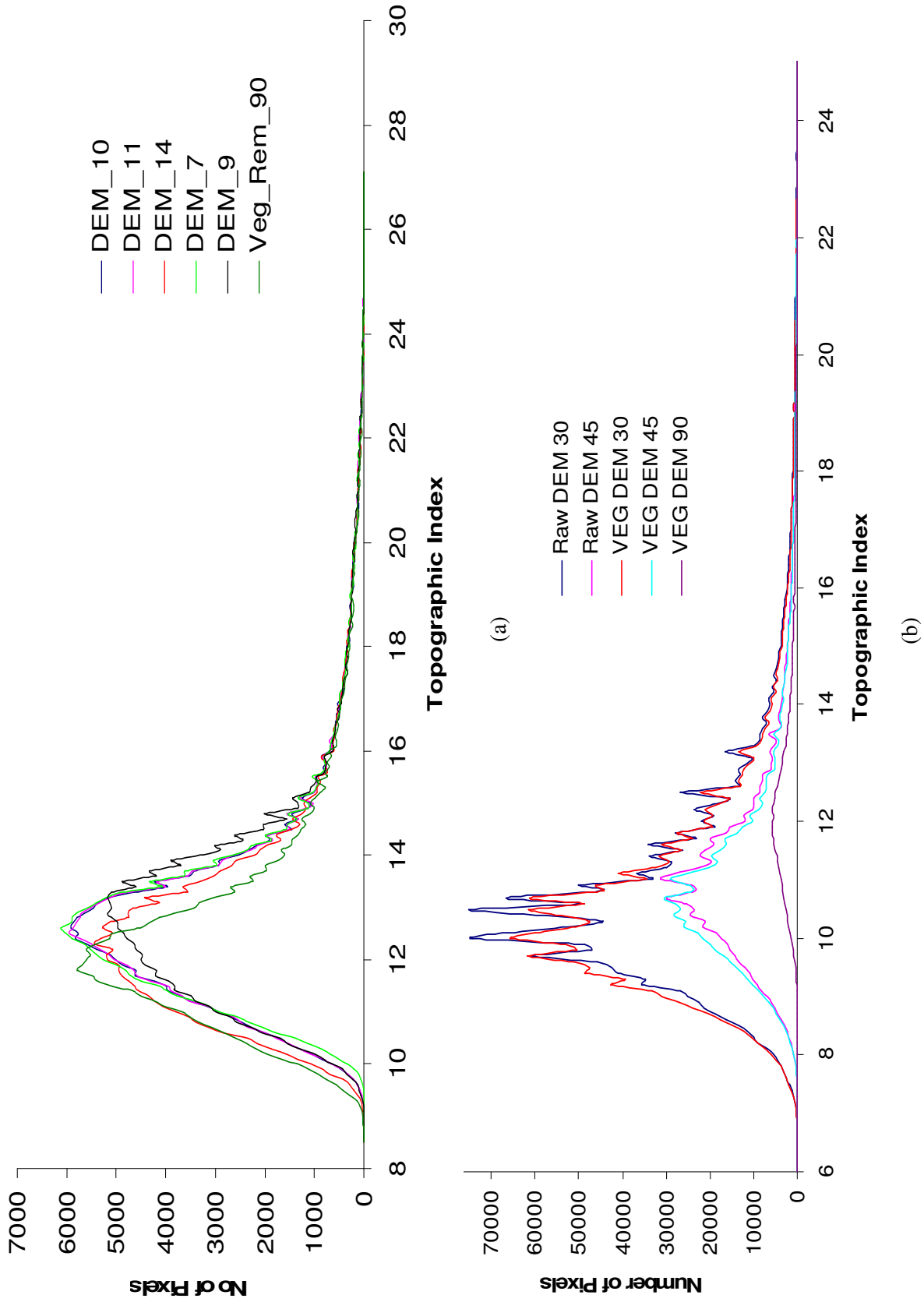
Figure 38 (a) Topographic Index Distribution of DEM improved by SCOP++ and Ilwis Map Calculation using vegetation height attribute map, (b) DTM Resolution Effect on Topographic Index Distribution
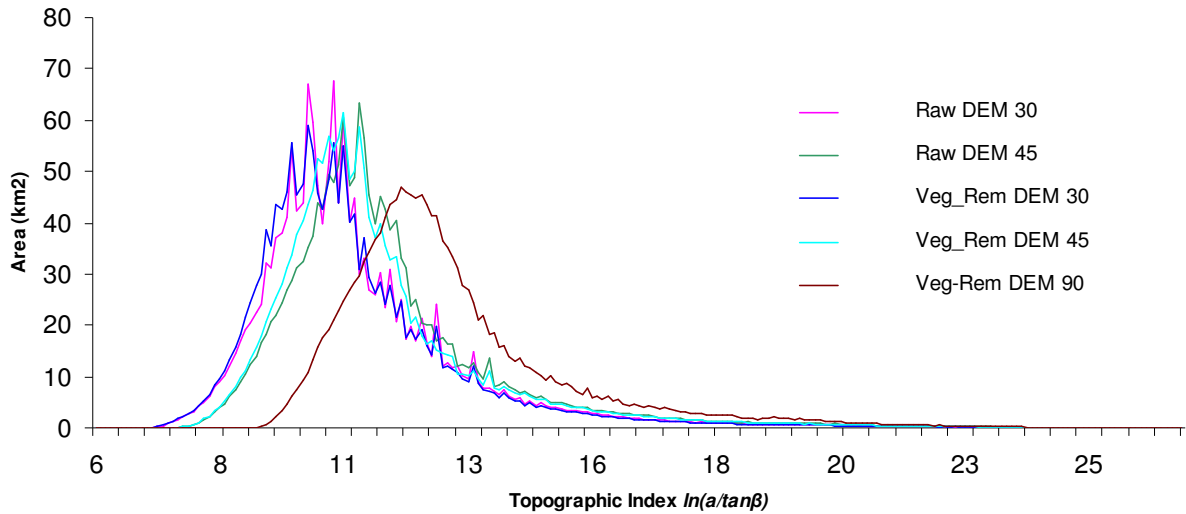
Figure 39 Topographic Index- Area distribution in Malewa catchment for different resolution SRTM raw DEM and Ilwis DTM

Table 8 Statistical Comparison of Topographic Index for the different resolution SRTM DTMs

DEM	Raw DEM 30	Raw DEM 45	Ilwis DTM 30	Ilwis DTM 45	Iwis DTM 90
Weighted average TI	11.01	11.51	10.91	11.36	12.78
Min TI	5.7	6.8	5.7	6.7	8.5
Max TI	27.6	27.6	27.5	27.6	17.2

7.   Conclusions and Recommendations

7.1.   Conclusions

Particular to the Malewa basin landcover condition and terrain complexity the following conclusions are drawn:

- The 3 arc second SRTM DEM horizontal shift is within one pixel when the projections and reference datum are entered appropriately in importing and exporting from one GIS software package to another package. Particular attention should be given to corner coordinates and the number of rows and columns. In some packages, for instance Ilwis, once proper georeferencing is made on the test satellite image, and the right corner coordinates and projection information are given to the DEM that can be the original projection information, the drainage extracted from it perfectly fits the drainage line in the satellite. But, in some packages this may not be the case. The projection information of the satellite image and the DEM should be reprojected to the same projection and datum. This is tested by extracting drainage network map from ASTER DEM and SRTM DEM, after reprojecting both into UTM coordinate system and WGS84 horizontal and vertical datum, and overlaying the drainage lines together that gave exact fit.
- The ASTER DEM generated in 30m resolution even after it is resampled to 90m resolution using bicubic resampling technique gives more detailed terrain feature than the 90m resolution raw SRTM DEM.

- From the vertical accuracy comparison of the ASTER DEM generated using ENVI-ASTER-DTM and the raw SRTM DEM applying both Triangulation Ground Control Points and GPS data, it is investigated that SRTM DEM is more accurate than the ASTER DEM. SRTM DEM has high correlation to the triangulation ground control points and the GPS data than the ASTER DEM; however, ASTER DEM gives much more ground feature details since it is generated from high resolution and seems not to be much affected by the bicubic resampling method as the averaging method applied to the SRTM DEM from 30m to 90m horizontal resolution.
- The vegetation cover filtering applied using SCOP++ performed well in flat areas with negligible modification of the terrain features by the linear prediction and trend surface fitting algorithms. It is found that the linear prediction algorithm used in SCOP++ has smoothening effects in complex terrain conditions and vegetated areas. It considerably affected the ridges and narrow valleys by trimming the ridge tops and raising up the valley bottoms. This can be improved by fine tuning the different strategy setups and

their different parameters, which may take several experimenting hours and expertise. Forcing down the raised valley surfaces by applying DEM optimization procedure available in different GIS/ Hydro packages after the filtering process can also be another option.

- The drainage networks derived from the improved DEMs are compared with the drainage networks extracted from the raw SRTM DEM overlaying on 15m resolution false colour composite ASTER image. All the DTMs with different quality levels found from the vegetation removal techniques applied gave satisfactory results relative to the network extracted from the raw SRTM DEM. Specially no significant difference is seen in well defined channel sections. However, some discontinuities of drainage lines are available in narrow drainage sections and flat areas that can be improved using more advanced flow direction computation algorithms. The high resolution DTMs found by resampling the Ilwis vegetation cover removed SRTM DEM performed well in delineating the lower order drainage lines from the confluences to where they start to form.

- The daily runoff output of the SWAT model when ASTER DEM is used is higher than when the SRTM DEM is used. The output does not show any differences for the DEM improvement applied. However, the runoff output is found sensitive to the resolution changes to the SRTM DEM. From this specific landcover condition and terrain characteristics it is concluded that the raw SRTM DEM can be used in SWAT runoff modeling depending on the desired time step. For time steps shorter than a day better model output is found when the DEM is resampled to higher resolution than trying to improve the quality of the DEM by vegetation cover removing. Data voids in the raw SRTM DEM can be filled using some of the interpolation techniques available in most of the GIS packages. Elevation information from pixels around the data void areas can be used for the interpolation to fill up the void space. It is also possible to convert the DEM into point data cloud, interpolate and fill the void areas of the original DEM by elevation information form this interpolated new DEM keeping the remaining pixels with elevation information in the original DEM unchanged.

- The Topographic Index has shown high heterogeneity in the catchment for the resolution changes than for the changes in the quality of DTMs. The smoothening of the terrain by the applied filtering procedure produced high index values. High resolution DTMs shown less index values with wider range of distribution. From this it is concluded that the index is more sensitive to resolution changes than the DTM quality.

7.2.　　Recommendations

The vertical and horizontal accuracy of the GPS used in this study is 10feet (3.048m) and 15m respectively. However, this has increased the RMSE calculated in the accuracy assessment relative to the result found when the Tri.GCPs are used. Therefore, more accurate GPS is highly recommended for such kind of assessment.

Inaccessibility to the 1 arc second resolution SRTM DEM was also one of the limitations of this study that could help in the assessment of the degree of the terrain detail loss when it is averaged to 3 arc second resolution DEM.

Further researches that incorporate detail comparison of DEMs generating technique from optical imageries and InSAR may reveal that whether InSAR gives more detail terrain information than optical parallax or vies versa; because ASTER DEM generated in 30m resolution gives more terrain detail after it is resampled to 90m resolution applying bicubic resampling technique.

The SWAT model used to assess the DEM quality and resolution effects is calibrated for monthly discharge output for the whole Naivasha catchment. When the calibrated parameters are used for the daily runoff modelling from the Malewa catchment only, the daily runoff output does not fit with the actual measurements at the river basin outlet point. The model gives much higher runoff output than the actual records. The whole DEM effect is based on the hypothesis that more detailed terrain information better represents the actual terrain characteristics and gives better accurate runoff output. This hypothesis is based on the model runoff outputs for the vegetation cover removed DEMs found by the two approaches used that have different accuracy level but gave exactly equal daily discharge values. Further study on model calibrated for daily time step is recommended to evaluate the volumetric runoff model output variation with respect to the DTM quality.

 In this study more emphasize is given to the DEM accuracy comparison, quality improvement effect on the SWAT model runoff output. Further studies are recommended on the DEM quality (detailed terrain features) effect after the model is calibrated for more accurate DEM that can be generated from very high resolution sources like LIDAR data or IKONOS Image with much focus on the model setup, calibration and validation.

It is also recommended that the evaluation procedures applied in this study are used to assess the sensitivity of fully distributed runoff models in which case the runoff output may be more sensitive to the DEM quality and resolution.

References

Abbott, M.B., J.C., Refsgaard, 1996. Distributed Hydrological Modelling. Kluwer Academic.

Abbott, M.B.J.C., Bathurst, J.A., Cunge, P.E.,O'Connell, J.,Rasmussen, 1986. An Introduction to the European Hydrological System-Systeme Hydrologique Europeen, "SHE", 1: History and philosophy of a physically-based, distributed modelling system. Journal of Hydrology, 87(1-2): 45-59.

Al-Sabbagh, M., 2001. Surface Runoff Modeling Using GIS and Remote Sensing: Case study in Malewa catchment, Naivasha, Kenya. MSc Thesis, ITC, Enschede, 82 pp.

Anderson, M.G., T.P.,Burt (Editor), 1995. Hydrological Forecasting. John Wiley & Sons Ltd.

Bamler, R., 1999. A world-Wide 30m Resolution DEM from SAR Interferometry in 11 days, Photogrammetric Week 99.

Bandaragoda, c., David, G.Tarboton, Ross, Woods, 2004. Application of TOPNET in the Distributed Model Intercomparison Project. Journal of Hydrology, 298: 178-201.

Barling, R., D., Moore I.,D., Grayson, R.,B., 1994. A quasi-dynamic wetness index for characterising the spatial distribution of zones of surface saturation and soil water content. Water Resources Research, 30.

Beven, K.J., 1985. Distributed Models. Hydrological forecasting. John Wiley & Sons Ltd.

Beven, K.J. (Editor), 1997. Distributed Hydrological Modelling: Application of the TOPMODEL Concept. Advances in Hydrological Processes. John Wiley & Sons.

Beven, K.J., 2000. Rainfall runoff modelling : the primer. Wiley & Sons, Chichester.

Beven, K.J., Lamb, R, Quinn, P F, Romanowicz, R and Freer, J,, 1995. TOPMODEL,. In: P. V., Singh (ed) (Editor), Computer Models of Watershed Hydrology, Water Resources Publications,, pp. 627-668.

Beven, K.J., O' Connel, P.E., 1982. On the role of Physically-Based Distributed Modelling in Hydrology, Wallingford, U.K, pp. Report,

No.81.

Brasington, J., Keith, Richards, 1998. Interactions between Model Predictions,

Parameters and DTM Scales for TOPMODEL. Computers & Geosciences, 24: 299-314.

Chow, V.t., 1988. Applied Hydrology. McGraw-Hill, New York.

Cuartero, A., Felicísimo, A.M., Ariza, F.J., 2004. Accuracy of DEM Generation from Terra-aster Stereo Data, XXth ISPRS Congress. Geo-Imagery Bridging Continents, Istanbul, Turkey, pp. 559.

De Ruyver, R., 2004. DEM optimization for hydrological modelling using SRTM for the 'Pantanal' region, Brazil, ITC, Enschede, 55 pp.

Di Luzio, M., R.Srinivasan, J.G.Arnold, S.L., Neitch, 2002. ArcView Interface For SWAT2000: Users Guide, Texas Water Resources Institute, College Station, Texas

TWRI Report TR-193.

Dingman, S., Lawrence, 2002. Physical Hydrology. Printice-Hall, Inc., Upper Saddle river, New Jersey.

Garberecht, J., L. W., Martz, 1999. Digital Elevation Model Issues in Water Resources Modelling, ESRI International User Conference. Digital Elevation Model Issues in Water Resources Modeling, Environmental Systems Research Institute, San Diego, California, pp. 1-17.

Hashimoto, T., 2000. DEM generation from stereo AVNIR

image. Advances in Space Research 25: 931-936.

Jacobsen, K., Recardo, Passini, 2002. Filtering of Digital Elevation Models, FIG/ASCM/ASPRS annual convention, Washington.

Koch, A., Peter, Lohmann, 2000. Quality Assessment and Validation of Digital Surface Models Derived From the Shuttle Radar Topography Mission (SRTM). IAPRS, Vol. XXXIII.

Kraus, K., Pefeifer, N., 1998. Determination of Terrain Models in Wooded Areas with Airborne Laser Scanner Data. ISPRS Journal of Photogrammetry & Remote Sensing, 53: 193-203.

Lanzl, F., Seige P., Lehmann F., Hausknecht, P., 1995. Using multispectral and stereo MOMS-02 data from the Priroda mission for remote sensing applications, ISSSR, International Symposium on Spectral Sensing Research, Melbourne, Australia,.

Lee, J., 1996. Digital Elevation Models: Issues of Data Accuracy and Applications, Proceedings of the ESRI User Conference.

Lee, J., Snyder, P., Fisher, P., 1992. Modelling the Effect of Data Errors on Feature Extraction From Digital Elevation Models. Photogrammertic Engineering and Remote Sensing, 58, No. 10: 1461-1467.

Li, Z., 1991. Effects of Check Point on the Reliability of DTM Accuracy Estimates Obtained from experimental test. Photogrammetric Engineering & Remote Sensing, 57: 1333-1340.

Lindström, G., Johansson, B., Persson, M., Gardelin, M., Bergström, S., 1997. Development and test of the distributed HBV-96 model J. Hydrol., 201: 272-288.

Maire, C., M.,Datcu, n.d. Synergy of Image and Digital Elevation Models (DEMs) Information for Virtual Reality.

Mather, M., Paul, 2004. Computer Processing of Remotely - Sensed Images: An Introduction. John Wiley & Sons Ltd, The Atrium, South Gate, Chichester, West Succex PO 19 8SQ, England.

Maune, D., F. (Editor), 2001. Digital Elevation Model Technologies and Applications: The DEM users Manual. American Society for Photogrammetry and Remote Sensing, Bethesda, Maryland, 539 pp.

Moore, I.D., Lewis, A.,J.C., Gallant (Editor), 1993. Terrain attributes: estimation methods and scale effects. Modeling Change in Environmental Systems.

Muthuwatta, L., Perakum, 2004. Long Term Rainfall-Runoff Lake Level Modeling of the Lake Naivasha Basin, Kenya. MSc Thesis, ITC, Enschede, 67 pp.

NDEP, 2004. Guidelines for Digital Elevation Data Version 1.0. National Digital Elevation Program.

Neitsch, S.L., J.G., Arnold, J.R.,Kiniry, J.R., Williams, K.W.King (Editor), 2002. Soil and Water Assessment Tool Theorotical Documentation: version 2000. Grassland, Soil & Water Research Laboratory, Temple, Texas GSWRL Report 02-01, Blackland Research and Extension Centre, Temple, Texas BRC Report 02-05. by Texas Water Resources Institute, College Station, Texas TWRI Report TR-191.

Pfeifer, N., Philipp, stadler, Christian, Briese, 2001. Derivation of Digital Terrain Models in the SCOP++ Environment, OEEPE Workshop on Airborne Laser scanning and Interferometric SAR for Digital Elevation Models, Stockholm.

Pinol, J., K. J.,Beven, Freer, J., 1997. Modelling the hydrological response of Mediterranean catchments, Prades, Catalonia - the use of distributed models as aids to hypothesis formulation. Hydrol., 11: 1287-1306.

Podder, A., Haque, 1998. Estimation of Long-Term Inflow into Lake Naivasha from the Malewa Catchment, Kenya. MSc. Thesis, ITC, Enschede, 84 pp.

Priebbenow, R., Clerici, E., 1988. Cartographic Applications of SPOT Imagery. International Archives of Photogrammetry, 57: 289-297.

Quinn, P.F., K.J.,Beven, P., Chevallier, O.,Planchon, 1991. The Prediction of Hillslope Flow Paths for Distributed Hydrological Modelling Using Digital Terrain Models, Hydrological Processes. John Wiley & Sons Ltd., pp. 59-79.

Rabus, B., Michael, Eineder, Achim, Roth, Richard, Bamler, 2003. The Shuttle radar Topography Mission- a New Class of Digital Elevation Models Acquired by Spaceborne Radar. Photogrammetry and Remote Sensing, 57: 241-262.

Reimold, G.R., J., Cooper, R., Romano, D., Cowan, C., Koeberl, 2004. A SRTM Investigation of Serra Da Cangalho Impact Structure, Brazil. W.U. Lunar and Planetary Science XXXV.

SHMI, 2003. HBV-Model (HBV-Model (Hydrologiska Byråns Vattenbalansacdeling).

SulSoft, 2002. ASTER DTM: Installation & User's Guide. SulSoft Ltda.

Sun, G., K.J.,Ranson, V. I.,Kharuk, K.,Kovacs, 2003. Validation of Surface Height from Shuttle Radar Topography Mission Using Shuttle Laser Altimeter. Remote Sensing of Environment, 88: 401-411.

Toutin, T., 1995. Generating DEM from Stereo Images with a Photogrammetric

Approach: Examples with VIR and SAR Data. Advances in Remote Sensing, 4 No 2: 110-117.

Vienna University of Technology, I.o.P.a.R.S., 2002-2003. SCOP++ Manual. IPF, TU Vienna and INPHO GmbH.

Viessman, W., Lewis,G.L.,Knapp,J.W., 1989. Introduction to Hydrology. Harper & Row.

Wagner, W.W., C., Eberhofer, M.,Hollaus, G. Summer, C., Eberhofer, M.,Hollaus, G., Summer, 2004. Robust Filtering of Airborne Laser Scanner Data for Vegetation Analysis, Proceedings of the ISPRS working group VIII/2. 'Laser-Scanners for Forest

and Landscape Assessment'. Institute for Forest Growth

Institute for Remote Sensing and Landscape Information Systems

Albert Ludwigs University, Freiburg, Germany.

Wechsler, S., P., 1999. Perceptions of Digital Elevation Model Uncertainty. URISA Journal.

Welch, R., Jordan T., Lang H., Murakami H.,, 1998. ASTER as a source for topographic data in the late 1990's. IEEE Transactions on Geosciences and Remote Sensing, 36: 1282-1289.

Weng, Q., 2002. Quantifying Uncertainty of Digital Elevation

Models Derived from Topographic Maps. In: P.v.O. D. Richardson (Editor), Advances in Spatial Data Handling. Springer-Verlag, New York, pp. 403-418.

Xiong, Z., Xiaojing, Huang, Leong, Keong, Kwoh ,Soo Chin Liew, 2002. Automated DEM generation from SPOT imagery. GIS development.net.

Zink, M., Geudtner, D., 1999. Calibration of the Interferometric X-SAR System on SRTM, CEOS SAR Workshop, Toulouse, France, ESA.

APPENDICES

Appendix A: SCOP++ Protocols of the applied Filtering Strategies

DEM 7

```
1------------------------------------------------------------------------
-
 ThinOut  VERS 5.2.2 step nb.0                        05Feb 08 14:13:13
------------------------------------------------------------------------
-
Input:               C:\INPHO_~1\SCOP__~1\test1\test1\test1_.all
Output:              C:\Inpho_Data\SCOP++_Projects\test1\test1\step0.tho
Cell size:           180.000
Method:              Lowest
Area:
  Left lower corner: 166021.440 9892000.000
  Size:              108000.000 108000.000
Nb of input points: 1442401
Nb of output points: 361201

 END SCOP.ThinOut


1------------------------------------------------------------------------
-
  Filter step nb.1                          05Feb 08 14:14:27
------------------------------------------------------------------------
-
Input:               C:\Inpho_Data\SCOP++_Projects\test1\test1\step0.tho
DTM:                 C:\Inpho_Data\SCOP++_Projects\test1\test1\step1.dtm
Output ground:       C:\Inpho_Data\SCOP++_Projects\test1\test1\step1.grd
Output vegetation:   C:\Inpho_Data\SCOP++_Projects\test1\test1\step1.veg


   DIGITAL ELEVATION MODEL
       MAP SHEET


   POSITION AND SIZE
       LEFT LOWER CORNER          EAST  ..........      166021.44
                                  NORTH ..........     9892000.00
       EXTENSION                  EAST  ..........      108000.00
                                  NORTH ..........      108000.00


   CHARACTERISTICS OF THE DEM
       GRID WIDTH                 EAST  .........          90.00
                                  NORTH .........          90.00
       NUMBER OF GRID LINES       EAST  .........             11
                                  NORTH .........             11
       NUMBER OF INTERPOLATED COMPUTING UNITS ....          14400
       NUMBER OF STORED GRID POINTS       .........        1742400
```

```
        NUMBER OF GRID INTERSECTIONS      .........              0


   INFORMATION ABOUT THE INTERPOLATION
        LINEAR PREDICTION
        NUMBER OF REFERENCE POINTS GIVEN ..........         361201
                SINGLE POINTS            ...........         361201
                HIGHS AND LOWS           ...........              0
                LINE POINTS              ...........              0
        AVERAGE FILTER VALUES
                SINGLE POINTS            ...........          1.182
                HIGHS AND LOWS           ...........           .000
                LINE POINTS              ...........           .000
        MAXIMUM FILTER VALUES
                SINGLE POINTS            ...........         73.606
                HIGHS AND LOWS           ...........           .000
                LINE POINTS              ...........           .000



1-----------------------------------------------------------------------
-
 SortOut  VERS 5.2.2 step nb.2                     05Feb 08 14:15:55
-----------------------------------------------------------------------
-
Input:                  C:\INPHO_~1\SCOP__~1\test1\test1\test1_.all
DTM:                    C:\Inpho_Data\SCOP++_Projects\test1\test1\step1.dtm
Output:                 C:\Inpho_Data\SCOP++_Projects\test1\test1\step2.sog
Lower distance:         -3.000
Upper distance:         3.000
Nb of input points:     1442401
Nb of output points:    937937


 END SCOP.SortOut


1-----------------------------------------------------------------------
-
  Filter step nb.3                              05Feb 08 14:22:05
-----------------------------------------------------------------------
-
Input:                  C:\Inpho_Data\SCOP++_Projects\test1\test1\step2.sog
DTM:                    C:\Inpho_Data\SCOP++_Projects\test1\test1\step3.dtm
Output ground:          C:\Inpho_Data\SCOP++_Projects\test1\test1\step3.grd
Output vegetation:      C:\Inpho_Data\SCOP++_Projects\test1\test1\step3.veg


   DIGITAL ELEVATION MODEL
        MAP SHEET


   POSITION AND SIZE
        LEFT LOWER CORNER         EAST  ..........       166021.44
                                  NORTH ..........      9892000.00
```

```
        EXTENSION                       EAST   ..........        108000.00
                                        NORTH  ..........        108000.00


    CHARACTERISTICS OF THE DEM
        GRID WIDTH                      EAST   .........            90.00
                                        NORTH  .........            90.00
        NUMBER OF GRID LINES            EAST   ........                 7
                                        NORTH  ........                 7
        NUMBER OF INTERPOLATED COMPUTING UNITS ....         40000
        NUMBER OF STORED GRID POINTS           .........      1960000
        NUMBER OF GRID INTERSECTIONS           .........            0


    INFORMATION ABOUT THE INTERPOLATION
        LINEAR PREDICTION
        NUMBER OF REFERENCE POINTS GIVEN ..........        937937
                SINGLE POINTS           ...........        937937
                HIGHS AND LOWS          ...........             0
                LINE POINTS             ...........             0
        AVERAGE FILTER VALUES
                SINGLE POINTS           ...........          .452
                HIGHS AND LOWS          ...........          .000
                LINE POINTS             ...........          .000
        MAXIMUM FILTER VALUES
                SINGLE POINTS           ...........        62.126
                HIGHS AND LOWS          ...........          .000
                LINE POINTS             ...........          .000
```

DEM 9

```
1----------------------------------------------------------------------
-
 ThinOut  VERS 5.2.2 step nb.0                      05Feb 08 16:15:09
----------------------------------------------------------------------
-
Input:             C:\INPHO_~1\SCOP___~1\test1\test1\test1_.all
Output:            C:\Inpho_Data\SCOP++_Projects\test1\test1\step0.tho
Cell size:         180.000
Method:            Lowest
Area:
  Left lower corner: 166021.440 9892000.000
  Size:              108000.000 108000.000
Nb of input points: 1442401
Nb of output points: 361201


 END SCOP.ThinOut


1----------------------------------------------------------------------
-
  Filter step nb.1                                 05Feb 08 16:16:11
```

```
-------------------------------------------------------------------------
-
Input:                  C:\Inpho_Data\SCOP++_Projects\test1\test1\step0.tho
DTM:                    C:\Inpho_Data\SCOP++_Projects\test1\test1\step1.dtm
Output ground:          C:\Inpho_Data\SCOP++_Projects\test1\test1\step1.grd
Output vegetation:      C:\Inpho_Data\SCOP++_Projects\test1\test1\step1.veg


   DIGITAL ELEVATION MODEL
        MAP SHEET


   POSITION AND SIZE
        LEFT LOWER CORNER           EAST   ..........      166021.44
                                    NORTH  ..........     9892000.00
        EXTENSION                   EAST   ..........      108000.00
                                    NORTH  ..........      108000.00

   CHARACTERISTICS OF THE DEM
        GRID WIDTH                  EAST   .........           90.00
                                    NORTH  .........           90.00
        NUMBER OF GRID LINES        EAST   .........              11
                                    NORTH  .........              11
        NUMBER OF INTERPOLATED COMPUTING UNITS ....           14400
        NUMBER OF STORED GRID POINTS        .........       1742400
        NUMBER OF GRID INTERSECTIONS        .........             0

   INFORMATION ABOUT THE INTERPOLATION
        LINEAR PREDICTION
        NUMBER OF REFERENCE POINTS GIVEN ..........          361201
                SINGLE POINTS           ...........          361201
                HIGHS AND LOWS          ...........               0
                LINE POINTS             ...........               0
        AVERAGE FILTER VALUES
                SINGLE POINTS           ...........            .180
                HIGHS AND LOWS          ...........            .000
                LINE POINTS             ...........            .000
        MAXIMUM FILTER VALUES
                SINGLE POINTS           ...........           2.827
                HIGHS AND LOWS          ...........            .000
                LINE POINTS             ...........            .000
```

DEM 10

```
1-------------------------------------------------------------------------
-
 ThinOut  VERS 5.2.2 step nb.0                       05Feb 08 16:35:44
-------------------------------------------------------------------------
-
Input:                  C:\INPHO_~1\SCOP___~1\test1\test1\test1_.all
```

```
Output:              C:\Inpho_Data\SCOP++_Projects\test1\test1\step0.tho
Cell size:           180.000
Method:              Lowest
Area:
  Left lower corner: 166021.440 9892000.000
  Size:              108000.000 108000.000
Nb of input points:  1442401
Nb of output points: 361201


 END SCOP.ThinOut


1------------------------------------------------------------------------
-
  Filter step nb.1                            05Feb 08 16:37:16
------------------------------------------------------------------------
-
Input:               C:\Inpho_Data\SCOP++_Projects\test1\test1\step0.tho
DTM:                 C:\Inpho_Data\SCOP++_Projects\test1\test1\step1.dtm
Output ground:       C:\Inpho_Data\SCOP++_Projects\test1\test1\step1.grd
Output vegetation:   C:\Inpho_Data\SCOP++_Projects\test1\test1\step1.veg


   DIGITAL ELEVATION MODEL
        MAP SHEET


   POSITION AND SIZE
        LEFT LOWER CORNER            EAST  ..........      166021.44
                                     NORTH ..........     9892000.00
        EXTENSION                    EAST  ..........      108000.00
                                     NORTH ..........      108000.00

   CHARACTERISTICS OF THE DEM
        GRID WIDTH                   EAST  .........          90.00
                                     NORTH .........          90.00
        NUMBER OF GRID LINES         EAST  .........             11
                                     NORTH .........             11
        NUMBER OF INTERPOLATED COMPUTING UNITS ....          14400
        NUMBER OF STORED GRID POINTS        .........      1742400
        NUMBER OF GRID INTERSECTIONS        .........             0

   INFORMATION ABOUT THE INTERPOLATION
        LINEAR PREDICTION
        NUMBER OF REFERENCE POINTS GIVEN ..........         361201
                SINGLE POINTS           ...........         361201
                HIGHS AND LOWS          ...........              0
                LINE POINTS             ...........              0
        AVERAGE FILTER VALUES
                SINGLE POINTS           ...........           .180
                HIGHS AND LOWS          ...........           .000
                LINE POINTS             ...........           .000
```

```
      MAXIMUM FILTER VALUES
              SINGLE POINTS           ...........          2.371
              HIGHS AND LOWS          ...........           .000
              LINE POINTS             ...........           .000




1------------------------------------------------------------------------
-
 SortOut  VERS 5.2.2 step nb.2                      05Feb 08 16:38:47
------------------------------------------------------------------------
-
Input:             C:\INPHO_~1\SCOP__~1\test1\test1\test1_.all
DTM:               C:\Inpho_Data\SCOP++_Projects\test1\test1\step1.dtm
Output:            C:\Inpho_Data\SCOP++_Projects\test1\test1\step2.sog
Lower distance:    -3.000
Upper distance:    3.000
Nb of input points: 1442401
Nb of output points: 953657


 END SCOP.SortOut


1------------------------------------------------------------------------
-
  Filter step nb.3                          05Feb 08 16:41:32
------------------------------------------------------------------------
-
Input:             C:\Inpho_Data\SCOP++_Projects\test1\test1\step2.sog
DTM:               C:\Inpho_Data\SCOP++_Projects\test1\test1\step3.dtm
Output ground:     C:\Inpho_Data\SCOP++_Projects\test1\test1\step3.grd
Output vegetation: C:\Inpho_Data\SCOP++_Projects\test1\test1\step3.veg


   DIGITAL ELEVATION MODEL
       MAP SHEET


   POSITION AND SIZE
        LEFT LOWER CORNER        EAST  ..........       166021.44
                                 NORTH ..........      9892000.00
        EXTENSION                EAST  ..........       108000.00
                                 NORTH ..........       108000.00

   CHARACTERISTICS OF THE DEM
        GRID WIDTH               EAST  .........           90.00
                                 NORTH .........           90.00
        NUMBER OF GRID LINES     EAST  .........               7
                                 NORTH .........               7
        NUMBER OF INTERPOLATED COMPUTING UNITS ....       40000
        NUMBER OF STORED GRID POINTS    .........       1960000
        NUMBER OF GRID INTERSECTIONS    .........             0
```

```
INFORMATION ABOUT THE INTERPOLATION
      LINEAR PREDICTION
      NUMBER OF REFERENCE POINTS GIVEN ..........          953657
             SINGLE POINTS          ..........          953657
             HIGHS AND LOWS         ..........               0
             LINE POINTS            ..........               0
      AVERAGE FILTER VALUES
             SINGLE POINTS          ..........            .107
             HIGHS AND LOWS         ..........            .000
             LINE POINTS            ..........            .000
      MAXIMUM FILTER VALUES
             SINGLE POINTS          ..........           1.974
             HIGHS AND LOWS         ..........            .000
             LINE POINTS            ..........            .000
```

DEM 14

```
1-----------------------------------------------------------------------
-
 ThinOut  VERS 5.2.2 step nb.0                         05Feb 08 17:20:19
-----------------------------------------------------------------------
-
Input:              C:\INPHO_~1\SCOP___~1\test1\test1\test1_.all
Output:             C:\Inpho_Data\SCOP++_Projects\test1\test1\step0.tho
Cell size:          180.000
Method:             Lowest
Area:
  Left lower corner: 166021.440 9892000.000
  Size:             108000.000 108000.000
Nb of input points: 1442401
Nb of output points: 361201


 END SCOP.ThinOut


1-----------------------------------------------------------------------
-
  Filter step nb.1                                    05Feb 08 17:32:43
-----------------------------------------------------------------------
-
Input:              C:\Inpho_Data\SCOP++_Projects\test1\test1\step0.tho
DTM:                C:\Inpho_Data\SCOP++_Projects\test1\test1\step1.dtm
Output ground:      C:\Inpho_Data\SCOP++_Projects\test1\test1\step1.grd
Output vegetation:  C:\Inpho_Data\SCOP++_Projects\test1\test1\step1.veg


   DIGITAL ELEVATION MODEL
```

MAP SHEET

POSITION AND SIZE
       LEFT LOWER CORNER   EAST 166021.44
                                   NORTH 9892000.00
       EXTENSION   EAST 108000.00
                                   NORTH 108000.00

CHARACTERISTICS OF THE DEM
       GRID WIDTH   EAST 30.00
                                   NORTH 30.00
       NUMBER OF GRID LINES   EAST   4
                                   NORTH   4
       NUMBER OF INTERPOLATED COMPUTING UNITS   1438743
       NUMBER OF STORED GRID POINTS   23019888
       NUMBER OF GRID INTERSECTIONS   0

INFORMATION ABOUT THE INTERPOLATION
       LINEAR PREDICTION
       NUMBER OF REFERENCE POINTS GIVEN   361201
               SINGLE POINTS   361201
               HIGHS AND LOWS   0
               LINE POINTS   0
       AVERAGE FILTER VALUES
               SINGLE POINTS 206
               HIGHS AND LOWS 000
               LINE POINTS 000
       MAXIMUM FILTER VALUES
               SINGLE POINTS 3.222
               HIGHS AND LOWS 000
               LINE POINTS 000

1--
-
 SortOut VERS 5.2.2 step nb.2   05Feb 08 17:36:43

-
Input: C:\INPHO_~1\SCOP__~1\test1\test1\test1_.all
DTM: C:\Inpho_Data\SCOP++_Projects\test1\test1\step1.dtm
Output: C:\Inpho_Data\SCOP++_Projects\test1\test1\step2.sog
Lower distance: -15.000
Upper distance: 15.000
Nb of input points: 1442401
Nb of output points: 1353730

 END SCOP.SortOut

1--
-

```
   Interpolation step nb.4                          05Feb 08 17:40:09
----------------------------------------------------------------------
-
Input:                    C:\Inpho_Data\SCOP++_Projects\test1\test1\step2.sog
DTM:                      C:\Inpho_Data\SCOP++_Projects\test1\test1\step4.dtm


   DIGITAL ELEVATION MODEL
        MAP SHEET


   POSITION AND SIZE
        LEFT LOWER CORNER         EAST  .......... 	      166021.44
                                  NORTH ..........       9892000.00
        EXTENSION                 EAST  ..........        108000.00
                                  NORTH ..........        108000.00

   CHARACTERISTICS OF THE DEM
        GRID WIDTH                EAST  .........            90.00
                                  NORTH .........            90.00
        NUMBER OF GRID LINES      EAST  .........                4
                                  NORTH .........                4
        NUMBER OF INTERPOLATED COMPUTING UNITS ....       160000
        NUMBER OF STORED GRID POINTS        .........    2560000
        NUMBER OF GRID INTERSECTIONS        .........          0

   INFORMATION ABOUT THE INTERPOLATION
        LINEAR PREDICTION
        NUMBER OF REFERENCE POINTS GIVEN ..........      1353730
                SINGLE POINTS           ...........      1353730
                HIGHS AND LOWS          ...........            0
                LINE POINTS             ...........            0
        AVERAGE FILTER VALUES
                SINGLE POINTS           ...........         .276
                HIGHS AND LOWS          ...........         .000
                LINE POINTS             ...........         .000
        MAXIMUM FILTER VALUES
                SINGLE POINTS           ...........        3.481
                HIGHS AND LOWS          ...........         .000
                LINE POINTS             ...........         .000
```

Appendix B: Triangulation Ground Control Points (Tri.GCPs) collected from Kenyan Survey Department in Different Projection, Datum, and Spheroid

Projection UTM Datum Arc 1960 Spheroid Clarke 1880 (Original data from Kenyan Survey Department)			Projection Geographic Lat/Lon Datum WGS 84 Spheroid WGS 84 (converted by ERDAS 8.7)			Projection UTM Datum WGS 84 Spheroid WGS 84 (converted by ERDAS 8.7)		
Xutm	Yutm	Z Arc1960	Xlat	Ylat	Zwgs84	Xutm	Yutm	Zwgs84
216573.1	9919905	2060	36.45441	-0.72666	2043.657	216573.1	9919905	2043.657
244848	9930828	3907	36.70835	-0.62805	3890.55	244848	9930828	3890.55
216971.6	9932384	2457	36.45805	-0.61387	2440.081	216971.6	9932384	2440.081
153459.3	9946170	3049	35.88801	-0.48903	3030.543	153459.3	9946170	3030.543
174813.3	9922477	3075	36.07954	-0.70319	3057.948	174813.3	9922477	3057.948
237730.8	9893875	2612	36.64425	-0.96206	2597.163	237730.8	9893875	2597.163
227574.5	9904995	2745	36.55311	-0.86148	2729.505	227574.5	9904995	2729.505
192218	9986767	2873	36.23597	-0.12231	2853.172	192218	9986767	2853.172
201518	9986444	2594	36.31945	-0.12525	2574.318	201518	9986444	2574.318
196161.2	9960584	2586	36.27132	-0.35894	2567.465	196161.2	9960584	2567.465
220496.5	9976969	2378	36.48982	-0.2109	2359.035	220496.5	9976969	2359.035
831295.5	9950942	2328	41.97688	-0.44597	2319.503	831295.5	9950942	2319.503
155084	9965580	2312	35.90266	-0.31368	2292.654	155084	9965580	2292.654
164509.7	9968207	2146	35.98725	-0.28997	2126.662	164509.7	9968207	2126.662
202454.7	9975150	2755	36.32785	-0.22732	2735.866	202454.7	9975150	2735.866
173279.9	9940355	2128	36.06587	-0.54165	2110.093	173279.9	9940355	2110.093
817588.3	9991507	2169	41.85377	-0.07948	2158.368	817588.3	9991507	2158.368
834657.8	9962251	2066	42.00702	-0.34379	2057.026	834657.8	9962251	2057.026
186857.1	9956176	1955	36.18779	-0.39875	1936.541	186857.1	9956176	1936.541
883698.7	9898852	2777	42.44741	-0.91618	2771.772	883698.7	9898852	2771.772
210717.2	9914979	1912	36.40181	-0.77114	1895.803	210717.2	9914979	1895.803
211097.5	9925567	1917	36.40528	-0.67546	1900.316	211097.5	9925567	1900.316
180381.1	9962938	2098	36.12968	-0.33762	2079.132	180381.1	9962938	2079.132
418246.7	9576348	1012	38.26455	-3.83527	1013.722	418246.7	9576348	1013.722
842733.2	9922465	3075	42.07966	-0.70319	3068.018	842733.2	9922465	3068.018
204008.6	9932179	2167	36.34166	-0.61567	2149.907	204008.6	9932179	2149.907
462427.5	9577228	1642	38.66246	-3.82756	1644.344	462427.5	9577228	1644.344
828600.8	9795690	2335	41.95413	-1.84871	2333.575	828600.8	9795690	2333.575
421312.4	9622787	2208	38.29249	-3.4152	2207.821	421312.4	9622787	2207.821
375982.7	9640667	1254	37.88464	-3.25308	1252.393	375982.7	9640667	1252.393
405768.1	9668033	1823	38.1529	-3.00579	1820.663	405768.1	9668033	1820.663
438037.2	9647398	1061	38.44317	-3.19265	1060.025	438037.2	9647398	1060.025

Appendix C: Field collected GPS data distribution in Malewa basin and Naivasha area.
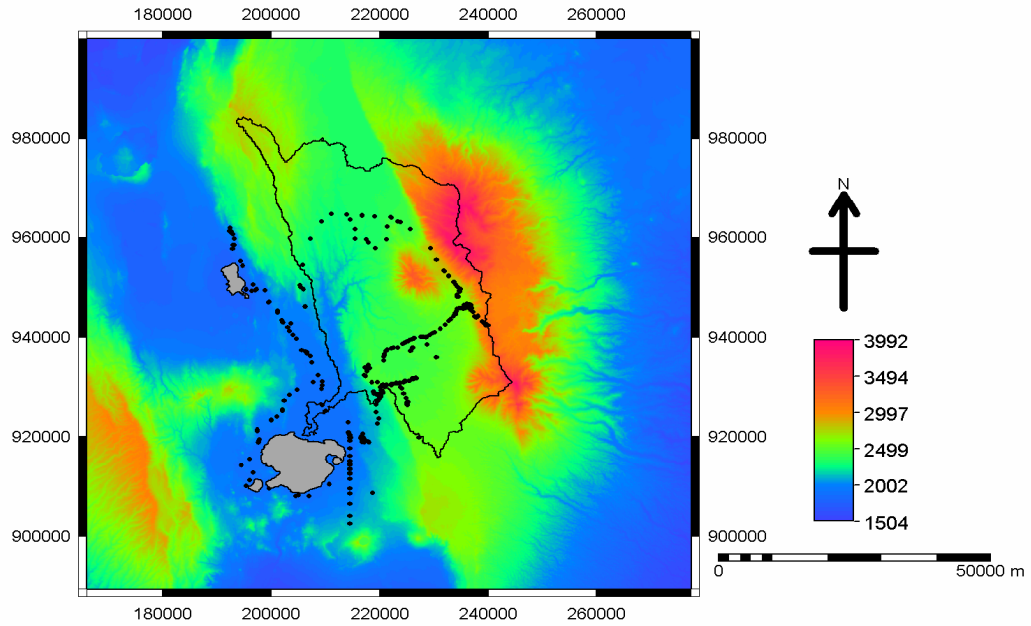
Appendix D: GPS data Collected in the Field

Projection	UTM				
Spheroid	Clarke 1880				
Datum	Arc1960				

X	Y	Z	X	Y	Z
204882	9908144	1890	216974	9932386	2456
195862	9911153	1915	217653	9934225	2444
196424	9912756	1903	217715	9934368	2447
204372	9908025	1910	217568	9934018	2446
197632	9919455	1904	217362	9933890	2438
197561	9919273	1910	217096	9933927	2410
197243	9921433	1955	217131	9933913	2414
197270	9921126	1941	217185	9933843	2405
199840	9923329	1986	217177	9933850	2411

199889	9923469	1991	217233	9933865	2422
200891	9924070	1987	217313	9933907	2435
201816	9925174	2010	217469	9933762	2448
201953	9925483	2023	217961	9933679	2442
202216	9927227	2036	217457	9933375	2454
203265	9928338	1976	217381	9933172	2456
204571	9929410	1929	217283	9932195	2465
207524	9930942	1932	218367	9930917	2465
210085	9938521	1970	219332	9931014	2476
210965	9937826	1971	220534	9935330	2444
210984	9937638	1951	220722	9936327	2408
210542	9941073	1979	220743	9936435	2408
210269	9945324	1980	220759	9936488	2410
212698	9947290	2014	220711	9936507	2410
212796	9947263	2011	221037	9937281	2433
206159	9944808	2028	221183	9937418	2437
205274	9950129	2195	221941	9937727	2458
207299	9962402	2332	222361	9937800	2463
212092	9964638	2273	223078	9937934	2457
212107	9964634	2279	224336	9938759	2456
219888	9969460	2357	224598	9938931	2449
219912	9969397	2361	224838	9939088	2436
220010	9969674	2366	225011	9939196	2438
239878	9942221	3174	225299	9939380	2445
227663	9938934	2441	225648	9939557	2450
214326	9920365	1909	226057	9939620	2437
214263	9920363	1902	226151	9939668	2426
214383	9919851	1899	226199	9939733	2420
214465	9919869	1907	227279	9940014	2456
214269	9919790	1896	227641	9940001	2463
214269	9919150	1898	227896	9939946	2463
214269	9917718	1911	228313	9939899	2461
214269	9916157	1927	228443	9939969	2461
214269	9915171	1952	229091	9940390	2479
214269	9914622	1960	229625	9940801	2486
214269	9914305	1966	229897	9940921	2495
214269	9914288	1966	230991	9941596	2513
214269	9913390	1985	231872	9942454	2540
214269	9913450	1987	232491	9943131	2548
214269	9912515	2005	232652	9943304	2548
214269	9912444	2004	232873	9943547	2561
214269	9911457	2030	233421	9944148	2570
214269	9911479	2031	233670	9944421	2572
214269	9909498	2055	233748	9944663	2579
214269	9909538	2062	233859	9945038	2583
214269	9908535	2078	234091	9945570	2588
214269	9908513	2079	234441	9945715	2581

214269	9906447	2118	234500	9945826	2575
214269	9906407	2118	234707	9945752	2569
214269	9904084	2147	234903	9945778	2580
214269	9904015	2144	235044	9945776	2591
214269	9902501	2129	235260	9945770	2610
226534	9931677	2454	235676	9945785	2621
226485	9931727	2456	235906	9946049	2631
226388	9931813	2457	235988	9946144	2630
225859	9931653	2453	236098	9946292	2635
225895	9931586	2454	236141	9946462	2639
225300	9931169	2432	236192	9946532	2639
225235	9931215	2427	236261	9946551	2643
224516	9931140	2455	236325	9946538	2649
224502	9931170	2452	236373	9946515	2649
224110	9930898	2444	236420	9946474	2654
224080	9930908	2441	236460	9946445	2660
223488	9930721	2442	236491	9946417	2661
223467	9930760	2444	236535	9946367	2666
222857	9930739	2452	236570	9946345	2668
222876	9930763	2452	236642	9946313	2670
222242	9930556	2447	236642	9946267	2669
222263	9930532	2450	236577	9946195	2674
222027	9930460	2446	236550	9946102	2678
221985	9930408	2447	236567	9946059	2683
221064	9930430	2453	236620	9946024	2684
221052	9930404	2453	236647	9945979	2685
220213	9930239	2429	236643	9945961	2688
220230	9930203	2433	236664	9945910	2693
219962	9929897	2388	236697	9945817	2701
219940	9929909	2386	236688	9945742	2705
220043	9929367	2340	236677	9945686	2708
220303	9928877	2299	220127	9929256	2356
220317	9928861	2299	220249	9929129	2345
220052	9928416	2256	220315	9929014	2337
220033	9928419	2256	220310	9928856	2323
219573	9928167	2238	220198	9928669	2311
219621	9928280	2241	220111	9928527	2294
219350	9928488	2237	220018	9928364	2277
219440	9928526	2240	220000	9928247	2270
218480	9908637	2088	219984	9928077	2269
199383	9946855	1910	219941	9927956	2262
199470	9946976	1918	219873	9927854	2260
196959	9949334	1873	219701	9927601	2260
196297	9949261	1848	219578	9927423	2252
194565	9954201	1857	219483	9927286	2247
194130	9955086	1857	219386	9927142	2245
192720	9957627	1868	219186	9925000	2218

192930	9958352	1919	219348	9922748	2151
192913	9958371	1920	217892	9918868	2099
192952	9959668	1955	217627	9919124	2110
192809	9960565	1980	216868	9919617	2104
192388	9961009	1980	216496	9920181	2091
192433	9961022	1980	216467	9920180	2094
192205	9961258	1998	216477	9920146	2090
192251	9961896	2045	216460	9920120	2078
197091	9949487	1881	216496	9920218	2087
195247	9949491	1808	216647	9920610	2081
195268	9949389	1803	214045	9920849	1951
201762	9943385	2020	214129	9920852	1904
203840	9940305	1978	213937	9922916	1913
206345	9936951	1942	202843	9941972	1988
216829	9919175	1977	201060	9944930	2017
216970	9918862	1981	196563	9950497	1877
216557	9919180	1970	206123	9937068	1947
216600	9919188	1969	209141	9930362	1914
216572	9919003	1984	209168	9926393	1921
216578	9919092	1970	219575	9923681	2123
216570	9919003	1973	220448	9930419	2432
216398	9919565	1964	222236	9930553	2435
216351	9919702	1963	223139	9930717	2433
216280	9919907	1958	224349	9931120	2442
216407	9919875	1965	224340	9931120	2441
216533	9919852	1987	226202	9931733	2450
216528	9919879	1998	226403	9931803	2448
216534	9919866	1990	230222	9935912	2477
216616	9919914	2047	228512	9938478	2442
216573	9919904	2045	225884	9937921	2435
216575	9919905	2059	225477	9937225	2441
216975	9932388	2439	227062	9934337	2446
224941	9926362	2410	214039	9920854	1900
224747	9926724	2414	206074	9946075	2007
224854	9926894	2421	205705	9949534	2109
224932	9926950	2400	205753	9949485	2110
225006	9927009	2400	205575	9954455	2189
224639	9927687	2399	207102	9959675	2195
224204	9928621	2387	210906	9964690	2243
223854	9929737	2374	213691	9964514	2254
223615	9929952	2374	216571	9964340	2291
220328	9928979	2231	216566	9964275	2294
224819	9926567	2404	218876	9964168	2293
209860	9925190	1913	221162	9962076	2347
209128	9929640	1911	221074	9959532	2344
208442	9932350	1928	218981	9957825	2321
206344	9936685	1944	217691	9958858	2263

203418	9942663	1987	217305	9959544	2293
203418	9942663	1992	215249	9959680	2215
198683	9949299	1937	215227	9961570	2282
221808	9963972	2389	214359	9963482	2274
221880	9963884	2392	202042	9942854	2027
223136	9963158	2402	203173	9941181	1993
223663	9962985	2405	204550	9939612	1967
225346	9961602	2430	205409	9937314	1956
229186	9957657	2791	207048	9936130	1954
231569	9953345	2789	207265	9934912	1964
233504	9951010	2735	209224	9931072	1928
233451	9950966	2714	197465	9918899	1928
233774	9950551	2701	195955	9915575	1934
234127	9948100	2578	194218	9914144	1946
233690	9944444	2561	195239	9910048	1928
224041	9938581	2443	199492	9909498	1956
220595	9936297	2418	206797	9908007	1926
220529	9936075	2426	210565	9910389	1940
220303	9928841	2302	201075	9945211	2021
219195	9926426	2226	201983	9943007	2027

Appendix E: Ilwis Script used to calculate Topographic Index

Parameter	Name	Type
%1	Original DEM	Raster Map
%2	Pixel Size	Value
%3	Flow accumulation map	Raster Map
%4	Threshold value	Value

// script to calculate morphometric variable.

dfdy_1.mpr{dom=value;vr=-1000:1000:0.1} = MapFilter(%1,DFDY.fil,value)
calc dfdy_1.mpr

dfdx_1.mpr{dom=value;vr=-1000:1000.7:0.1} = MapFilter(%1,DFDX.fil,value)
calc dfdx_1.mpr

// slope map in percentage
slp_perc=100*(hyp(dfdx_1,dfdy_1)/(%2))
calc slp_perc.mpr

// slope map in degrees
slp_deg=RADDEG(ATAN(slp_perc/100))
calc slp_deg.mpr

// process to remove 0 degrees from slope map to 0.1 degrees to avoid undefined cells or 0 values
mau=iff(slp_deg=0,0.1,slp_deg)
calc mau.mpr

// Giving a threshold to rivers
raster_flow.mpr{dom=bool;vr=True:False}=iff(%3>=%4,1,?)
calc raster_flow.mpr

// Wetness index factor
Wet_indx=LN((%3*%2*%2)/(TAN(DEGRAD(mau))))
calc Wet_indx.mpr
//end